

**EVALUATION OF MAGNETIC,  
DIELECTRIC AND MECHANICAL PROPERTIES  
OF RUBBER FERRITE COMPOSITES**

*Thesis submitted to the*  
**COCHIN UNIVERSITY OF SCIENCE AND TECHNOLOGY**  
*In partial fulfilment of the requirements  
for the award of the degree of*

**DOCTOR OF PHILOSOPHY**

*By*  
**M. A. SOLOMAN**

**DEPARTMENT OF POLYMER SCIENCE AND RUBBER TECHNOLOGY  
COCHIN UNIVERSITY OF SCIENCE AND TECHNOLOGY  
COCHIN – 682 022, INDIA  
JULY 2002**

*Dedicated to*

*My Loving Parents .....*

# CERTIFICATE

*This is to certify that the thesis entitled "Evaluation of Magnetic, Dielectric and Mechanical Properties of Rubber Ferrite Composites" is based on the bonafide research work carried out by Mr. M.A.Soloman under my guidance, in the Department of Polymer Science and Rubber Technology, Cochin University of Science and Technology, Cochin - 682 022, and no part of the work reported in this thesis has been presented for the award of any degree from any other institution.*



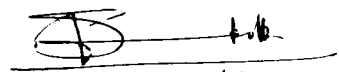
**Dr. Philip Kurian**  
Reader  
Department of Polymer Science  
and Rubber Technology  
Cochin University of Science  
and Technology

Cochin-22  
19<sup>th</sup> July 2002

## *Declaration*

*I hereby declare that the work presented in this thesis entitled "Evaluation of Magnetic, Dielectric and Mechanical Properties of Rubber Ferrite Composites" is based on the original research work carried out by me under the guidance and supervision of Dr. Philip Kurian, Reader, Department of Polymer Science and Rubber Technology, Cochin University of Science and Technology, Cochin-682 022 and no part of the work reported in this thesis has been presented for the award of any degree from any other institution.*

Cochin - 22  
19<sup>th</sup> July 2002

A handwritten signature in black ink, consisting of a stylized 'S' followed by a horizontal line and the initials 'A.S.'.

**M. A. Soloman**

## ACKNOWLEDGEMENT

*This thesis would not have been possible without the interaction and support of many people. I have great pleasure to acknowledge them for their contributions.*

*Dr. Philip Kurian, Reader, Department of Polymer Science and Rubber Technology, Cochin University of Science and Technology, Cochin, my supervising teacher was the main source of encouragement and support for the completion of this work. With great pleasure, I express my deep sense of gratitude for his inspiring guidance and competent advice without which the successful completion of this work would not have been possible.*

*I am thankful to Dr. K.E. George, Head of the Department of Polymer science and Rubber Technology and Dr. A.P. Kuriakose, Emeritus professor and former Head of Department of Polymer science and Rubber Technology for providing me the necessary facilities. With pleasure I thank all faculty members, non-teaching staff and friends of the Department of Polymer science and Rubber Technology for their help throughout the course of this work.*

*I express my wholehearted gratitude to Dr. M.R. Anantharaman, Department of Physics, Cochin University of Science and Technology, for his constant advice and encouragement, which helped me for the successful completion of this thesis. I am thankful to Prof. K. P. Rajappan Nair, Prof. M. Sabir and Dr. Elizabeth Mathai, former Heads of Department of Physics, for providing me the necessary facilities.*

*It gives me immense pleasure to take this opportunity to express my sincere thanks to Dr.P.A.Joy, Scientist, NCL, Pune, Dr.S.Venkatachalam, Sr. Scientist, VSSC, Thiruvananthapuram, Dr.Jossit Kurian, Deputy Director and Mr.Arjun Pillai of CFSC, Manjeri, Dr. Seshadri, Mr. Mathew, and Mr. Vibin of Philips Carbon India Ltd. for their help in completing this work.*

*Words are insufficient to express my gratitude to my colleagues and friends Mrs. Prema. K. H, Mr. Mathew George, Mr. Mohammed Jamal, Mr. E.M. Mohammed Mr. C. Joseph Mathai, Mr. Santhosh. D. Shenoy, Mr. S. Saravanan, Mr. U. Sajeev,*

*Mrs. K. A. Malini, Miss. S Sindhu, Miss Swapna S. Nair, Mrs. Asha Mary John, Mr. Saji Augustine, Mr. S. Shaji, and Mr. P.A. Nelson for their support at various stages of this work. Also I thank Dr. Cyriac Mathew and Dr. R. Sreelatha Kutty for their help in the early stages of my work.*

*I take this opportunity to acknowledge with thanks the help received from the Management, Principal and colleagues of St. Albert's College, Ernakulam. I owe a deep sense of gratitude to Prof. Mathew Pylee, former Principal of St. Albert's College, Ernakulam, who inspired me much.*

*I wish to thank the University Grants Commission for the award of the two years of Teacher Fellowship for the completion of the research work.*

*At this moment I remember with love and thanks, the inspiration, love and the blessings of my parents and other family members. Finally I thank the support and inspiration I received from my wife JOVI and my little son.*

*Above all, I thank God Almighty for his blessings*

**M. A. Soloman**

## *Preface*

---

Ceramic magnetic materials used in various devices have the inherent drawback that they are not easily machinable to obtain complex shapes. Plastic magnets and elastomer magnets, on the other hand have several advantages, as they are flexible, easily machinable and mouldable. They are light in weight and low in cost. Hence plastic magnets and rubber ferrite composites have the potential in replacing the conventional ceramic type of magnetic materials for applications where flexibility is an important criterion. Moreover, these composites are also important because of their microwave absorbing properties. Recent studies have indicated that the addition of fillers like carbon black on rubber ferrite composites enhances the microwave absorbing properties of the composites. Hence, studies pertaining to the incorporation of carbon black along with magnetic fillers in elastomer matrixes assume significance.

The hard ferrites are an important class among the ferrite materials due to their importance as permanent magnets and high density magnetic recording media. Since their discovery by Philips in 1950's, the M-type hexaferrite have continued to be of great interest for applications such as permanent magnets, plastoferrites, injection-moulded pieces, microwave devices and magnetic recording media. This is because of their relatively high coercivity, excellent chemical stability and corrosion resistance. Furthermore, their magnetic properties can be modified for various applications by proper choice of the constituents and appropriate preparative techniques.

In the present study the preparation and characterisation of rubber ferrite composites (RFC) containing barium ferrite (BaF) and strontium ferrite (SrF) have been dealt with. The incorporation of the hard ferrites into natural and nitrile rubber was carried out according to a specific recipe for various loadings of magnetic fillers. For this, the ferrite materials namely barium ferrite and strontium ferrite having the general formula  $MO_6Fe_2O_3$  have been prepared by the conventional ceramic techniques. After characterisation they were incorporated into the natural and nitrile rubber matrix by mechanical method. Carbon black was also

incorporated at different loading into the rubber ferrite composites to study its effect on various properties. The cure characteristics, mechanical, dielectric and magnetic properties of these composites were evaluated. The ac electrical conductivity of both the ceramic ferrites and rubber ferrite composites were also calculated using a simple relation. The results are correlated.

The results of the investigation on the 'Evaluation of Magnetic, Dielectric and Mechanical Properties of Rubber Ferrite Composites' in this thesis are classified into seven chapters.

**Chapter 1** gives a general introduction on the natural and synthetic rubber. Magnetic materials, their classification and applications are also dealt with in this chapter. A brief introduction to ferrites, magnetoplumbite structure and rubber ferrite composites are also provided in this chapter.

An outline about the equipments, materials used and the experimental techniques employed for the preparation and characterisation of samples are included in **Chapter 2**. The instruments used and the procedures adopted for the measurement of mechanical, dielectric and magnetic properties at various stages are also cited in this chapter.

**Chapter 3** deals with the preparation and characterisation of the ferrites and its incorporation into rubber matrixes. Structural evaluations of the prepared BaF and SrF samples were carried out using X-ray diffraction (XRD) method. These samples were checked for their monophasic characteristics before they were incorporated in to the matrix. RFCs were prepared by incorporating these precharacterised powder samples at various loading into natural and nitrile rubber according to a specific recipe. The preparation of RFCs containing carbon black is also included in this chapter

The cure characteristics and mechanical properties of the RFCs are discussed in **Chapter 4**. Cure characteristics of the RFCs were carried out using a Goettfert Elastograph model 67.85. Vulcanisation of these samples was then done on an electrically heated hydraulic press up to their respective cure times. The mechanical properties of these prepared RFCs were found out using an Instron Universal Testing Machine (UTM), model 4411 Test System.



The dielectric studies of these magnetic fillers and RFCs were carried out using a dielectric cell and an impedance analyser, model: HP 4285A in the frequency ranges from 100 KHz to 8 MHz and are presented in **Chapter 5**.

Magnetic properties of both ceramic fillers and RFCs were evaluated and dealt in **Chapter 6**. The correlation of the properties was carried out with a view to tailor making materials with specific magnetic properties. The variation of coercivity, saturation magnetisation and magnetic remanence for different filler loadings were compared and correlated. Magnetic measurements of ceramic BaF, SrF and the RFCs were carried out using vibrating sample magnetometer (VSM), model: 4500 (EG&G PARC).

**Chapter 7** is the concluding chapter of the thesis. In this chapter, the important observations and results are discussed and compared. Commercial and technical importance of RFCs and its possible applications are discussed in this chapter. The scope for further work is also dealt with in this chapter.

# CONTENTS

	<b>Page</b>
<b>Chapter 1</b>	
<b>INTRODUCTION</b>	01
1.1 Polymers	02
1.2 Magnetic Materials	07
1.3 Different Kinds of Magnetism	14
1.4 Application of Magnetic Materials	17
1.5 Rubber Ferrite Composites (RFC)	20
1.6 Present Study	22
References	24
<b>Chapter 2</b>	
<b>EXPERIMENTAL TECHNIQUES</b>	29
2.1 Materials Used	29
2.2 Experimental Methods	34
2.3 Physical Test Methods	39
2.4 Electrical Characterisation	40
2.5 Magnetic Characterisation	45
References	49
<b>Chapter 3</b>	
<b>PREPARATION AND CHARACTERISATION OF RUBBER FERRITE COMPOSITES</b>	53
3.1 Synthesis of Ceramic Ferrites	54
3.2 Structural Evaluation	55
3.3 Incorporation of Fillers in Rubber Matrix	58
3.4 Compounding	59

3.5	Determination of Cure Characteristics of RFCs	61
3.6	Preparation of Test Specimens	61
3.7	Conclusion	61
	References	62
<b>Chapter 4</b>		
<b>CURE CHARACTERISTICS AND MECHANICAL PROPERTIES OF RUBBER FERRITE COMPOSITES</b>		<b>63</b>
4.1	Introduction	63
4.2	Cure Characteristics	64
4.3	Mechanical Properties	73
	4.3.1 Stress Strain Properties of Rubber Ferrite Composites	74
	4.3.1.1 Natural Rubber based RFCs	74
	4.3.1.2 Nitrile Rubber based RFCs	82
	4.3.1.3 Abrasion Resistance	88
4.4	Conclusion	89
	References	90
<b>Chapter 5</b>		
<b>DIELECTRIC PROPERTIES OF RUBBER FERRITE COMPOSITES</b>		<b>91</b>
5.1	Introduction	91
5.2	Dielectric Measurements	92
	5.2.1 Ceramic Samples	93
	5.2.2 Dielectric Properties of Gum Natural Rubber Vulcanisate	96
	5.2.3 Dielectric Properties of Gum Nitrile Rubber Vulcanisate	97
5.3	Dielectric Properties of NR based RFCs	97
5.4	Dielectric Properties of NBR based RFCs	123
5.5	AC Conductivity Studies	132
5.6	Conclusion	142
	References	144

## **Chapter 6**

<b>MAGNETIC PROPERTIES OF RUBBER FERRITE COMPOSITES</b>	<b>147</b>
6.1 Introduction	147
6.2 Magnetic Measurements	148
6.2.1 Ceramic Samples	148
6.2.2 Rubber Ferrite Composites based on NR	150
6.2.3 Rubber Ferrite Composites based on NBR	159
6.3 Tailoring of Magnetic Properties of RFCs	166
6.4 Conclusion	168
References	169

## **Chapter 7**

<b>SUMMARY AND CONCLUSION</b>	<b>170</b>
7.1 Summary	171
7.2 Conclusion	174
7.3 Future Outlook	176
<b>List of abbreviations and symbols</b>	<b>177</b>
<b>List of publications</b>	<b>180</b>

# Chapter 1

---

## INTRODUCTION

Rubber ferrite composites are magnetic polymer composites consisting of ferrite fillers and natural/synthetic rubber matrix. These magnetic composites have a variety of applications as flexible magnets, pressure / photo sensors and microwave absorbers. One of the familiar applications of rubber magnets is the refrigerator door seal. They are lightweight, soft, elastic, stable, flexible, easy to be processed, energy saving and low cost.

Flexible magnetic composites can be prepared by embedding magnetic fillers into polymer matrixes according to suitable recipes. The mouldability into complex shapes is one of the advantages of these composite materials. Rubber magnets thus produced by the incorporation of the magnetic materials into various matrixes like natural and synthetic rubber have several advantages over the conventional ceramic magnets, due to its flexible nature. Hence, they have the potential of replacing the conventional ceramic materials.

Polymers and magnetic materials play a very important role in our day to day life. Both natural and synthetic polymers are truly indispensable to mankind. The polymers, which include rubber, plastics and fibers, make life easier and more comfortable. They are used in the manufacture of textiles, building materials, transportation, communication, packing materials, chairs, pipes, hoses, fancy decorative articles, toys etc.

Magnetic materials are equally important and are widely used by man from the very common machineries to the most sophisticated equipments. They are used in instruments like television sets, telephones, refrigerators, washing machines, vacuum cleaners, hearing aids, automobile parts, as permanent magnets in computers, as magnetic sensors on credit cards and in theft control devices, in magnetic recording media and various microwave absorbing devices. Magnetic materials include metals, alloys and ceramics.

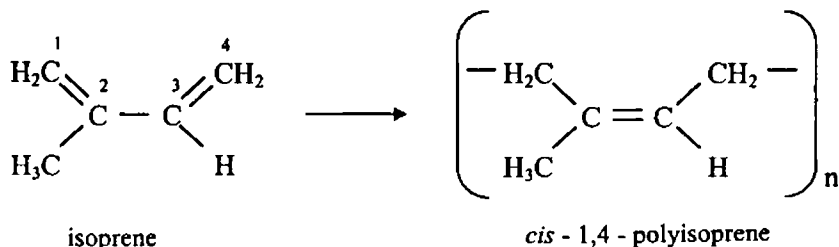
The permanent magnets play an important role in the science and technology of the present day. Alnicos (Al, Ni & Co), barium ferrite and strontium ferrite dominate the permanent magnet market. Of these barium ferrite and strontium ferrite are frequently known as the "Ceramic Magnets". The rare earths have been used in the new generation permanent magnets<sup>1</sup>. The discovery of Nd<sub>2</sub>Fe<sub>14</sub>B magnets, in 1984, has ushered a new era for the rare earth-transition based permanent magnets. Today's high-performance magnets are mostly made from Nd<sub>2</sub>Fe<sub>14</sub>B.

## 1.1 POLYMERS

### 1.1.1 Natural Rubber

Natural rubber (NR) is obtained from the sap of a tree called 'caoutchou' or 'weeping wood' and is botanically known as 'Hevea Brasiliensis', named after the large forest tree, which is its outstanding source. The English term "Rubber" was coined by Joseph priestly in 1770, since the material could erase pencil marks. The chemical name of natural rubber is polyisoprene, since it is a polymer of isoprene.

Faraday in 1821 found that natural rubber has an empirical formula of C<sub>5</sub>H<sub>8</sub> and it was Greville Williams (1860), who recognised that rubber was a polymer of isoprene.



The polymer chains in natural rubber have a perfectly *cis*-1, 4 structure. Hence the chemical name is *cis*-1, 4-polyisoprene<sup>2</sup>. The stereo regularity of the natural rubber imparts a good regularity to the rubber chains, because of this the natural rubber crystallises on stretching, resulting in high gum strength.

The raw natural rubber possesses considerable strength and appreciable elasticity and resilience at room temperature. It is sensitive to hot and cold and hence oxidises to a sticky product. For this reason rubbers have to be vulcanised for achieving optimum properties. During the process of vulcanisation, cross-linking occurs between the long chain molecules to obtain a continuous network of flexible, elastic chains. The three dimensional structure so produced restricts the free mobility of the molecules and the product obtained have reduced tendency to crystallise, improved elasticity, and substantially constant modulus and hardness over a wide range of temperature. The number of crosslinks formed, also referred to as degree of vulcanisation has an influence on the elastic and other properties of the vulcanisate. Vulcanisation can be carried out by means of various chemical reactions, depending on the chemical structure of the polymer. However, the most common practice for unsaturated elastomers such as natural rubber and the synthetic polydienes involve the treatment with sulphur and its compound.

Vulcanisation with sulphur alone is a slow process and requires large amount of sulphur, high temperatures and long heating periods. Hence accelerators are used in combination with vulcanising agents to reduce the time and/or temperature of vulcanisation. In certain cases accelerator activators and co-activators are also used. These form chemical complexes with the accelerators and increase the rate of vulcanisation and improve the properties of the final vulcanisate.

The discovery of Hancock in 1824 that rubber could be masticated was of greatest technical importance to the rubber industry. The addition of compounding ingredients is greatly facilitated by this treatment, which is usually carried out on two roll mills or in internal mixers or in continuous mixers. The process of mastication is accompanied by a marked decrease in the molecular weight of the rubber. When the mastication is complete, compounding ingredients are added, and the rubber mix is prepared for vulcanisation. The details are cited elsewhere<sup>3</sup>.

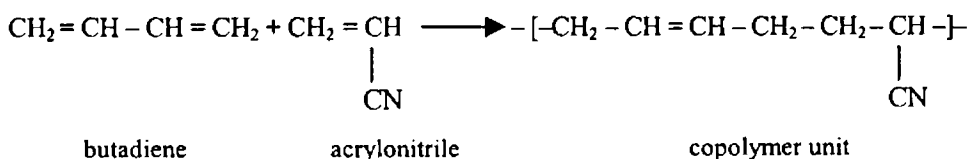
For many applications, however, even the vulcanised rubbers do not exhibit satisfactory tensile strength, modulus, stiffness, abrasion resistance and tear resistance. These properties can be enhanced by the addition of certain fillers to the rubber before vulcanisation. The fillers for rubber can be classified in two, inert fillers and reinforcing fillers. Inert fillers like clay, whittings, talc etc make the rubber mixture easier to handle before vulcanisation but have little effect on its physical properties. Reinforcing fillers, however, improve the physical properties of the vulcanised rubber. Carbon black is an outstanding reinforcing filler for both natural and synthetic rubbers.

Rubbers that retain double bonds after vulcanisation, such as natural rubber, styrene butadiene rubber and nitrile rubber, are sensitive to heat, light, and oxygen. Unless protected with antioxidants (Maasen 1965), the rubbers age by an autocatalytic process accompanied by an increase in oxygen content. As a result, softening or embrittlement of rubber occurs indicating degradation. Many rubbers are sensitive to the attack by ozone, requiring protection by antiozonants (Cox 1965). Natural rubber is far more sensitive than most of the other elastomers to both oxygen and ozone attack.

Rubber has certain unique properties, which makes it a useful material for products of commercial importance. In the vulcanised state it is elastic, and after stretching it returns to its original shape and in the unvulcanised state it is plastic; i.e., it flows under the effect of heat or pressure. Rubber is a poor conductor of electricity and hence it is very valuable as an electrical insulator. Some of the applications include the manufacture of automobile tyres, mechanical goods, footwear, hoses, beltings, adhesives and latex based products like gloves, foam rubber and thread.

### 1.1.2 Nitrile Rubber

Nitrile rubber, otherwise known by the generic name Buna-N or NBR, is a special purpose synthetic rubber. It is a copolymer of butadiene and acrylonitrile. The basic polymerisation reaction in the production of nitrile rubber is





Oil resistance is the most important property of nitrile rubber. NBR has good resistance to oils, greases, petroleum hydrocarbons and other non-polar solvents. Hence it is used in the manufacture of products like oil seals, O-rings, gaskets, fuel and oil hoses, including high pressure hoses, for hydraulic and pneumatic applications, friction covering, linings, containers, work boots, shoe soling and heels, conveyor belts, in membranes, etc. The presence of the nitrile group ( $C\equiv N$ ) on the polymer is responsible for this property. Nitrile rubbers are sometimes blended with plastics to obtain useful products<sup>4</sup>.

The commercially available nitrile rubbers differ from one another in three aspects: acrylonitrile content, temperature employed for polymerisation, and Mooney viscosity. However the acrylonitrile content is the one that has the most profound affect on the properties of a vulcanised nitrile rubber, influencing its resistance to oils and fuels.

The acrylonitrile (ACN) content varies usually from 20 - 50 % by weight and accordingly NBR is classified in to three namely, low ACN content NBR with less than 25%, medium with 25 – 35% and high content ACN NBR with 35 - 50%. The oil resistance of the nitrile rubbers varies greatly with their composition. Increasing the acrylonitrile content increases the oil resistance. For instance, when the ACN content is 18%, the NBR has fair oil resistance and when the ACN content is 40%, the polymer is extremely resistant to oil. This is because the incorporation of the polar monomer acrylonitrile changes the polarity of the polymer. Most of the fuels and lubricants are non polar and swell the non polar elastomer, such as NR, with a resultant loss in properties. The amount of acrylonitrile affects several properties of the elastomer. The properties like tensile strength, hardness, abrasion resistance, heat resistance and gas impermeability increases with the increasing ACN content, whereas other properties like resilience, low temperature flexibility, plasticiser compatibility decreases with the increasing ACN content. Other properties affected by monomer ratio are processability, cure rate, heat resistance and resistance to permanent set. With increased ACN content processing is easier, cure rate is faster and heat resistance better, but the resistance to permanent set decreases. Other important characteristics, which can affect the properties of nitrile rubber, especially the processing properties, are Mooney viscosity and gel content.

Basically nitrile rubbers are compounded much like natural rubber <sup>5</sup>. The compounding ingredients used are the same though they differ slightly in the amount. Vulcanisation of nitrile rubber is usually accomplished with sulphur, accelerator and zinc oxide and fatty acid as activator. In special cases peroxide may also be used. Sulphur is less soluble in NBR than in NR and only small amounts are used. But corresponding increases in the accelerators are required.

NBR shows no self-reinforcing effect, as there is no stress induced crystallisation. Since it does not crystallise, reinforcing fillers are necessary to obtain optimum tensile strength, tear strength and abrasion resistance. Carbon black is the most widely used filler and the reinforcement is proportional to the fineness of the black. Non black fillers used are various types of silica, calcium carbonate, hard clay, talc and other inorganic fillers. Fine precipitated silica is most reinforcing among the non black fillers. Semi-reinforcing fillers are also used for obtaining suitable physical properties and to bring down the raw material cost.

Plasticisers are used in almost all nitrile rubber compounds to improve processability and low temperature flexibility. Generally used plasticisers are the phthalate type esters.

Nitrile rubber requires age resistors in order to give longer service. Either the amine or the hindered phenolic type antioxidants are generally used.

The important industrial applications of NBR include the manufacture of cables for the petroleum, coal-mining and quarrying industries, transport, shipbuilding, power distribution, domestic and miscellaneous applications<sup>6,7</sup>. The other fields that account for most of the uses of NBR are the automobile, aircraft, oil, textile and printing industries.

It has already mentioned in this chapter that reinforcing fillers are required to improve the properties of NBR. The present study involves the use of magnetic fillers, namely barium ferrite and strontium ferrite, so as to obtain rubber magnets or flexible magnets. High abrasion furnace black (HAF) is added as a reinforcing filler along with ferrite fillers and its effect on different properties of the vulcanisate are studied and are explained in subsequent chapters.

## 1.2 MAGNETIC MATERIALS

Magnetic materials have wide range of applications, and these applications impose certain requirements on the magnetic materials. Hence, the wide variety of magnetic materials can be sharply divided into two groups, namely, magnetically soft and magnetically hard<sup>8,9</sup>.

### 1.2.1 Soft Magnetic Materials

Soft magnetic materials have high permeability, low coercive force and small hysteresis loss. They are easy to magnetise and demagnetise and have flux multiplying power. Soft magnetic materials are used in applications requiring frequent reversals of the direction of magnetisation.

Soft magnetic materials can be divided into four main groups, according to their function. Heavy duty flux multipliers, light duty flux multipliers, square loop materials, and microwave system components.

Heavy duty flux multipliers are used in the cores of transformers, generators, and motors. The electrical steel, that form the cores of transformers, generators and motors are subjected to alternating and rotating magnetic fields, and the minimisation of the energy loss per cycle is a design objective. The electrical steel is the cheapest magnetic material.

Light duty flux multipliers are the cores of small, special purpose transformers, inductors etc used mainly in communications equipment. Soft ferrites and nickel-iron alloys fall in this class.

Square loop materials are used in computers and in magnetic amplifiers and other saturable core devices. They include soft ferrites and nickel-iron alloys.

Microwave system components comprise soft ferrites and garnets. There are various soft magnetic materials like Fe-Si or Fe-Ni alloys, ferrimagnetic oxides like ferrites. Ferrites have the general formula  $M^{2+}Fe^{3+}_2O^{2-}_4$  (where  $M^{2+}$  is  $Ni^{2+}$ ,  $Fe^{2+}$  etc.).

Soft magnetic materials are normally used for iron cores of transformers, motors, and generators, where high permeability, low coercive force and small hysteresis loss are required<sup>10</sup>.

### **1.2.2 Hard Magnetic Materials**

Hard magnetic materials have high coercivity, high remanence and large hysteresis loss. They are difficult to magnetise and demagnetise. Hard magnetic materials are used to produce permanent magnets<sup>11</sup>. The purpose of a permanent magnet is to provide a magnetic field in a particular volume of space. A magnetic field can be produced by current in a conductor or by poles in a magnet. For many applications a permanent magnet is the better choice, since it provides a constant field without the continuous expenditure of electric power and without the generation of heat. A magnet is fundamentally an energy-storage device. This energy is put into it when it is first magnetised and it remains in the magnet indefinitely, if properly made and properly handled. Such magnets are called 'Permanent magnets'.

Hard magnetic materials are used as permanent magnets for various kinds of electric meters, loudspeakers and in other apparatus for which high coercivity, high remanence and large hysteresis loss are desirable.

Based on the composition and structural features, permanent magnetic materials are classified into

1. Martensitic or quench hardened alloys.
2. Dispersion hardened alloys.
3. Work hardened alloys.
4. Order hardened or super lattice forming alloys.
5. Metallic powders, self bonded.
6. Metallic powders, bonded with a bonding agent
7. Ceramic powders, self bonded.
8. Ceramic powder, bonded with a bonding agent.
9. Miscellaneous, which possess some unusual features and not coming in the above mentioned categories.

Hard magnetic materials include ferrites, alloy magnetic steels, permanent magnet alloys, special alloys, carbon steels, magnetic steels, rare-earth based

magnets, etc. The permanent magnets play a very important role in our day to day life. Alnico (Al, Ni & Co), barium ferrite and strontium ferrite are the most widely used permanent magnet materials. Recently, rare earth transition metal based permanent magnets, especially Nd-Fe-B magnets having unique properties are used in the modern technological devices<sup>12</sup>.

### 1.2.3 Ferrites.

The field of magnetic oxides is one of the areas in magnetism, where significant advances have been made since the beginning of the 20<sup>th</sup> century. Here the development of ferrites and the advances made in this area are noteworthy. Ferrites are a group of technologically important ferrimagnetic materials. The advent of ferrites began with the search for magnetic materials of unusually high resistivities to minimise eddy current losses. The term ferrites refers to all magnetic oxides containing iron as the major metallic component<sup>13</sup>. It is the systematic study by Snoek<sup>14</sup> in 1946 that culminated in the introduction of magnetic ferrites having technically and commercially viable properties. Research activities on ferrites in the last five decades, has led to the development of these magnetic materials.

Ferrites are mixed metal oxides with iron (III) oxides as their main components. They exhibit a substantial spontaneous magnetisation and phenomena like magnetic saturation and hysteresis. Ferrites crystallise in three different crystal structures, namely, spinels, garnets and magnetoplumbites<sup>15-17</sup>.

Spinel ferrites have a cubic structure with general formula  $MOFe_2O_3$ , where M is a divalent metal ion like Mn, Ni, Fe, Co, Mg etc. Garnets have a complex cubic structure having a general formula  $Ln_3^{III}Fe_2O_{12}$ , where  $Ln^{III} = Y, Sm, Eu, Gd, Tb, Dy, Ho, Er, Tm$  or Lu. The third type magnetoplumbite is having a hexagonal structure with general formula  $MO_6Fe_2O_3$ , where M is a divalent metal such as Ba, Sr and Pb. The most important in the group of magnetoplumbite is barium ferrite  $BaO_6Fe_2O_3$ .

Magnetically, ferrites are classified into two groups, namely, soft and hard<sup>16</sup>. Further, depending on its symmetry, the magnetic ferrites fall mainly into two groups, cubic and hexagonal<sup>18</sup>. Barium and strontium ferrites belong to the class of

hexagonal ferrites. Both of these are hard ferrites as well<sup>13,15,17,19-23</sup>. They are normally prepared using the ceramic technique<sup>24-34</sup>.

The ferrimagnetic materials have great commercial importance due to their unique properties like large magnetisation values, high resistivity and low eddy current losses. They have advantages such as applicability at higher frequency, lower price and greater electrical resistance<sup>35</sup>. The practical applications of ferrites have been exploited by utilising these advantages.

Ferrites in general find extensive applications<sup>36-43</sup> in a number of devices like inductor and transformer cores, antenna cores, magnetic amplifiers, deflection yokes in television sets, hearing aids, computer peripherals, memory and switching applications in digital computers and data processing circuits<sup>44</sup>, modulators, circulators, isolators, phase shifters, other high frequency devices and also for various microwave applications<sup>17, 45-48</sup>. Other applications of ferrites involve the use in temperature sensors, magnetostrictive delay lines, magnetic resonators, ferrite filters<sup>49</sup>, ferrite radiators<sup>50,51</sup>, ferrite power limiters and so on. They are usually employed in the ceramic form. These ceramic magnets have the inherent drawback that they are not easily machinable to obtain complex shapes.

### 1.2.3.1 Soft Ferrites

The ferrites, which are easy to magnetise and demagnetise, are termed as soft ferrites. Soft ferrites have a cubic crystal structure. The general formula is  $MOFe_2O_3$ , where M is a divalent metal ion like Mn, Ni, Fe, Mg etc. These ferrites have saturation magnetisation ( $M_s$ ) value less than that of iron and its alloys and have low dc permeability. So they are inferior to magnetic metals and alloys for applications involving static or moderate-frequency fields. Non-magnetic zinc ferrite is often added to increase the saturation magnetisation.

These ferrites have extremely high electrical resistivity with good magnetic properties, so they can operate with virtually no eddy current loss at high frequencies. This fact accounts for all the applications of soft ferrites.

The largest production of soft ferrites by weight is that of deflection yoke rings<sup>52</sup> for picture tubes in television receivers. There are many other significant

applications<sup>10</sup> of soft ferrites such as recording heads, antenna rods, proximity sensors, humidity sensors, interference suppression cores, etc.

### 1.2.3.2 Hard Ferrites

The ferrites, which are hard to magnetise and demagnetise, are termed as hard ferrites. Hard ferrites have hexagonal crystal structure. The general formula is  $MO_6Fe_2O_3$ , where M is a divalent metal ion like Ba, Sr and Pb. In the group of hard ferrites, magnetoplumbites or M-type hexagonal ferrites ( $MO_6Fe_2O_3$ ) are widely used in many technological applications due to their superior magnetic properties.

The most important among the hard ferrites is barium ferrite. It has a fairly large crystal anisotropy (anisotropy constant,  $K = 3.3 \times 10^6$  ergs / cm<sup>3</sup>). The Curie point is 450°C. Barium ferrite was developed into a commercial magnet material in 1952 in Netherlands by the Philips Company, which called it ferroxdure. Some American trade names are Indox, Ferrimag, etc. Strontium ferrite has almost identical properties except that anisotropy constant is somewhat larger. In the recent years, it has been replaced to some extent by strontium ferrite. Sometime the general term 'hexaferrite' is used for both the materials.

Hexaferrites are widely used as permanent magnet materials<sup>53</sup> in applications where a very high resistance to demagnetisation (high coercivity) is required and the flux density does not need to be as high as in the metal magnetic materials. Other important advantages are very low cost, lightweight, high chemical stability, availability of the raw material and absence of eddy currents. One rapidly increasing application of the hard ferrite involves its incorporation into rubber or plastic matrixes thereby forming a versatile flexible magnet. Looking into the industrial perspective, one can see that the total world production of hard ferrites is almost the double that of the soft ferrites.

### 1.2.4 Magnetoplumbite structure

The hexagonal ferrites were discovered and investigated at the Philips Research Laboratories<sup>13</sup>. The determination of their structure by Braun<sup>54</sup> was the

basis for understanding the crystallographic building principle and the magnetic properties of these compounds. Of the several ferrimagnetic materials found with the hexagonal structure,  $\text{BaFe}_{12}\text{O}_{19}$  ( $\text{BaO}\cdot 6\text{Fe}_2\text{O}_3$ ), often referred to, as barium ferrite has the structure of naturally occurring mineral called Magnetoplumbite<sup>55</sup>. The term magnetoplumbite was coined by a group of Swedish investigator<sup>56</sup>. Magnetoplumbite has the approximate formula,  $\text{PbFe}_{7.5}\text{Mn}_{3.5}\text{Al}_{0.5}\text{Ti}_{0.5}\text{O}_{19}$ . Its structure was first described by Adelsköd<sup>57</sup>.

These classes of ferrites having composition  $\text{MO}_6\text{Fe}_2\text{O}_3$  ( $\text{M}=\text{Ba}^{2+} / \text{Sr}^{2+} / \text{Pb}^{2+}$ ), which is isostructural to mineral magnetoplumbite are commonly known as M-type hexagonal ferrites<sup>58</sup>. Materials of this type are very strongly uniaxial with a high value of K (anisotropy constant), and are used in making permanent magnets<sup>59</sup>. The magnetoplumbite structure can be visualised with help of figure 1.1. The atoms lie in mirror planes containing the c-axis and in the figure; the atoms and symmetry elements are shown for one such mirror plane. Atoms that do not lie on a three-fold symmetry axis (the full vertical line) appear three times within a unit cell, in the same plane perpendicular to the c-axis. Their other positions are readily obtained by rotation of the figure about the three-fold axis through  $120^\circ$  and  $240^\circ$ .

In Figure 1.1, the 'blocks' S,R,S\*, and R\* are designated; the S-block has the formula  $\text{Fe}_6\text{O}_8$  and the R-block  $\text{BaFe}_6\text{O}_{11}$ . Between S and S\*, and between R and R\* a  $180^\circ$  rotation about the c-axis occurs. Thus the structure of the M-type material may be written as  $\text{SRS}^*\text{R}^*$  or chemically  $2(\text{BaFe}_{12}\text{O}_{19})$ , i.e. two formula units per unit cell.

Figure 1.1 depicts the unit cell of  $\text{BaFe}_{12}\text{O}_{19}$ . All atoms lie in mirror planes containing the c-axis and atoms in one such plane are shown, together with the blocks S, S\*, R and R\* (after Braun 1957).



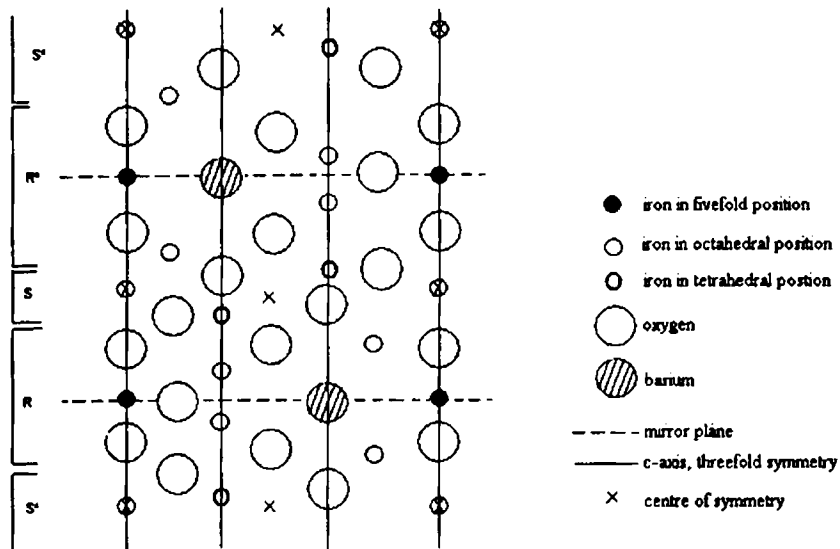


Fig 1.1 The unit cell of  $\text{BaFe}_{12}\text{O}_{19}$

A third type of block, the T-block is shown in figure 1.2, where the symbolism is that used in figure 1.1. The T-block consists of four oxygen layers with an oxygen ion replaced by  $\text{Ba}^{2+}$  in each of the middle layers. The formula for a T-block is thus  $\text{Ba}_2\text{Fe}_8\text{O}_{14}$ .

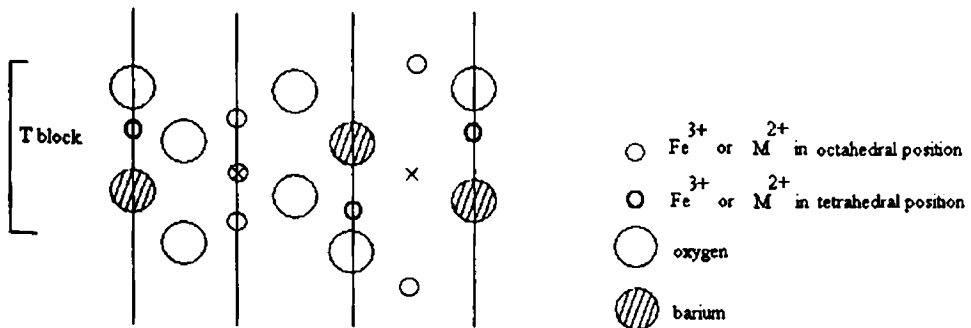


Fig 1.2 The T - block structure found in hexagonal iron oxides

Depending on the blocks R,S,R\*,S\*, and T a range of hexagonal structures can be synthesised. The compounds are designated M,W,Y,Z,X, and U as follows.

Type	Unit cell structure	Formula	Approx. cell size (Å°)	
			A	C
M	SRS*R*	Ba Fe <sub>12</sub> O <sub>19</sub>	5.9	23.3
M <sub>2</sub> W	SSR*S*S*R	Ba M <sub>2</sub> Fe <sub>16</sub> O <sub>27</sub>	5.9	32.3
M <sub>2</sub> Y	STSTST	Ba <sub>2</sub> M <sub>2</sub> Fe <sub>12</sub> O <sub>22</sub>	5.9	43.5
M <sub>2</sub> Z	RSTSR*S*T*S*	Ba <sub>3</sub> M <sub>2</sub> Fe <sub>24</sub> O <sub>41</sub>	5.9	56
M <sub>2</sub> X	3(RSR*SS)	Ba <sub>2</sub> M <sub>2</sub> Fe <sub>28</sub> O <sub>46</sub>	5.9	84
M <sub>2</sub> U	RSR*S*T*S*	Ba <sub>4</sub> M <sub>2</sub> Fe <sub>36</sub> O <sub>60</sub>	5.9	113

Where M is a divalent transition metal ion.

### 1.3 DIFFERENT KINDS OF MAGNETISM

The origin of magnetism can be attributed to the orbital and spin motion of electrons<sup>13,17,45,60</sup>. Magnetic moments of important magnetic atoms such as iron, cobalt and nickel are caused by spin motion of electrons. Depending on the magnetic properties and how the material reacted to a magnetic field, the magnetism exhibited by different materials can be divided in the following categories<sup>13,15-17,19,45,61-64</sup>. They are diamagnetism, paramagnetism, ferromagnetism, antiferromagnetism and ferrimagnetism.

Apart from this, magnetism like superparamagnetism, metamagnetism and parasitic magnetism etc are known. They are not included in this list, since they can be considered as derivatives from one of the above.

#### 1.3.1 Diamagnetism

The diamagnetic property is associated with completely filled shells in an atom. In diamagnetic materials the constituent atoms or molecules have all their electrons paired up in such a way that their magnetic dipole moments cancel each other. Hence there are no dipoles to be aligned by the field. In fact, an applied magnetic field is opposed by changes in the orbital motion of the electrons of a diamagnetic substance. This property can be understood as an example of Lenz's

law, which states that an applied magnetic field produces a field that opposes its cause. The diamagnetic materials have the relative permeability  $\mu_r < 1$  and susceptibility  $\chi$  is a small negative value. The negative value of diamagnetic materials is in accordance with the Lenz's law. Super conductors are perfect diamagnets with  $\chi = -1$

There are various diamagnetic materials; the strongest among them are metallic bismuth and organic molecules such as benzene. Other examples include metals like Cd, Cu, Ag, Sn, and Zn.

### 1.3.2 Paramagnetism

Paramagnetic substances have intrinsic permanent magnetic moments. When an external field is applied, they tend to align themselves parallel to the field, thereby intensifying the lines of force in the direction of the applied field. This result in an over all magnetic moment that adds to the magnetic field. Paramagnetism is independent of the applied field but is temperature dependent.

For ideal paramagnetic materials, the relative permeability  $\mu_r > 1$  and susceptibility  $\chi$  is small positive and varies inversely with the absolute temperature. Paramagnets are governed by Curie's law, which states that  $\chi$  is proportional to  $1/T$ ,  $T$  being the absolute temperature.

Paramagnetic materials usually contain transition metals or rare earth materials that possess unpaired electrons.

### 1.3.3 Ferromagnetism

A ferromagnetic substance has a net magnetic moment even in the absence of the external magnetic field. This is because of the strong interaction between the magnetic moments of the individual atoms or electrons in the magnetic substance that causes them to line up parallel to one another. When the many individual magnetic dipole moments produced in a material are appreciable, there can be long range interactions. This results in large scale areas of magnetism called domains. In ferromagnetic materials, the dipoles within a domain are all aligned and the domains tend to align with an applied field. The energy expended in reorienting the

domains from the magnetised back to the demagnetised state manifests itself in a lag in response, known as hysteresis.

For ferromagnetic materials, the relative permeability  $\mu_r > 1$  and susceptibility  $\chi$  is large positive and varies with the absolute temperature. They obey the Curie – Weiss law,

$$\chi = \frac{C}{(T - \theta)}, \text{ where } C \text{ and } \theta \text{ are Curie Weiss constants.}$$

An important property of ferromagnets is the Curie temperature, named after the French physicist Pierre Curie, who discovered it in 1895. Above the Curie temperature ferromagnets become paramagnets, since there is sufficient thermal energy to destroy the interaction between atoms that creates domains. i.e. ferromagnetic materials, when heated, eventually lose their magnetic properties. This loss becomes complete above the Curie temperature. The Curie temperature of metallic iron is about 770°C.

Ferromagnetism is exhibited mostly by metals and alloys. Iron, Cobalt and Nickel are all examples of ferromagnetic materials. Chromium dioxide is another material that exhibits ferromagnetism.

#### **1.3.4 Anti ferromagnetism**

Antiferromagnetism is a weak magnetism, which is similar to paramagnetism in the sense of exhibiting a small positive susceptibility. The substances in which the magnetic moments interact in a way, such that it is energetically favorable for them to line up antiparallel are called antiferromagnets.

The behavior of antiferromagnetic substances to an applied magnetic field depends up on the temperature. At low temperatures, the arrangement of the atomic dipoles is not affected, and the substance does not respond to an applied magnetic field. When the temperature is increased, some atoms are loosened and align with the magnetic field. This results in a weak magnetism in the substance.

There is a temperature analogous to Curie temperature called the Neel temperature, above which antiferromagnetic order disappears. Above the Neel temperature the substance becomes paramagnetic. Most antiferromagnetics are ionic compounds, namely, oxides, sulphides, chlorides and the like.  $\text{MnO}$ ,  $\text{Cr}_2\text{O}_3$ ,  $\text{MnS}$ ,  $\text{NiCl}_2$  etc are some examples of antiferromagnetic materials.

### **1.3.5 Ferrimagnetism**

The term 'Ferrimagnetism' was proposed by Neel in order to explain the magnetism of ferrites. Ferrimagnets are a form of antiferromagnet in which the opposing dipoles are not equal so they do not cancel out. Just like ferromagnetics, ferrimagnetic materials exhibit a substantial spontaneous magnetisation, which makes them industrially important. Ferrimagnets are good insulators, making them very useful in preventing energy losses due to eddy currents in transformers.

At a certain temperature, called the Curie point, the arrangement of the spins become random, and the spontaneous magnetisation vanishes. Above this Curie point, the substance exhibits paramagnetism. The most important ferrimagnetic substances are ferrites and the naturally occurring mineral magnetite.

## **1.4 APPLICATION OF MAGNETIC MATERIALS**

Man has used magnetic materials for thousands of years. Today they play an important role and are widely spread in daily life applications. For instance, they are found in numerous products such as home appliances, electronic products, automobiles, communication and data processing devices and equipments. These materials include metals, metal oxides, alloys, ionic compounds, ceramics and polymers.

The most important use of magnets at home is in the electric motors. All electric motors work on the principle of an electromagnet. These motors run the pumps, fans, refrigerators, vacuum cleaners, washing machines, mixers etc. Audiotape and videotape players have electromagnets called heads that record and read information on tapes covered with tiny magnetic particles. Magnets in speakers

transform the signal into a sound by making the speakers vibrate. An electromagnet called a deflection yoke in TV picture tubes helps form images on a screen<sup>10,14</sup>. Magnets are also used in certain modern switches and other electrical accessories.

An important engineering application of magnetic materials is as permanent magnets<sup>16,65</sup>. The earliest and for a long time the only; application of the permanent magnet was in the compass needle. Today the application of the permanent magnet, in industry, transportation, in the automobile, aircraft, shipbuilding, power distribution etc form a long list. The magnets used in the industry include electromagnetic powered devices such as crane, cutters, fax machines, computers etc. They are also used in electric indicators, integrating and recording meters, process variable sensors, transmitters, analysers and controllers, alarm monitoring systems in control panels and so on. In transportation, systems that use electromagnetic materials are trains, tractors, subways, trolleys, monorails, escalators, elevators, cycle dynamos etc. Scientists and engineers have developed trains that use electromagnetism to float it above the track. They use the force of a magnet to levitate the train. It eliminates friction so it has an advantage of higher speeds over ordinary trains. In the automobile, magnets are used in the magneto-ignition system, parts in wipers, horns, starters, switches, induction motors, etc. In the power sector, the major application of magnets is in the generators and transformers. Generators in power plants rely on magnets like the ones found in electric motors to produce electricity. Transformers are devices that use electromagnetism to change high voltage electricity to low voltage electricity needed in homes and industries.

The branch of magnetism finds lots of application in science and medicine. The bending magnets are very powerful magnets that help control beams of atomic particles, which are boosted into high speed devices called particle accelerators. An important application of magnetism in medicine is magnetic resonance imaging (MRI). The technique is used primarily in medical settings to produce high quality images of the inside of the human body. MRI is based on the principles of nuclear magnetic resonance (NMR), a spectroscopic technique used by scientists to obtain microscopic, chemical and physical information about molecules. The principle of

MRI is applicable in the human body because we are all filled with small biological magnets, the most abundant and responsive of which is the nucleus of the hydrogen atom, the proton. The principle of MRI takes advantage of the random distribution of protons, which possess fundamental magnetic properties. Magnetic bottles are created to hold plasmas, which is so hot they would melt any container made of ordinary material, so they hold it in a magnetic field.

Magnetic materials are used at both radio and microwave frequencies. There are numerous applications below microwave frequencies. Some of these are used as cores in inductors, flyback transformers, magnetic memories and switching devices. The memory and switching applications in digital computers and data processing circuits involves the use of microsecond pulses for transmitting, storing, and reading information expressed in a binary code. Other non-microwave applications are transformers and tuned inductors. Applications at the microwave frequencies include the use in making microwave devices such as waveguide isolators, which can transmit in one direction but attenuate in the other. It is also used in various polarization rotators, resonance isolators, modulators, phase shifters, circulators and as microwave gyrators.

Composites magnetic materials find large variety of applications because of their remarkable properties. They are used in magnetic recording media, color imaging, magnetic memories for computers, magnetic fluids, magnetic refrigeration, etc. Magnets based on rubber ferrite composites find applications in many devices because of their easy mouldability, flexibility and microwave absorbing properties.

Magnetic ceramics or ferrites are very well established groups of magnetic materials. Research activity on ferrites in the last five decades, has led to development of these magnetic materials. Magnetic ceramics participate in virtually every area of application. Even though magnetic ceramics are very well established, improvements and innovations continue to take place; many new and exciting applications, theories and preparation technologies are currently under development. Hence the study of ferrites and magnetic composites assumes significance.

## **1.5 RUBBER FERRITE COMPOSITES (RFC)**

A composite can be defined as the material created when two or more distinct components are combined<sup>66</sup>. These composite materials, which comprise two physically distinct phases – a soft material and a hard reinforcing material, enjoy the conjoint properties of both the phases. If formulated and fabricated properly, composites can offer a combination of properties and a diversity of applications unattainable with metals, ceramics, or polymers alone. Thus composites have exceptional and superior properties that surpass the performance of the individual components. There are natural (e.g. wood, teeth, bone etc.) as well as synthetic (e.g. alloys) composites. In polymers they include copolymers and blends, reinforced plastics and material such as carbon black and non-black reinforced rubber vulcanisate.

Polymer matrix composites are often termed as advanced composite materials. These are the commonly used advanced composites, which can be fashioned into a variety of shapes and sizes. They provide great strength and stiffness along with a resistance to corrosion.

Composite magnetic materials (composites with two or more phases where at least one phase is magnetic) have the advantage that their physical properties can be modified so as to tailor materials for various applications.

In magnetic polymer composites, both the magnetic filler and the polymer matrix chosen affect processability and physical properties of the final product. Hence the proper selection of fillers and the matrix is very important to tailor make composites for various applications. The polymer must have appropriate physical properties and reasonable stability. Also factors like percolation limits and nature of the matrix namely saturation/ unsaturation / polarity of the rubber all influences the final properties of the composites. The macroscopic parameters of the composites like modulus and tensile strength would be influenced by the interaction between the filler and the matrix. The role of fillers in modifying the properties of the composites is to be understood properly for developing RFCs with the required properties for various applications. Thus a systematic study of these composites would be very useful to design materials for specific applications.



Flexible rubber magnets and plastic magnets are usually made by mixing ferrite with an appropriate polymer using suitable compounding ingredients according to specific recipe<sup>9,67,68</sup>. Flexible magnets with appropriate magnetic properties can be made by a judicious choice of magnetic fillers. The impregnation of magnetic filler into the matrix not only imparts the magnetic properties but also modifies the dielectric properties of the composites.

The incorporation of ferrite powders in natural or synthetic rubbers produce flexible ferrites or rubber ferrite composites<sup>10,69-71</sup>, which has many novel applications as magnets. For instance, the resistance to mutual demagnetisation is as good as that of sintered isotropic ferrite, and the brittleness is replaced by flexibility. Compared with alloy magnets the holding power is low, but it is sufficient for many purposes, where cheapness and adaptability are more important. Rubber ferrite composites (RFCs) can be synthesised by the incorporation of ferrite powders in natural or synthetic rubber matrixes. Both the soft and hard ferrites can be embedded in the polymer matrix. Soft ferrites like nickel-zinc ferrite, manganese-zinc ferrite have been incorporated in the polymer matrixes (both natural and synthetic) to produce RFCs<sup>72</sup>. The incorporation of hard ferrites in the elastomer matrix can not only bring economy but also produce flexible permanent magnets which find extensive applications<sup>73,74</sup>.

Rubber Ferrite Composites have enormous application potential in electrical and electronic industries in different forms. These involve the use in magnetic memories for computers, magnetic fluids, magnetic refrigeration, magnetostrictive transducers, color imaging and in many applications that can be achieved by ceramic materials. The rubber ferrite composites are useful as microwave absorbing materials due to its dielectric properties and design flexibility. Some of these materials are used as electromagnetic wave absorbers in the VHF and UHF bands<sup>75,76</sup>. Thus they find applications in the microwave and radar technology applications.

The addition of carbon black is known to reinforce the matrixes; moreover, earlier studies have indicated that the addition of fillers like carbon black on rubber ferrite composites enhances the microwave absorbing properties of the composites<sup>77-81</sup>. Therefore, studies pertaining to the incorporation of carbon black along with magnetic fillers in elastomer matrixes are interesting and assume significance.

## **1.6 PRESENT STUDY**

Composites can offer a combination of properties and a diversity of applications unobtainable with the individual components. This is exploited in the preparation of rubber ferrite composites. Here the useful properties of the polymer matrix and the ferrite filler are advantageously used for the production of RFCs. The matrix and the filler are chosen to obtain the optimum properties for specific applications. The magnetic polymer composites have the advantage that their physical properties can be modified so as to tailor make materials for various applications.

In the present study the hexagonal hard ferrite, namely barium ferrite,  $\text{BaFe}_{12}\text{O}_{19}$  (BaF) and strontium ferrite,  $\text{SrFe}_{12}\text{O}_{19}$  (SrF) have been prepared by the conventional ceramic techniques and characterised by XRD. These pre-characterised magnetic filler are then incorporated into two different matrixes, namely natural rubber (NR) and nitrile rubber (NBR) separately. The incorporation is carried out according to a specific recipe and for various loadings of ferrite filler and N330 (HAF) carbon black. The hard ferrites are selected, to produce flexible permanent magnets. Possible value addition to the abundantly available natural resource, natural rubber is also aimed at by undertaking this study. The nitrile rubber is chosen considering its superior and special purpose applications. The structural, magnetic, mechanical and electrical characterisation of these ceramic filler as well RFC have been carried out and the results are correlated.

The main objectives of the present work can be summarised as follows:

- Preparation of barium ferrite and strontium ferrite using ceramic technique.
- Characterisation of the prepared ferrites using X-ray diffraction technique (XRD).
- The incorporation of these ferrites into elastomer matrix to produce rubber ferrite composites (RFC).
- Evaluation of the processability and mechanical properties of the RFCs.

- **Analysis of the dielectric properties of the ceramic BaF and SrF and RFCs at various frequencies and temperatures**
- **Magnetic characterisation of the prepared ferrite and RFCs using Vibration Sample Magnetometer (VSM)**
- **Study the effect of loading of ferrite fillers on processing, mechanical, dielectric and magnetic properties of RFCs.**
- **Study the effect of carbon black on the processing, mechanical, dielectric and magnetic properties of RFCs.**
- **Correlation of properties.**

**REFERENCES**

1. Muller K.H, G. Krabbes, J. Fink, S. Grub. A. Kirchner, G. Fuchs, L. Schultz, J. Magn. Magn. Mater, **226-230** (2001) 1370-1376.
2. Maurice Morton, 'Rubber Technology', 3<sup>rd</sup> edition, 1995, Van Nostrand Reinhold Company, New York.
3. Fred W Billmeyer Jr, 'Textbook of Polymer Science', 4<sup>th</sup> edition, 1994, John Wiley & Sons, Inc., New York.
4. Brydson J. A, 'Plastic Materials', 5<sup>th</sup> edition, 1989, Butterworth Scientific, London.
5. Werner Hofmann, 'Rubber Technology Handbook', 1989, Hanser Publishers, Munich Vienna, New York.
6. Colin W. Evans, 'Developments in Rubber and Rubber Composites – 2', 1983, Applied Science Publishers Ltd, London and New York.
7. Penn W. S, 'Synthetic Rubber Technology', Vol-1, 1960, Staples Printers Limited.
8. "Doug" DeMaw. M. F, 'Ferromagnetic-Core Design and Application Handbook', 1981, Prentice-Hall, Englewood Cliffs, New Jersey.
9. John Delmonte, 'Metal-Filled Plastics', Reinhold Publishing Corporation, New York.
10. Snelling. E.C and A.D. Giles, 'Ferrites for Inductors and Transformers', Research Studies press Ltd, John Wiley & Sons Inc. New York.
11. Alex Goldman, 'Modern Ferrite Technology', 1990, Ferrite Technology worldwide, Inc., Published by Van Nostrand Reinhold, 115 Fifth Avenue, New York.
12. Krishnamurty. N and Ashok Kumar Suri, 'Rare Earths and Their Role in Modern Life', 2001, Published by Indian Association for Radiation Protection, BARC, Trombay, Mumbai.
13. Smit. J and H.P.J. Wijn, 'Ferrites', 1959, Philips Technical library.
14. Snoek, J.L. 'New Developments in Ferromagnetic Materials', 1947, Elsevier Publishing Company, Inc., New York-Amsterdam.
15. Cullity B.D, 'Introduction to Magnetic Materials', 1972, Addison- Wesley Publishing Company, Inc., Philippines.

16. Soshin Chikazumi and Stanley H. Charap: 'Physics of Magnetism', 3<sup>rd</sup> Edn, 1964, John Wiley & Sons, Inc., New York.
17. Murthy V.R.K and B. Viswanathan, 'Ferrite Materials', 1990, Science and Technology, Narosa Publishing House.
18. Cullity. B.D, 'Elements of X-ray diffraction', 2<sup>nd</sup> Edn, 1978, Addison-Wesley Publishing Company, Inc., Philippines.
19. Hadfield D, 'Permanent Magnets and Magnetism', 1962, John Wiley and sons, Inc., London.
20. Hiroaki Nishio, Hitoshi Taguchi, Fumihiko Hirata and Taku Takeishi, IEEE, Trans. Magn, 29, 6 (1993).
21. Xinyong Li, Gongxuan Lu, Shuben Li, J. Mater. Sci. Lett., 15 (1996) 397-399.
22. Wartewig P, K. Melzer, M. Krause and R. Tellgren, J. Magn. Magn. Mater., 140-144 (1995) 2101-2102.
23. Wang J. F, C. B. Ponton and I. R. Harris, J. Magn. Magn. Mater., 234 (2001) 233-240.
24. Benito. G, M. P. Morales, J. Reequena, V. Raposo, M. Vazquez, and J. S. Moya, J. Magn. Magn. Mater., 234 (2001) 65-72.
25. B. V. Bhise, M.B. Dangare, S.A. Patil, S.R. Sawant, J. Mater. Sci. Lett. 10 (1991) 922.
26. Sawadh. P. S, and Kulkarni. D.K, Materials Chemistry and physics, 63 (2000) 170-173.
27. Ahmed. M. A, Phys. Stat. Sol. A 111 (1989) 567.
28. Valenzuela R, 'Magnetic Ceramics', 1994, Cambridge, Cambridge University Press.
29. Haneda. K, and Kojima. H, J. Amer. Ceram. Soc., 57 (1974) 68.
30. Sung-Soo Kim and Dae-Hee Han, IEEE Trans. Magn., 30, 6 (1994).
31. Daniels. J.M and Rosencwaig, Can.J.Phys. 48 (1970) 381.
32. Leung. L.K, Evans. B.J, and Morrish. A.H, phys. Rev. B 8 (1973) 29.
33. Patil. A.N, Patil. M.G, Patankar. K.K, Mathe. V.L, Mahajan. R.P and Patil. S. A, Bull. Mater. Sci., 23, 5 (2000) 447-452.
34. Murthy. S.R, Bull. Mater. Sci., 24, 4 (2001) 379-383.

35. Mitsuo Sugimoto, *J. Amer. Cer. Soc.*, Sugimoto, **82**, 2 (1999) 269- 280.
36. Ronald F. Soohoo, 'Theory and Applications of Ferrites', 1960, Engle wood Cliffs, Prentice-Hall, Inc., New Jersey.
37. Kato, V. and Takei. T, 'Permanent oxide magnet and its characteristics', *J. Instn. Elect. Engrs, Japan*, **53** (1933) 408.
38. Kawai. N, 'Formation of a solid solution between some ferrites', *J. Soc. Chem. Ind. Japan*, **37** (1934) 392.
39. Snoek. J. L, 'Magnetic and electrical properties of the binary systems  $MO.Fe_2O_3$ ', **3** (1936) 363, *Physica*, Amsterdam.
40. Owens. C.D, 'A survey of the properties and applications of ferrites below microwave frequencies', *Proc. Inst. Radio. Engrs.*, **44** (1956) 1234-1248.
41. Snelling. E. C, 'Ferrites for linear applications', Part 1, Properties. *IEEE Spectrum*. **9**, 1 (1972) 46-47.
42. Watanabe. H, Iida. S and Sugimoto, 'Ferrites', *Proceedings of ICF3* (1981) M. Centre for Academic Publications, Japan.
43. Thomas. G, 'Advances in ferrites', Vol.1 *ibid.*197 (1989).
44. Papiian W.N, *Proc. I.R.E.*, (1952) 475.
45. Benjamin Lax, Kenneth J Button, 'Microwave Ferrites and Ferrimagnetics', 1962, Mc Graw-Hill Book Co.
46. Bate and Alstad, *IEEE Trans. Magn.*, **5** (1969) 823-839.
47. Iimura, Tsutomu, (*Magn.Electron.Mater.Res.Lab; Hitachi Met.Ltd.*, Kumagaya, Japan 360), *Zairyo Kagaku*, **27**, 3 (1990) 179-187.
48. Shin. J. Y and J. H. Oh, *IEEE Trans. Magn.*, **29**, 6 (1993) 3437-3439.
49. Nelson C.E, "Ferrite-Tunable Microwave Cavities and the Introduction of a New Reflectionless, Tunable Microwave Filter," *proc. I.R.E.*, **44** (1956) 1449.
50. Angelakos D.J and M.M. Korman, "Radiation from Ferrite-Filled Apertures", *Proc. I.R.E.* (1956) 1463.
51. Tyras G and G. Held, "Radiation from a Rectangular waveguide Filled with Ferrite", *Trans. I.R.E. on Microwave Theory and Techniques*, *MTT-6*, **3** (1958) 268.

52. Barten, P.G.J. and Kaashoek, J. IEEE Trans. Consum. electron., CE-24, 3 (1978) 481-488.
53. van den Broek, C.A.M. and Stuijts, A.L. Ferroxdure. Philips Tech. Rev., 37, 7 (1977) 157-175.
54. Braun P. B, 'The crystal structures of a new group of ferromagnetic compounds', Philips Res. Repts., 12 (1957) 491-545.
55. Jan Smit, 'Magnetic Properties of Material', 13, 29 (1971) Inter University Electronics series, McGraw-Hill Company.
56. Aminoff G, Geol. Foren. Stockholm, Forth, 47 (1925) 283.
57. Adelsköd V, Arkiv Kemi. Mineral. Geol., 12A (1938) 1-9.
58. Standley K. J, 'Oxide Magnetic Materials', 2<sup>nd</sup> edition, 36 (1972) Clarendon Press, Oxford.
59. Craik D. J and R. S. Tebble, 'Ferromagnetism and Ferromagnetic Domains', 1965, North-Holland Publishing Company, Amsterdam.
60. Daniel C. Mattis, The theory of Magnetism, 1965, Harper and Row Publishers New York.
61. Crangle. J, The Magnetic Properties of Solids, 1977, Edward Arnold Publishers Ltd.
62. Keer H.V, Principles of solid state physics, 1993, Willey Eastern Ltd., New Delhi.
63. Ami E. Berkowitz and Eckart Kneller, Magnetism and Metallurgy, 1969, Academic Press Inc.
64. Brailsford. F, Physical principles of magnetism, 1966, D Van Nostrand Co. Ltd.
65. Holzbock. W. G, 'Instruments for measurements and control' 2<sup>nd</sup> edition, 1962, Van Nostrand Reinhold Company, New York.
66. Encyclopedia of Polymer Science and Engineering, Vol.3.
67. Katz H. S and J. V. Milewski, 'Handbook of Reinforcement of Plastics', 1978, Vannostrand Reinhold, New York.
68. Jozef Slama, Anna Gruskova, L'udovit Keszegh, Mojmir Kollar, IEEE Trans. Magn., 30, 2 (1994) 1101-1103.

69. Safari Ardi M, Dick W and McQueen D.H, *Plastic Rubber and Composites Processing Applications*, **24** (1995) 157-164.
70. Anantharaman M.R, S. Jagatheesan, S. Sindhu, K.A. Malini, C. N. Chinnasamy, A. Narayansamy, P. Kurian and K. Vasudevan, *Plastic Rubber and Composites Processing Applications*, **27**, 2 (1998) 77-81.
71. Anantharaman M.R, S. Sindhu, S. Jagatheesan, K.A. Malini and Philip Kurian, *Journal of Physics D Applied Physics* **32** (1999) 1801-1810.
72. Anantharaman. M.R, K.A.Malini, S.Sindhu, E.M. Mohammed, S.K. Date, P.A.Joy and Philip Kurian, *Bull. Mater. Sci.*, **24**, 6, (2001) 623-631.
73. Praveen Singh & T.C. Goel, *Indian J. Pure and Appl Phys.*, **38** (2000) 213-219.
74. Anantharaman M. R, P. Kurian, B. Banerjee, E. M. Mohammed, and M. George, *Kautschuk Gummi Kunststoffe, Germany*, **6**, 49 (1996) 424- 426.
75. Grunberger W, B. Springmann, M. Brusberg, M. Schmidt and R. Jahnke, *J. Magn. Mater.*, **101** (1991) 173-174.
76. Naito Y and K. Suetake, *IEEE Trans. Micro Wave Theory and Tech.*, MTT-19, 1 (1971) 65-72.
77. Mirtaheri S.A, J.Yin, H. Seki, T. Mizumoto and Y.Naito, *Trans. IEICE*, **72**, 12 (1989) 1447-1452.
78. Dishovski N, A.Petkov, Iv. Nedkov and Iv.Razkazov: *IEEE Trans Magn.*, **30**, 2 (1994) 969-970.
79. Ganchev S.I, J. Bhattacharyya, S. Bakhtiari, N. Quaddoumi, D. Brabdenburg and R.Zoughi, *IEEE Trans. Microwave Theory and Tech.*, **42**, 1 (1994) 18-24.
80. Kim S.S, S.B.Jo, K.I.Gueon, K.K.Choi, J.M.Kim and K.S.Churn: *IEEE Trans. Magn.*, **27**, 6 (1991) 5462-5464.
81. Kwon H.J, J.Y. Shin and J.H.Oh: *J. Appl. Phys.*, **75**, 10 (1994) 6109-6111.



# Chapter 2

---

## EXPERIMENTAL TECHNIQUES

The materials used and the experimental procedures adopted in the present investigations are given in this chapter.

### 2.1. MATERIALS USED

#### 2.1.1 Elastomers

##### 2.1.1.1 Natural Rubber (NR)

ISNR –5 used in this study was supplied by the Rubber Research Institute of India, Rubber Board, Kottayam. The Bureau of Indian Standard (BIS) specifications for this grade of natural rubber are given below.

Dirt content, % by mass (max.)	0.05
Volatile matter, % by mass (max.)	0.80
Nitrogen, % by mass (max.)	0.60
Ash content, % by mass (max.)	0.60
Initial plasticity, P <sub>0</sub> (min.)	30.00
Plasticity retention Index (PRI) (min.)	60.00

### **2.1.1.2 Acrylonitrile - butadiene rubber (Nitrile Rubber) (NBR)**

Nitrile rubber used in this study was Aparene- N 553 manufactured by Apar Polymers Ltd, Gujarat, India. It had the following specifications

Acrylo nitrile content (% by weight)	34
Mooney Viscosity, ML (1+4) at 100°C	50

### **2.1.2 Compounding ingredients**

#### **2.1.2.1 Zinc oxide**

M/S. Meta Zinc Ltd., Bombay, supplied zinc oxide for the study. It had the following specifications:

Specific gravity	5.5
Zinc oxide content, (% by mass)	98
Loss on heating (2hrs at 100°C), (%)	0.5

#### **2.1.2.2 Stearic acid**

Stearic acid used for the study, supplied by Godrej Soaps (Pvt.) Ltd., Bombay, having the following specifications:

Melting point, (°C)	65
Acid number	200
Specific gravity	0.8
Ash content, % by mass (max.)	0.1

#### **2.1.2.3 Sulphur**

Standard Chemical Company, Madras, supplied Sulphur. It had the following specifications:

Specific gravity	2.05
Ash content, % by mass (max.)	0.10
Solubility in CS <sub>2</sub> , (%)	98

#### **2.1.2.4 Fillers**

##### **2.1.2.4.1 Carbon black**

High abrasion furnace black (HAF N-330) used in these experiments was supplied by M/S. Philips Carbon Ltd., Cochin and had the following specification.

Appearance	Black granules
DBP absorption, (cc/ 100 g)	102 ± 5
Pour density, (g/cc)	0.39
Iodine number	82
Loss on heating/hr (max) at 125°C, (%)	2.5

##### **2.1.2.4.2 Barium Ferrite**

Barium ferrite (BaF) prepared by the ceramic technique was used for the preparation of RFCs.

##### **2.1.2.4.3 Strontium Ferrite**

Strontium ferrite (SrF) used for the preparation of RFCs was prepared by the ceramic technique

#### **2.1.2.5 Accelerator**

##### **2.1.2.5.1 N – Cylohexyl Benzthiazyl Sulphenamide (CBS)**

The sample had the following specifications:

Ash content, % by mass (max.)	0.5
Moisture % by mass (max.)	0.5
Specific gravity	1.27

#### **2.1.2.6 Plasticisers**

##### **2.1.2.6.1 Aromatic oil**

Aromatic oil supplied by Hindustan Organic Chemicals having the following specifications was used for the study.

Aniline point, (C)	43
Ash content, % by mass (max.)	0.01
Viscosity gravity constant	0.96
Specific gravity	0.98

#### **2.1.2.6.2 Diocetyl phthalate (DOP)**

The dioctyl phthalate used was supplied by Rubo Synthetic Impex Ltd., Bombay and had the following specifications.

Specific gravity	0.98
Viscosity (cps)	60

#### **2.1.2.7 Antioxidant (Vulkanox SP)**

Commercial phenolic type of antioxidant, Vulkanox SP was supplied by Bayer India Ltd.

### **2.1.3 Other reagents used**

#### **2.1.3.1 Barium Carbonate**

Barium carbonate (Analytical Reagent grade) used for the preparation of barium ferrite was supplied by Qualigens Fine Chemicals, a Division of Glaxo India Limited, Dr. Annie Besant Road, Mumbai 400 025. It had the following specifications.

Molecular Weight	197.35
Assay (acidimetric), (%)	99

#### **2.1.3.2 Strontium Carbonate**

Qualigens Fine Chemicals supplied strontium carbonate (AR grade) used for the preparation of strontium ferrite. It had the following specifications.

Molecular Weight	147.63
Minimum assay (acidimetric), (%)	99

### **2.1.3.3 Ferrous Sulphate**

Qualigens Fine Chemicals supplied ferrous sulphate (AR grade) used for the preparation of barium and strontium ferrite. It had the following specifications.

Molecular Weight	278.02
Minimum Assay (by $\text{KmnO}_4$ ), (%)	98

### **2.1.3.4 Oxalic acid**

Oxalic acid used for the preparation of ferrous oxalate dihydrate was supplied by Qualigens Fine Chemicals. It had the following specifications.

Molecular Weight	126.07
Assay (acidimetric), (%)	99.5

### **2.1.3.5 Sulphuric acid**

AR grade sulphuric acid used for the preparations was supplied by Qualigens Fine Chemicals. It had the following specifications.

Molecular Weight	98.08
Assay (acidimetric), (%)	97-99
Wt. Per ml at 20°C, (g)	1.835

## **2.1.4 Solvents**

### **2.1.4.1 Acetone**

Acetone (AR grade) used for the preparations was supplied by Qualigens Fine Chemicals. It had the following specifications.

Minimum assay by GLC, (%)	99.5
Wt. Per ml at 20°C, (g)	0.789-0.791
Refractive index	1.35-1.36

## 2.2 EXPERIMENTAL METHODS

The conventional method for preparing ferrites is the ceramic technique<sup>1-16</sup>, which involve the firing of mixtures of iron oxide and the oxides of the corresponding metal at high temperature. Several other procedures have been employed to prepare the ferrite samples, including chemical co precipitation<sup>17-19</sup>, glass crystallization<sup>20-22</sup>, combustion method<sup>23,24</sup>, organometallic precursor method<sup>25</sup>, the pyrosol method<sup>26</sup>, ball milling<sup>27-29</sup>, hydrothermal synthesis<sup>30,31</sup>, sol-gel<sup>32-41</sup>, aerosol synthesis<sup>42,43</sup>, colloidal synthesis<sup>44</sup>, cryochemical method<sup>45</sup>, microemulsion<sup>46</sup>, liquid mix technique<sup>47,48</sup>, lyophilization (freeze-drying) and coprecipitation<sup>49</sup>, ion-exchange resin method<sup>50</sup> etc. Some of these methods have the advantages such as to reduce the particle size and low temperature preparation. But in general all these methods are more complex and more expensive than the ceramic method. In the present work, the ceramic technique was adopted because it provides a comparatively easier route for the bulk preparation of both barium and strontium ferrites.

### 2.2.1 Ceramic Technique

Ceramic technique was employed to synthesise the barium and strontium ferrites having the general formula  $MO_6Fe_2O_3$  Where M stands for barium or strontium. Ferrous oxalate dihydrate precursors were utilised for the synthesis of these ferrites. Ferrous oxalate dihydrate (FOD) was first prepared by the coprecipitation technique. Analytical grade ferrous sulphate and oxalic acid were utilised for this purpose. Appropriate amounts of the chemicals were weighed and aqueous solutions of ferrous sulphate and oxalic acid were made using distilled water. One or two drops of sulphuric acid were added in order to prevent the oxidation of ferrous sulphate before making the solution. Ferrous sulphate solution was heated to 60°C. Preheated oxalic acid (60°C) was added drop by drop to this solution with the help of a separating funnel aided by constant stirring. When the reaction was over, the solution was filtered and the precipitate washed with boiling water. This was repeated to remove the excess of oxalic acid, if any, present in the solution. The precipitate was then dried in a hot air oven at 100°C. Fine yellow coloured particles of FOD were obtained. AR grade of barium carbonate and

strontium carbonate were the other precursor materials employed for the preparation of barium ferrite and strontium ferrite.

Pure  $\alpha$ - $\text{Fe}_2\text{O}_3$ , prepared by the decomposition of the freshly prepared ferrous oxalate dihydrate was mixed with appropriate amounts of the AR grade barium carbonate and strontium carbonate. A slurry was made by using AR grade acetone in an agate mortar. They were homogenised thoroughly by mixing for a long time and pre-sintered at  $500^\circ\text{C}$  for three hours in a furnace under ambient atmosphere. The homogenisation and pre-sintering were carried out three time. The pre-sintered powder sample of the BaF and SrF was then pressed in a hydraulic press into cylindrical pellets by using a mould of die steel having a diameter of 12 mm. The final sintering of the powder sample and the pellet in the furnace was carried out at  $1200^\circ\text{C}$  for 24 hours. They were then cooled under ambient conditions and these powders and pellets were used for further characterisation and studies. The properties of the final product depend on the sintering temperature, time, cooling rate and environment.

### 2.2.2 Structural Evaluation of Barium/Strontium Ferrite by X-Ray Powder Diffraction

The X-ray powder diffraction technique was used to evaluate the various structural parameters namely relative intensity ' $I/I_0$ ', inter atomic spacing ' $d$ ', and lattice parameter ' $a$ '. The identification of the phase was also conducted by using X-ray diffraction. The powder diffractograms of the samples were recorded by employing Rigaku D Max -C, X-ray powder diffractometer using  $\text{Cu K}_\alpha$  radiation of wavelength ( $\lambda$ )  $1.54098 \text{ \AA}$ . From the XRD spectrum obtained ' $I/I_0$ ', ' $2\theta$ ' and ' $\beta$ ' values corresponding to each peaks were noted and the different parameters were calculated by using the following relations. Inter atomic spacing was calculated by utilising the relation<sup>51-53</sup>

$$d = \frac{\lambda}{2 \sin \theta} \quad (2.1)$$

where ' $\lambda$ ' is the wavelength of the X-ray radiation used.

The particle size was calculated from the XRD data by using Scherer formula, which is given by

$$D = \frac{0.9 \lambda}{\beta \cos\theta} \quad (2.2)$$

where 'β' is the full width half maximum of the intensity.

Surface area of the ceramic samples can be calculated by using the empirical relation

$$S = \frac{6000}{D\rho} \text{ m}^2/\text{g} \quad (2.3)$$

where 'D' is particle size in nm and 'ρ' is the density of the sample in g/cm<sup>3</sup> <sup>54</sup>.

### 2.2.3 Mixing and processability study of the compounds using Brabender Plasticorder

Brabender plasticorder has been widely used for measuring processability of polymer. This torque rheometer is essentially a device for measuring the torque generated due to the resistance of a material to mastication or flow under preselected conditions of shear and temperature. The heart of the torque rheometer is a jacketed mixing chamber whose volume is approximately 40 cc for the model used (PL 3S). Mixing and shearing of the material in the mixing chamber is done by horizontal rotors with protrusions. The resistance put up by the test material against rotating rotors in the mixing chamber is indicated with the help of a dynamometer balance. The dynamometer is attached to a mechanical measuring system, which records the torque. A dc thyristor controlled drive is used for speed control of the rotors (0 to 150 rpm). The temperature can be varied up to 300°C. A thermocouple with a recorder is used for temperature measurements. Different types of rotors can be employed depending upon the nature of the polymer used. The rotors can be easily mounted using the simple fastening and coupling system. The rubber was charged into the mixing chamber after setting the test conditions. When the nerve of the rubber had disappeared, the compounding ingredients were added as per sequence given in ASTM D 3182 (1982). The final torque displayed on the dial gauge was noted. The compound was discharged after completion of the mixing. Mixing time and temperature were controlled during the process. The homogenisation of the compound was carried out using a two roll mill.



### 2.2.4 Homogenisation of the rubber compounds

The mixing of rubber with the compounding ingredient was done in a Brabender Plasticorder and the homogenisation of the compound was carried out on a laboratory (15x33 cm) two roll mill at a friction ratio of 1:1.25. The temperature of the rolls was maintained at  $60\pm 5^\circ\text{C}$  and the compound was homogenised by passing six times endwise through a tight nip and finally sheeted out at nip gap of 3 mm.

### 2.2.5 Determination of cure characteristics

The cure characteristics of the mixes were determined using a Goettfert elastograph model 67.85. It is a microprocessor controlled rotorless cure meter with a quick temperature control mechanism and well defined homogeneous temperature distribution in the test chamber. It uses two directly heated, opposed biconical dies that are designed to achieve a constant shear gradient over the entire sample chamber. In this instrument, a circular shaped test specimen is kept in the lower half of the cavity, which is oscillated through a small deformation angle ( $\pm 0.2^\circ$ ). The frequency of oscillations is 50 cycles/minute. The torque transducer on the upper die senses the force being transmitted through the rubber sample. The following data can be obtained from a typical elastograph cure curve as shown in figure 2.1.

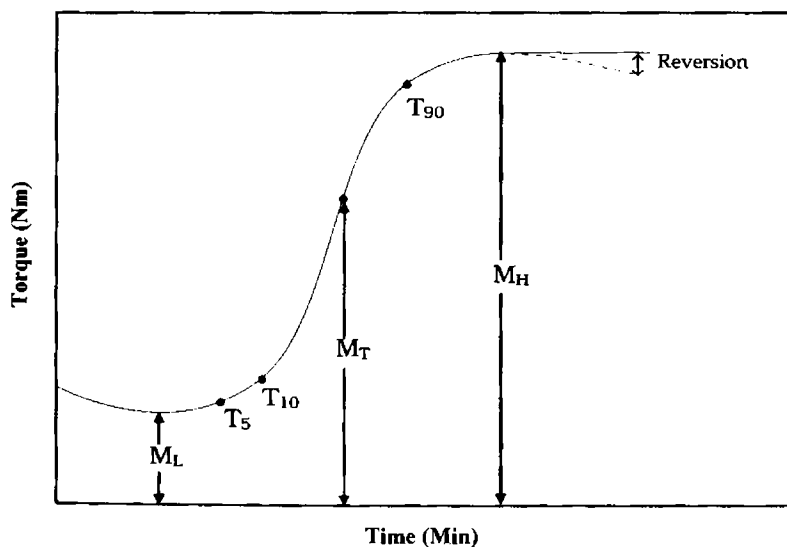


Fig 2.1 A typical cure curve obtained from the elastograph

- (i) Minimum torque,  $M_L$   
Torque obtained by mix after homogenising at the test temperature and before the onset of cure.
- (ii) Maximum torque,  $M_H$   
Maximum torque recorded at the completion of cure.
- (iii) Torque,  $M_T$   
Torque at any given time T
- (iv) Optimum Cure time,  $T_{90}$   
This is the time taken for obtaining 90% of the maximum torque
- (v) Scorch time,  $T_{10}$   
It is the time taken for two unit rise (0.02 Nm) above minimum torque (i.e. about 10% vulcanization).
- (vi) Induction time,  $T_5$   
It is the time taken for one unit rise above minimum torque (i.e. about 5 % vulcanization).
- (vii) Cure rate index  
Cure rate index is calculated from the following equation.  
Cure rate index =  $100 / T_{90} - T_{10}$   
Where,  $T_{90}$  and  $T_{10}$  are the times corresponding to the optimum cure and scorch respectively.

The elastograph microprocessor evaluates the vulcanisation curve and prints out the data after each measurement.

### 2.2.6 Moulding of Test Specimens

The test specimens for determining the physical properties are prepared in standard moulds by compression moulding on an electrically heated press having 45 × 45 cm platens at a pressure of 140 Kg cm<sup>-2</sup> on the mould. The rubber

compounds are vulcanised up to their respective optimum cure time at 150°C. Mouldings are cooled quickly in water at the end of the curing cycle and stored in a cool and dark place for 24 hours and are used for subsequent physical tests. For samples having thickness more than 6 mm (abrasion resistance, compression set etc.) additional curing time based on the sample thickness is given to obtain satisfactory moulding.

## **2.3 PHYSICAL TEST METHODS**

### **2.3.1 Stress Strain Properties**

Tensile properties of the vulcanisate are determined as per ASTM D 412 (1980) using dumb-bell specimens on an Instron Universal Testing Machine, Model 4411 Test System. All tests are carried out at 28±2°C. Dumbbell specimens for the tests are punched out from the compression moulded sheets along the mill grain direction using a standard die. The thickness of the narrow portion is measured by bench thickness gauge. The sample is held between the two grips on the UTM, the upper grip of which is fixed. The rate of separation of the power actuated lower grip is fixed at 500 mm/min. The tensile strength, elongation at break and modulus at different elongations are recorded and evaluated after each measurement by the microprocessor.

### **2.3.2 Abrasion resistance**

The abrasion resistance of the samples is determined using a DIN abrader (DIN 53516). Cylindrical samples of 15 mm diameter and 20 mm length is kept on a rotating sample holder and 10 N load was applied. Initially a pre run is given for the sample and its weight taken. The weight after the final run is also noted. The difference in weight is the weight loss on abrasion. It is expressed as the volume of the test piece abraded by its travel through 42 m on a standard abrasive surface. The volume loss on abrasion was calculated as follows:

$$V = \Delta M / \rho$$

Where V = volume loss,  $\Delta M$  = mass loss, and  $\rho$  = density of the sample.

Abrasion resistance is the reciprocal of volume loss on abrasion.

### **2.3.3 Hardness**

Hardness is defined as the resistance of a material to deformation, particularly permanent deformation, indentation or scratching. Durometer hardness tester is used for measuring the relative hardness of soft materials. It is based on the penetration of specified indenter forced into the material under specified conditions. It consists of a pressure foot, an indenter and a dial gauge. The indenter is spring loaded and the point of the indenter protrudes through the opening in the base. There are several instruments used to measure the hardness of soft sponge up to ebonite type material. The most commonly used are Durometers Type A and Type D. The basic difference between the two types is the shape and dimension of the indenter. The hardness numbers derived from either scale are just numbers without any units. Type A Durometer is used for measuring the hardness of relatively soft materials and Type D Durometer is used for measuring the hardness of harder material. The hardness measured using Type A Durometer is expressed in a unit called 'Shore A' and that measured using Type D is called 'Shore D'. On shore A scale 0 would be soft and 100 hard<sup>54-58</sup>.

The hardness (Shore A) of the moulded samples were tested by using Zwick 3114 hardness tester in accordance with ASTM D 2240 – 86. The tests were carried out on a mechanically unstressed sample of 12 mm diameter and minimum 6 mm thickness. The test is conducted by first placing the specimen on a hard, flat surface and the pressure foot of the instrument is pressed onto the specimen. A load of 12.5N was applied and after ensuring firm contact with the specimen, the readings were taken after 10 seconds of indentation.

## **2.4 ELECTRICAL CHARACTERISATION**

### **2.4.1 Dielectric Constant**

The investigation of the dielectric properties helps us in understanding the nature and structure of the materials. An accurate measurement of these properties will provide valuable information about the electrical behaviour of the materials and its usefulness for various applications. This helps to improve the design and quality of the existing devices. Hence an exact knowledge of the dielectric

properties of a material is a prerequisite for many technological applications. Information on dielectric properties is also very useful for improving the microwave absorbing properties of the ferrites. The most important among the dielectric properties is the dielectric constant or permittivity. The permittivity is defined as the ratio of the field strength in vacuum to that in the material for same distribution of charges. Dielectric constant is dependent on parameters like frequency, temperature, orientation, composition, pressure and molecular structure of the material. Applications in the microwave processing of food, rubber, plastics and ceramics would benefit from the knowledge of dielectric properties.

An electrical conductor charged with a quantity of electricity  $q$  at a potential  $V$  is said to have a capacity  $C=q/V$ . The capacity of a simple parallel plate capacitor is given by

$$C = \frac{\epsilon A}{d} \quad (2.4)$$

where  $A$  is the area of the parallel plates,  $d$  is the separation between the plates and  $\epsilon$  is the ratio of dielectric constant of the medium between the plates to that of free space.

This equation is exploited in evaluating the dielectric constant of the ceramic barium and strontium ferrites and rubber ferrite composites containing BaF/SrF in natural and nitrile rubber.

The dielectric properties of the ceramic samples and the RFCs were studied using a dielectric cell and an impedance analyser (Model: HP 4285A) in the frequency range 100KHz to 8 MHz. A dielectric cell was fabricated for this purpose. Figure 2.2 shows a schematic diagram of the fabricated dielectric cell.

BaF and SrF samples, prepared by ceramic technique were made in the form of pellets having diameter of 12mm diameter. These were then loaded onto the spring loaded sample holder assembly. The capacitance values at different frequencies ranging from 100 KHz to 8 MHz were noted. The dielectric constant was calculated using the formula

$$C = \frac{\epsilon_0 \cdot \epsilon_r \cdot A}{d} \quad (2.5)$$

where  $A$  is the area of the sample pieces used and  $d$  their thickness.  $\epsilon_0$  and  $\epsilon_r$  are the dielectric constant of air and the sample respectively and  $C$  is the capacitance value.

The dielectric constants were evaluated for RFCs containing different loadings of the BaF and SrF, both with and without carbon black in NR and NBR matrix. For this disc shaped samples having diameter 12 mm were punched out from the rubber sheet. The dielectric cell is provided with provisions for heating and the measurements were carried out from 303K to 393K for all samples.

Dielectric phenomenon arises from the interactions of the electric field with different charged species such as electrons, protons, ions and also the electron shells and nuclei which constitute the dielectric material. In any dielectric material there will be some power loss because of the work done to overcome the frictional damping forces encountered by the dipoles during their rotations.

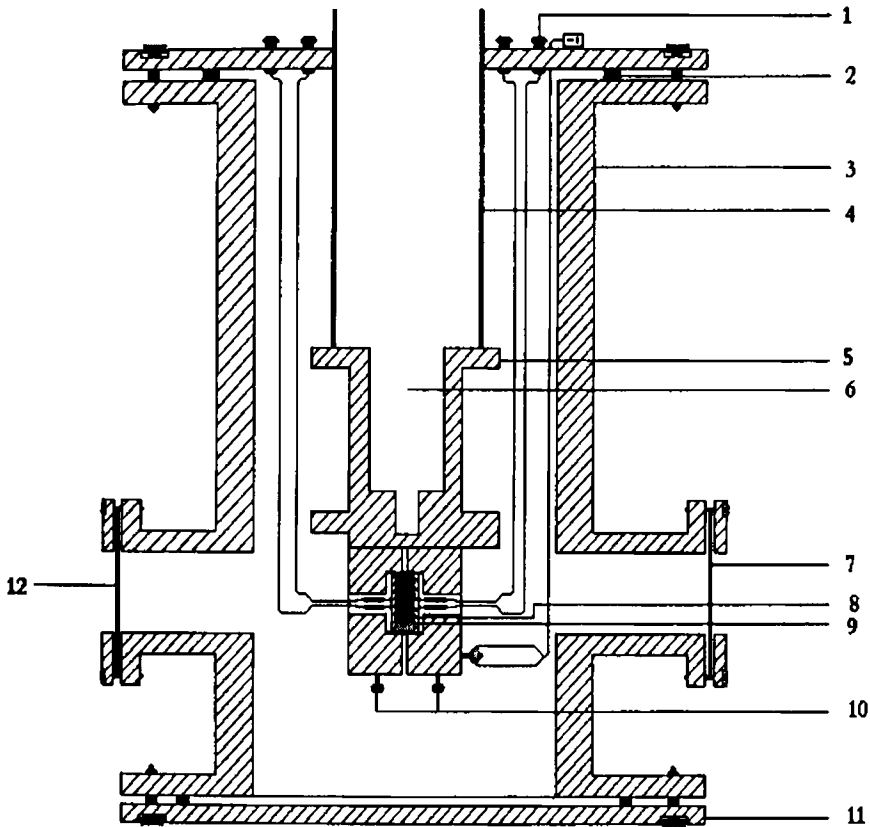
When an ac sinusoidal voltage source is placed across the capacitor, the resulting current will be made of a charging current and a loss current that is related to the dielectric permittivity. Here we have considered only in the relative permittivity ( $\epsilon_r$ ) of the material and the loss ( $\tan \delta$ ). Permittivity describes the interaction of a material with an electric field. The relative permittivity is given by  $\epsilon_r = \epsilon / \epsilon_0$ . The complex relative permittivity is given by

$$\epsilon_r^* = \frac{\epsilon^*}{\epsilon_0} = \frac{\epsilon' - j\epsilon''}{\epsilon_0} \quad (2.6)$$

Where ' $\epsilon_0$ ' is the permittivity of free space, which is  $8.854 \times 10^{-12}$  F/m in SI units. The real part of dielectric permittivity ( $\epsilon'$ ) is a measure of how much energy from an external electric field is stored in a material. The imaginary part of the dielectric permittivity ( $\epsilon''$ ) is called the loss factor. It is a measure of the energy dissipation or heat generation in the material when an external electric field is applied. The loss current will be always in phase with the applied voltage. But the charging current will be always out of phase and in ideal case the phase change will be  $90^\circ$ . If loss current ' $I_L$ ' and charging current ' $I_C$ ' makes angles ' $\theta$ ' and ' $\delta$ ' respectively with the total current ' $I_T$ ' passing through the capacitor, the dielectric

loss is given by 'tanδ', which is the ratio of the imaginary and real parts of the dielectric constant.

$$\tan \delta = \epsilon''/\epsilon' \quad (2.7)$$



- |                         |                      |
|-------------------------|----------------------|
| 1. BNC                  | 7. Glass Window      |
| 2. Neoprene O Ring      | 8. Copper Electrodes |
| 3. MS Chamber           | 9. Sample            |
| 4. SS Pipe              | 10. Fixing Screws    |
| 5. Sample Holder        | 11. MS Flange        |
| 6. Liq. Nitrogen Cavity | 12. To Vacuum pump   |

**Fig. 2.2 Schematic representation of dielectric cell**

The special feature of this measurement is that the entire data acquisition and evaluation of the dielectric constant were automated based on a software package

developed and modified by us. This was done with the help of a base package supplied by National Instruments called 'LabVIEW', which in turn is based on G Programming. LabVIEW is a programming language for data acquisition, analysis, simulation or computer control of instruments, techniques or processes. LabVIEW is an acronym for Laboratory Virtual Instrument Engineering Workbench and is an object oriented language and its style, syntax and data flow is different from conventional linear programming languages. Appropriate modifications were incorporated in the software so as to enable the data acquisition automatic and visual observation of the graphs on the computer screen. The characteristic feature of this automatic data acquisition is that it has been possible to acquire 20,000 data points or more in a matter of 5 to 10 minutes. By using the modified package the data can be plotted and analysed.

#### 2.4.2 AC conductivity measurements

The ac electrical conductivity of both the ceramic and rubber ferrite composites was evaluated by calculating the ac conductivity values using dielectric parameters. The dielectric studies of both ceramic and rubber ferrite composites were carried out using a dielectric cell and an impedance analyzer (Model: HP 4285A). Disc shaped samples were used to find out the dielectric constant. The capacitance and dielectric loss in the frequency range 100KHz – 8MHz were found out. Dielectric constant or relative permittivity was calculated using the formula

$$\epsilon_r = \frac{C.d}{\epsilon_0.A} \quad (2.8)$$

where d is the thickness of the sample, C the capacitance and A the area of cross section of the sample.  $\epsilon_r$  is the relative permittivity of the material which is a dimensionless quantity. The ac conductivity of these samples were then evaluated using the relation

$$\sigma_{ac} = 2\pi f \tan\delta \epsilon_0 \epsilon_r \quad (2.9)$$

where f is the frequency of the applied field and  $\tan\delta$  is the loss factor. The principle and the theory underlying the evaluation of  $\sigma_{ac}$  from dielectric measurements are based on a treatment dealt by Goswamy<sup>64</sup>. The measured values of  $\epsilon_r$  and  $\tan\delta$  from the dielectric measurements for both ceramic and RFCs were used for the calculation of the ac conductivity.



## 2.5 MAGNETIC CHARACTERIZATION

The magnetic characterization of both the ceramic BaF/SrF and rubber ferrite composites (RFC) were carried out using a Vibrating Sample Magnetometer.

### 2.5.1 Vibrating Sample Magnetometry

Instrument used for the magnetic measurements is a Vibrating Sample Magnetometer (VSM), model: 4500 (EG&G PARC). A simplified block diagram is given in figure 2.3 and the VSM set up used for the study is given in figure 2.4. Magnetic properties of the rubber ferrite composites for different loadings of the magnetic filler with and without carbon black were carried out. Parameters like Saturation magnetisation ( $M_s$ ), Magnetic remanence or Retentivity ( $M_r$ ) and Coercivity ( $H_c$ ) were evaluated from the hysteresis loops obtained at room temperature.

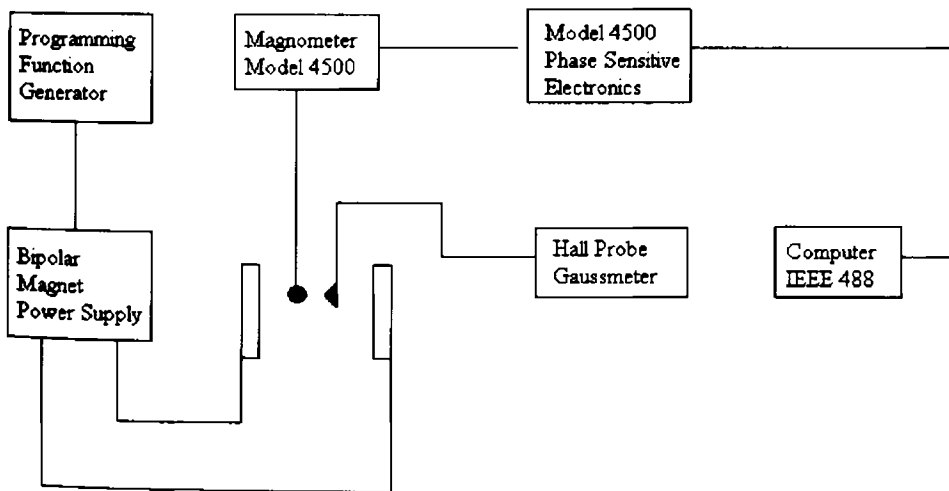
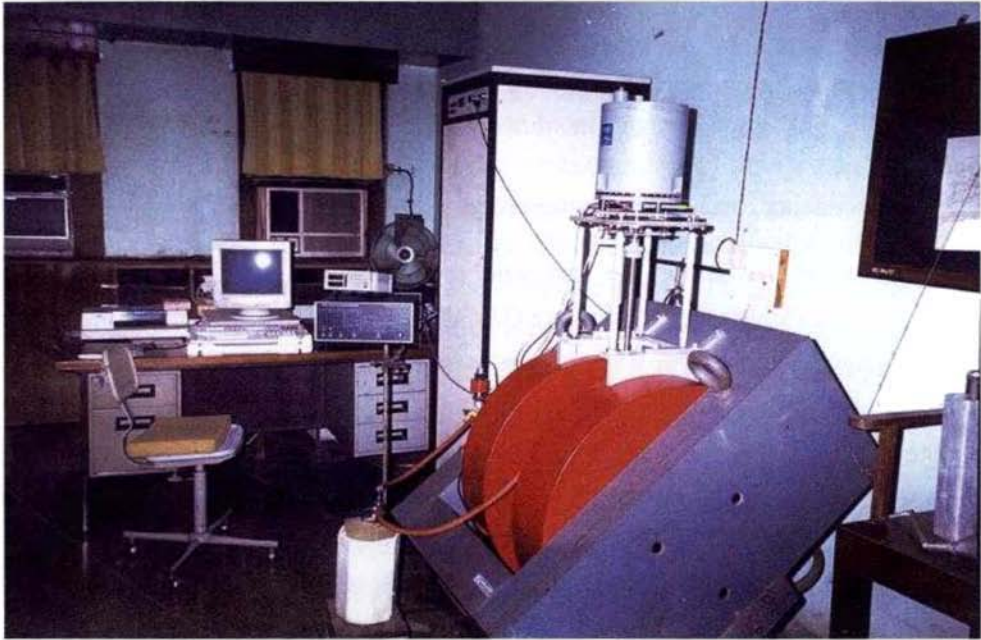


Fig. 2.3 Block diagram of VSM setup



**Fig 2.4 VSM set up used for the magnetic measurements**

### **2.5.2 Principle and Theory involved in VSM**

When a sample material is placed in a uniform magnetic field, a dipole moment is induced in the sample. The amount of magnetic flux linked to any coil placed in the vicinity of this magnetic moment is given by

$$\phi = \mu_0 n \alpha M \quad (2.10)$$

$\mu_0$  – permeability of free space

$n$  – number of turns per unit length of coil

$M$  – magnetic moment of the specimen

$\alpha$  – Geometric moment decided by position of moment with respect to coil as well as shape of coil.

$$\text{Anharmonic oscillator of the type } Z = Z_0 + A \exp(j\omega t) \quad (2.11)$$

induces an emf in the stationary detection coil. The induced emf is given by

$$V = -\frac{d\phi}{dt} = -j\omega\mu_0 nMA\left(\frac{\partial\alpha}{\partial z}\right)e^{j\omega t} \quad (2.12)$$

If amplitude of vibration (A), frequency and  $\frac{\partial\alpha}{\partial z}$  are constant over the sample zone then induced voltage is proportional to the magnetic moment of the sample. This is the basic idea behind VSM<sup>59-63</sup>.

When the magnetic material is placed in a uniform magnetic field, a dipole moment is induced which is proportional to the susceptibility of the sample and the applied field. If the sample is made to undergo sinusoidal motion, an electrical signal can as well be induced in suitably located stationary pick up coils. This signal, which is at the vibration frequency, is proportional to the magnetic moment and vibration amplitude. This means of producing an electrical signal related to the magnetic properties of a sample material is the basic principle used in the design of a VSM to measure the magnetic properties.

In model PARC 4500 VSM the material under study is contained in a sample holder, which is centered in the region between the poles of a laboratory electromagnet. A slender vertical sample rod connects the sample holder with a transducer assembly located above the magnet. The transducer converts a sinusoidal ac drive signal in to a sinusoidal vertical vibration of the sample rod and the sample is thus made to undergo a sinusoidal motion in a uniform magnetic field. Coils mounted on the poles of the magnet pick up the signal resulting from the sample motion. This ac signal at the vibrating frequency is proportional to the magnitude of the moment induced in the sample. However it is also proportional to the vibration amplitude and frequency. A servo system maintains constancy in the drive amplitude and frequency so that the output accurately tracks the moment level without degradation due to variation in the amplitude and frequency of vibration.

The servo technique uses a vibrating capacitor located beneath the transducer to generate an ac control signal that varies solely with the vibration

amplitude and frequency. The signal, which is at the vibration frequency, is fed back to the oscillator where it is compared with the drive signal so as to maintain constant drive output. It is also phase adjusted and routed to the signal demodulator where it functions as the reference drive signal. The signal originating from the sample in the pick up coils is then buffered, amplified and applied to the demodulator. There it is synchronously demodulated with respect to the reference signal derived from the moving capacitor assembly. The resulting dc output is an analog signal, which depends only on the magnitude of the magnetic moment, and not influenced by the amplitude and frequency drifts.

The system is provided with facilities for low temperature measurements as well for the thermomagnetisation measurements. That is, the variation of saturation magnetisation with temperature can be studied by using this system.

## REFERENCES

- 1 B.V. Bhise, M.B. Dangare, S.A.Patil, S.R.Sawant, *J. Mater. Sci. Lett.* **10** (1991) 922.
- 2 Sawadh. P. S, and Kulkarni. D.K, *Materials Chemistry and physics*, **63** (2000) 170-173.
- 3 Ahmed. M.A, *Phys. Stat. Sol. A* **111** (1989) 567.
- 4 Valenzuela R, 'Magnetic Ceramics'; Cambridge, Cambridge University Press, 1994.
- 5 Swallow. D, and Jordan. A. K, 'The fabrication of ferrites', *Proc. Br. Ceram. Soc.*, **2** (1964) 1-17.
- 6 Stuijts. A. L, 'Microstructural considerations in ferromagnetic ceramics', *Proc. 3<sup>rd</sup> Int. Mater. Symp. on Ceramic Microstructures*, Univ. Calif. Berkeley, (1966).
- 7 Heck. C, and Weber. J, 'How firing atmospheres influence ferrite properties', *Ceramic Ind.*, (1961), **77**, part 1, 5, 75; part 2, 6, 66.
- 8 Jackson. H, 'Kilns for the manufacture of ferrites', *Proc. Br. Ceram. Soc.*, **2**, (1964) 43-53.
- 9 Stijntjes, T. G. W, Presented at ICF4, *Advances in Ceramics* **16** (1985) 493.
- 10 Haneda. K, and Kojima. H, *J. Amer. Ceram. Soc.* **57**, (1974) 68.
- 11 Benito. G, M.P. Morales, J. Reequena, V.Raposo, M.Vazquez, and J.S. Moya, *J. Magn. Magn. Mater.*, **234** (2001) 65-72.
- 12 Sung-Soo Kim and Dae-Hee Han, *IEEE Trans.Magn.*, **30,6** (1994).
- 13 Daniels. J.M and Rosencwaig, *Can.J.Phys.* **48** (1970) 381.
- 14 Leung. L.K, Evans. B.J, and Morrish. A.H, *phys. Rev. B* **8** (1973) 29.
- 15 Patil. A.N, Patil. M.G, Patankar. K.K, Mathe. V.L, Mahajan. R.P and Patil. S.A, *Bull. Mater. Sci.*, **23**, 5 (2000) 447-452.
- 16 Murthy. S.R, *Bull. Mater. Sci.*, **24**, 4 (2001) 379-383.
- 17 Haneda. K, Miyakana. C, and Kojima. C, *J. Amer. Ceram. Soc.* **57** (1974) 354.

- 18 Roos. W, *J. Am. Ceram. Soc.* **63** (1980) 601.
- 19 Sankaranarayanan. V.K, and Khon. D.C, *J. Magn. Magn. Mater.*, **120** (1993) 73.
- 20 Shirk. B. T and Buessem. W. R, *J. Am. Ceram. Soc.* **53** (1970) 192.
- 21 Kubo. O, Ido. T, and Yokoyama. H, *IEEE Trans. Magn*, **MAG-18** (1982) 1122.
- 22 Battle. M, Garcia del Muro, Labarta. A, Martinez. B and Gornert. P, *J. Magn. Magn. Mater.*, **140-144** (1995) 473.
- 23 Castro. S, Gayoso. M, Rivas. J, Greneche. J. M, Mira. J, and Rodriguez. C, *J. Magn. Mag. Mater.*, **152** (1996) 61-69.
- 24 Castro. S, Gayoso. M, Rodriguez. C, Mira. J, Rivas. J, Paz. S and Greneche. J. M, *J. Magn. Magn. Mater.*, **140-144** (1995) 2097-2098.
- 25 Licci. F, Turilli. G, and Besagni. T, *IEEE Trans. Magn.* **24** (1988) 593.
- 26 Cabanas. M. V, Gonzalez-Calvet. J. M et al, *J. Solid State. Chem.* **101** (1992) 265.
- 27 Mendoza-Suarez. G, Matutes-Aquino. J. A, Escalante-Garcia. J.I, Mancha-Molinar. H, Rios-Jara. D, and Johal. K. K, *J. Magn. Magn. Mater.*, **223** (2001) 55-62.
- 28 Ding. J, Maurice. D, Miao. W.F, McCormick. P.G, and Street. R, *J. Magn. Magn. Mater.*, **150** (1995), 417
- 29 Jin. Z, Tang. W, Zhang. J, Lin. H, and Du. Y, *J. Magn. Magn. Mater.*, **182** (1998), 231.
- 30 Wang. J. F, Ponton. C. B, and Harris. I. R, *J. Magn. Mag. Mater.*, **234** (2001), 233-240.
- 31 Lin. C.H, Shin. Z.W, Wang. M.L and Yu. Y.C, *IEEE Trans. Magn.* **26** (1990) 15.
- 32 Zhong. W, Ding. W. P, Zhang.N, Hong. J.M, Yan. Q. J, and Du. Y.W, *J. Magn. Magn. Mater.*, **168** (1997) 196.
- 33 Zhong. W, Ding. W. P, Jiang Y.M, Zhang.N, Zhang.J.R, Du. Y.W, and Yan. Q. J, *J. Am. Ceram. Soc.* **80**, (1997) 3258.
- 34 Wang. L and Li. F. S, *J. Magn. Mag. Mater.*, **223** (2001) 233-237.

- 35 Mendoza-Suarez. G, Corral-Huacuz. J. C, Contreras-Garcia. M E, and Juarez-Medina. H, *J. Magn. Mag. Mater.*, **234** (2001) 73-79.
- 36 Martinez Garcia. R, Reguera Ruiz. E, Estevez Rams. E, and Martinez Sanchez. R. *J. Magn. Mag. Mater.*, **223** (2001) 133-137.
- 37 Jae-Gwang Lee, Jae Yun Park and Chul Sung Kim, *J. Mater. Sci.*, **33** (1998) 3965-3968.
- 38 Estevez Rams. E, Martinez Garcia, Reguera, Montiel Sanchez. H, and Madeira H.Y, *j. Phys; Appl.Phys.***33** (2000) 2708-2715.
- 39 Bernier. J. C, *Mater. Sci. Eng. A* **109** (1989) 233.
- 40 Mastsumoto. M, Morisako. A, Haeiwa. T, Naruse. K, and Karasawa. T, *IEEE Transl. J. Mag. Japan* **6** (1991) 648.
- 41 Qingqing Fang, Yanmei Liu, Ping Yin and Xiaoguang Li, *J. Magn. Magn. Mater.*, **234** (2001) 366-370.
- 42 Cabanas. M.V, Gonzalez-Calbet. J. M, and Vallet-Regi. M, *J. Mater. Res.* **9** (1994) 712.
- 43 Kaczmarek. W. A, Ninham. B. W, and Calka. A, *J. Appl. Phys.*, **70** (1991) 5909.
- 44 Matijevic. E, *J. Colloid Interface Sci.* **117** (1987) 593.
- 45 Kuz' Mitcheva. T. G, Ol'Khovik. L. P, and Shabatin. V. P, *IEEE Trans. Magn.* **31** (1995) 800.
- 46 Pillai. V, Kumarand. P, and Shah. D.O, *J. Magn. Mag. Mater.*, **116** (1992) L299.
- 47 Licci. F and Besagni. T, *IEEE Trans. Magn. MAG-20* (1984) 1639.
- 48 Srivastava. A, Singh. P and Gupta. M.P, *J. Mater. Sci.* **22** (1987) 1489.
- 49 Calleja. A, Tijero. E, Martinez. B, Pinol. S, Sandiumenge. F and Obradors. X, *J. Magn. Magn. Mater.*, **196-197** (1999) 293-294. ♣
- 50 Zhong Wei et al, *J. Applied Phys.* **85,8** (1999).
- 51 Keer H.V, *Principles of solid state physics* Willey Eastern Ltd. New Delhi (1993).

- 52 Cullity. B.D, 'Elements of X-ray diffraction', (Philippines, Addison-Wesley Publishing Company, Inc.) 2<sup>nd</sup> Edn. (1978).
- 53 Charles Kittel, Introduction to Solid State Physics, 1997, John Wiley and Sons, New York.
- 54 Blow C.M. and C. Hepburn, 'Rubber Technology and Manufacture', 2<sup>nd</sup> edition, (1985), Butterworths Publishers, London.
- 55 Vishu Shah, handbook of plastic testing technology, John Wiley and Sons Inc, USA 1998.
- 56 Allen W, Natural Rubber and the Synthetics, 1972, Granada Publishing Ltd.
- 57 Steven Blow. Hand book of Rubber Technology, 1998, Galgotia Publishing Pvt. Ltd.
- 58 Charles A Harper, Handbook of Plastic, Elastomers and Composites, 2<sup>nd</sup> edition, McGraw Hill Inc.1992.
- 59 Brailsford. F, Physical principles of magnetism, 1966, D Van Nostrand Co. Ltd.
- 60 Haberey. F and H.J.P. Wijn, Phys. Stat. Sol. (a) 26 (1968) 231.
- 61 Krishnan R.V. and A. Banerjee, Rev. Sci. Instrum., 70, 1 (1999) 85.
- 62 Simon Foner, Rev. Sci. Instrum. 30, 7 (1959) 548-557.
- 63 Joseph A. Pesch, Rev. Sci. Instrum, 54, 4 (1983) 480.
- 64 Goswami A, Thin Film Fundamentals, (1996) New age international Publishers Ltd., New Delhi.



# Chapter 3

## PREPARATION AND CHARACTERISATION OF RUBBER FERRITE COMPOSITES

This chapter deals with the preparation and characterisation of barium and strontium ferrite and its incorporation into the rubber matrixes to prepare rubber ferrite composites (RFC). The details of the characterisations carried out by employing various analytical tools at appropriate stages are depicted in the form of a flowchart as shown in figure 3.1.

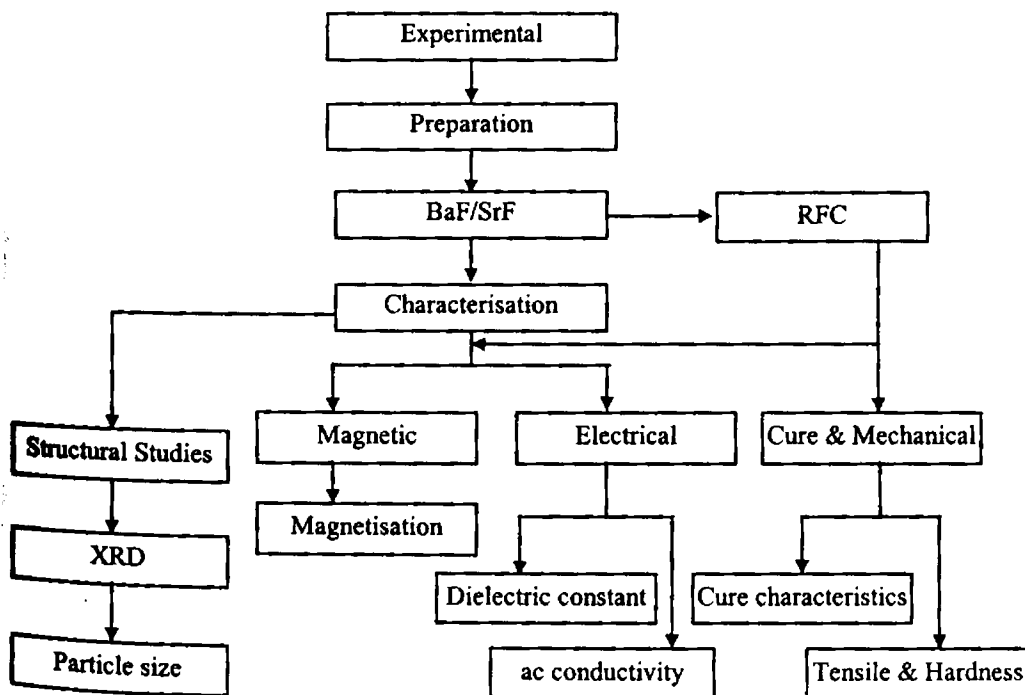


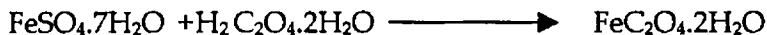
Fig 3.1 Flow chart for the preparation and characterisation of RFC

### 3.1 SYNTHESIS OF CERAMIC FERRITES

Both barium ferrite and strontium ferrite have been prepared by the ceramic techniques<sup>1-7</sup>. Ferrous oxalate dihydrate (FOD) precursors were employed for the synthesis of these ferrites. For the preparation of precursors the following method was employed. Ferrous oxalate dihydrate was first prepared by the co-precipitation technique.  $\alpha$ -Fe<sub>2</sub>O<sub>3</sub> was prepared by the decomposition of freshly prepared ferrous oxalate dihydrate.

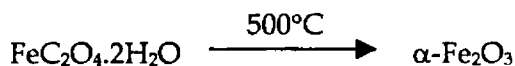
#### 3.1.1 Preparation of Ferrous Oxalate Dihydrate

AR grade of ferrous sulphate and oxalic acid were utilised for this purpose. Appropriate amounts of the chemicals were weighed and aqueous solutions of ferrous sulphate and oxalic acid were made by using distilled water. One or two drops of sulphuric acid were added in order to prevent the oxidation of ferrous sulphate before making the solution. Ferrous sulphate solution was heated to 60°C. Preheated oxalic acid (60°C) was added drop by drop to this solution with the help of a separating funnel aided by constant stirring, using a magnetic stirrer. When the reaction is over, the solution is filtered and the precipitate obtained is washed with boiling water. This was repeated to remove the excess of oxalic acid, if any, present in the solution. The precipitate was dried in a hot air oven at 100°C. Fine yellow coloured particles of FOD were obtained.



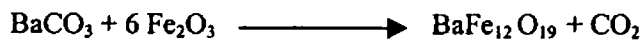
#### 3.1.2 Preparation of $\alpha$ -Fe<sub>2</sub>O<sub>3</sub>(haemitite)

$\alpha$  - Fe<sub>2</sub>O<sub>3</sub> was prepared by the decomposition of freshly prepared ferrous oxalate dihydrate (FOD). The decomposition of FOD at 500°C for three hours yielded haemitite ( $\alpha$ -Fe<sub>2</sub>O<sub>3</sub>).



### 3.1.3 Preparation of Barium and Strontium Ferrites

Appropriate amounts of the AR grade barium carbonate and strontium carbonate and  $\alpha\text{-Fe}_2\text{O}_3$  were taken and a slurry was made using AR grade acetone. This mixture was thoroughly mixed using an agate mortar. The mixing was continued for one hour to produce a homogeneous mixture of fine particles. After drying, this homogeneous mixture was pre-sintered at around  $500^\circ\text{C}$  for six hours in a muffle furnace. The pre-fired samples were again mixed to ensure homogeneity and again pre-fired at the same temperature. The pre-sintered powder sample of the BaF and SrF were then pressed in a hydraulic press into cylindrical pellets by using a mould of die steel having a diameter of 12 mm. Final sintering of the pre-sintered powder sample and the pellet were done at  $1200^\circ\text{C}$  by keeping it inside the furnace for 24 hours. They were then cooled under ambient conditions. The final sintered samples were again grinded in an agate mortar for one hour to ensure homogeneity. These finely ground powder and pellets were used for the characterisation and for the preparation of RFCs. The properties of the final product depend on the sintering temperature, time, cooling rate and environment.



## 3.2 STRUCTURAL EVALUATION

The barium ferrite and strontium ferrite powder prepared by the ceramic technique were analysed by x-ray powder diffraction (XRD) technique using X-ray diffractometer (Rigaku Dmax-C) with  $\text{Cu K}_\alpha$  ( $\lambda = 1.5405 \text{ \AA}$ ). The details are cited in chapter 2. From the X ray powder diffractograms recorded for BaF and SrF, parameters namely, inter atomic spacing ( $d$ ), relative intensity ( $I/I_0 \times 100$ ), and particle size ( $D$ ) were determined. The evaluation of the structural parameters indicated that the compounds were monophasic without any detectable impurities and were crystalline in nature. The XRD spectra of these ferrites are shown in figures 3.2 and 3.3.

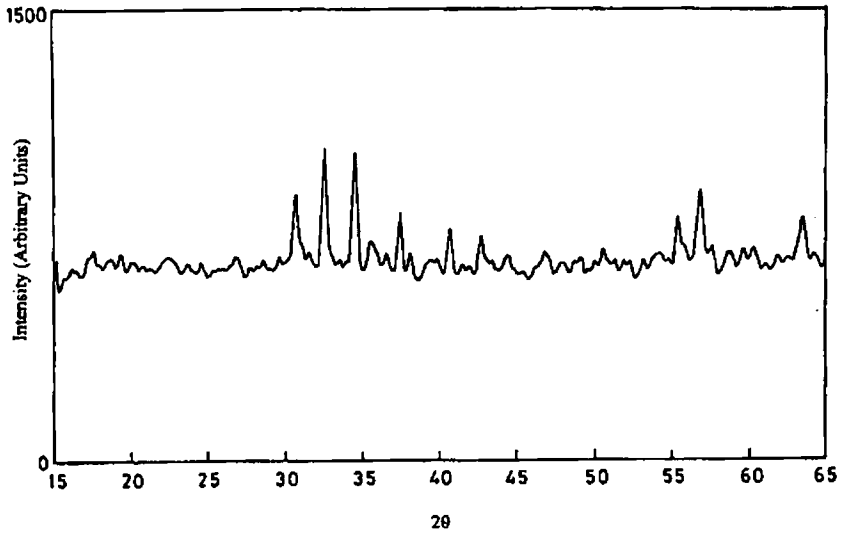


**Fig 3.2 XRD spectrum of barium ferrite**

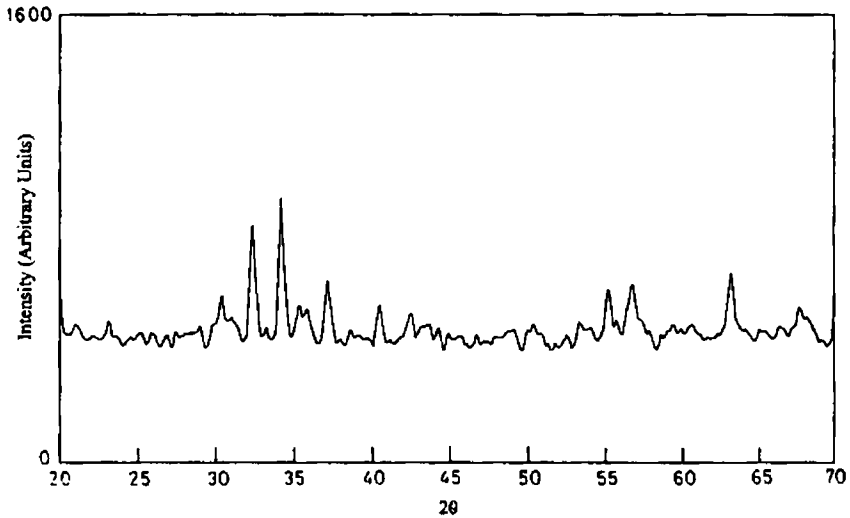


**Fig 3.3 XRD spectrum of strontium ferrite**

The interatomic spacing and their relative intensities matched well with that of the reported values in the literatures<sup>8,9</sup>. The XRD data are given in tables 3.1 and 3.2.

**Table 3.1 X-ray diffraction data for barium ferrite**

Inter atomic spacing, $d$ ( $\text{\AA}^\circ$ )	Relative intensity, $I / I_0 \times 100$
2.757	100
2.605	97
2.920	55
1.619	52
1.468	51
2.406	47
2.223	47
1.659	42
1.625	37
1.467	32
2.460	29

**Table 3.2 X-ray diffraction data for strontium ferrite**

Inter atomic spacing, $d$ ( $\text{\AA}^\circ$ )	Relative intensity, $I / I_0 \times 100$
2.6086	100
2.7527	74
2.4088	49
1.4659	43
1.6585	40
2.8644	36
1.6169	35
2.5336	35
2.9285	33
2.2229	33
2.4961	31

The particle size of the prepared ceramic sample depends very much on the preparation methods and sintering conditions. Since the particle size and surface area are inversely proportional, the increase in particle size, naturally decrease the surface area and vice-versa. The average particle size was calculated from the x-ray spectra using the Debye Scherrer formula (eqn.2.2) The average particle size of BaF lie in the range 60-70 nm and had a surface area of 20-25 m<sup>2</sup>/g, whereas that of SrF is in the range 25-35 nm with the surface area of around 50 m<sup>2</sup>/g.

However, it is to be noted here that the particle size 'D' determined by the Debye Scherrer formula represents only the average distribution of the particles and hence the surface area calculated by the formula  $S = \frac{6000}{D_p} \text{ m}^2/\text{g}$  is only indicative, unlike that obtained from technique like BET (Branauer, Emmett and Teller).

### 3.3 INCORPORATION OF FILLERS IN RUBBER MATRIX.

The barium and strontium ferrites thus prepared and characterised were then incorporated in natural rubber and nitrile rubber matrix according to the recipe cited in table 3.3 and 3.4 respectively. Compounds were prepared for various loadings of BaF and SrF, ranging from 40 to 120 phr in steps of 20.

**Table 3.3 Recipe used for compounding of natural rubber with barium and strontium ferrite**

Ingredients	Weight in grams					
	A0	B0	C0	D0	E0	F0
Natural rubber	100.0	100.0	100.0	100.0	100.0	100.0
Zinc oxide	5.0	5.0	5.0	5.0	5.0	5.0
Stearic acid	1.5	1.5	1.5	1.5	1.5	1.5
Sulphur	2.5	2.5	2.5	2.5	2.5	2.5
CBS	0.8	0.8	0.8	0.8	0.8	0.8
Antioxidant (SP)	1.0	1.0	1.0	1.0	1.0	1.0
BaF/SrF	0	40	60	80	100	120

**Table 3.4** Recipe used for compounding of nitrile rubber with barium and strontium ferrite

Ingredients	Weight in grams					
	A1	B1	C1	D1	E1	F1
Nitrile rubber	100.0	100.0	100.0	100.0	100.0	100.0
Zinc oxide	5.0	5.0	5.0	5.0	5.0	5.0
Stearic acid	1.5	1.5	1.5	1.5	1.5	1.5
Sulphur	1.5	1.5	1.5	1.5	1.5	1.5
CBS	1.5	1.5	1.5	1.5	1.5	1.5
Antioxidant (SP)	1.0	1.0	1.0	1.0	1.0	1.0
BaF/SrF	0	40	60	80	100	120

### 3.4 COMPOUNDING

The mixing was first carried out in a Brabender Plasticorder model PL 3S at 70°C for ten minutes at a speed of 50 rpm. This was then homogenised by using a two roll mixing mill (15 X 33 cm) as per ASTM D 3182-89. The details of the mixing conditions are given in chapter 2.

Studies carried out earlier<sup>10</sup> on RFC have shown that the percolation threshold was not reached even at a loading of 120 phr of magnetic fillers. Hence the 80 phr loading of BaF/SrF were taken as the control compound for further loadings of carbon black. RFC containing carbon black was prepared for various loadings namely 10 to 50 phr, in steps of 10. The carbon black used was N330 (HAF), the properties of which are given in chapter 2.

The tables 3.5 and 3.6 shows the recipe used for the preparation of RFC containing carbon black for NR and NBR respectively. It may be noted that the compounds D0 and D1 represent the base RFC containing the 80 phr of barium ferrite and strontium ferrite in NR and NBR respectively.

**Table 3.5 Recipe used for compounding of natural rubber containing ferrite filler and carbon black**

Ingredients	Weight in grams					
	D0	D01	D02	D03	D04	D05
Natural rubber	100.0	100.0	100.0	100.0	100.0	100.0
Zinc oxide	5.0	5.0	5.0	5.0	5.0	5.0
Stearic acid	1.5	1.5	1.5	1.5	1.5	1.5
Sulphur	2.5	2.5	2.5	2.5	2.5	2.5
CBS	0.8	0.8	0.8	0.8	0.8	0.8
Antioxidant (SP)	1.0	1.0	1.0	1.0	1.0	1.0
BaF/SrF	80	80	80	80	80	80
Carbon black	0	10	20	30	40	50
Aromatic oil	0	1	2	3	4	5

**Table 3.6 Recipe used for compounding of nitrile rubber containing ferrite filler and carbon black**

Ingredient	Weight in grams					
	D1	D11	D12	D13	D14	D15
Nitrile rubber	100.0	100.0	100.0	100.0	100.0	100.0
Zinc oxide	5.0	5.0	5.0	5.0	5.0	5.0
Stearic acid	1.5	1.5	1.5	1.5	1.5	1.5
Sulphur	1.5	1.5	1.5	1.5	1.5	1.5
CBS	1.5	1.5	1.5	1.5	1.5	1.5
Antioxidant(SP)	1.0	1.0	1.0	1.0	1.0	1.0
BaF/SrF	80	80	80	80	80	80
Carbon black	0	10	20	30	40	50
DOP	0	1	2	3	4	5



### **3.5 DETERMINATION OF CURE CHARACTERISTICS OF RUBBER FERRITE COMPOSITES**

After the mixing and homogenisation, the compound was matured for a period of 24 hours. Cure characteristics of the rubber compounds were estimated using Goettfert elastograph model 67.85. The cure characteristics namely scorch time, optimum cure time, cure rate index, minimum torque and maximum torque were determined from the cure graph. The details of the measurement and the results/discussion are cited in chapter 2 and 4 respectively.

### **3.6 PREPARATION OF TEST SPECIMENS**

The cure time required for each RFC samples was determined from the respective cure curves. The compounds were then vulcanised at 150°C on an electrically heated laboratory hydraulic press up to their respective cure times to make sheets of the sample. The entire test was carried out according to the ASTM standards. The details are described in chapter 2.

### **3.7 CONCLUSION**

Hexagonal hard ferrites namely barium ferrite and strontium ferrites were prepared by the ceramic techniques. They were then characterised by using the X-Ray Diffraction technique. Rubber ferrite composites (RFCs) containing various loadings of BaF and SrF were synthesised by the incorporation of these ferrites into both natural rubber and nitrile rubber matrix. The carbon black filled RFCs were prepared by incorporating varying amount of carbon black into RFC containing an optimum quantity of ferrite. This method of preparation can be adopted for the synthesis of RFCs intended for microwave applications.

**REFERENCES**

1. Benito. G, Morales. M. P, Requena. J. Raposo. V, Vazquez. M, and Moya. J.S, J. Magn. Mag. Mater., **234** (2001), 65-72.
2. H.P. Steier, J.Requena, J.S.Moya, J. Mater. Res. **14** (1999) 3647.
3. Shintaro Hayashi, Proceedings of the International Conference, Japan,(1970) 542-544.
4. H. Taguchi, Recent improvements of ferrite magnets, J. Phys. IV France, **7** C1-299, (1997).
5. Sung-Soo Kim and Dae-Hee Han, IEEE Trans. on Magn., **30**, 6 (1994) 4554- 4556.
6. D.C. Khan, M. Misra, Bull. Mater. Sci. **7** (1985) 253.
7. K. Ishino, Y. Narumiya, Cerm. Bull. **66** (1987) 1469.
8. Joint Committee on Powder Diffraction and Standards - *ICDD C*, **39**-1433, 1990.
9. Joint Committee on Powder Diffraction and Standards - *ICDD C*, **33**-1340, 1990.
10. K.A. Malini, E.M. Mohammed, S. Sindhu, P.A. Joy, S.K Date, S.D. Kulkarni, P. Kurian, and M.R. Anantharaman, J. Magn. Sci., **36** (2001) 5551-5557.

# Chapter 4

---

## **CURE CHARACTERISTICS AND MECHANICAL PROPERTIES OF RUBBER FERRITE COMPOSITES**

### **4.1 INTRODUCTION**

Rubber ferrite composites, as mentioned earlier are composite materials with ferrite fillers as one of the constituents and natural or synthetic rubber as the base matrix<sup>1-3</sup>. In these composites both the magnetic filler and the polymer matrix chosen affect the processability and other physical properties of the final product. In tailoring composites for various applications it is necessary to select the proper filler and polymer matrix. The physical and chemical properties of the magnetic composites will possibly be influenced by the interactions with the filler and the matrix.

The knowledge of cure characteristics throws light on the processability of the composites. Information regarding particle size and surface area of the filler are also valuable tools in explaining the surface activity with respect to the components present in the polymer matrix. The processability and other physical properties of the final product depend not only on the filler properties but also on factors like percolation limit or nature of the matrix, like saturation/ unsaturation / polarity of the rubber.

It is important to study the processability of the polymers since the final vulcanised product is to be prepared by moulding. Thus it is necessary to evaluate the cure parameters. The cure parameters namely the maximum torque, minimum torque, scorch time and cure time were evaluated. The variation in the cure

parameters with loading of fillers was also studied. The mechanical properties of these composites containing various loadings of the magnetic filler were investigated. The effect of carbon black on the cure characteristics and mechanical properties of these RFC were also studied. The preparation of RFC and analysis of cure characteristics and mechanical properties assume significance not only in tailor making compounds, but also in understanding various properties and the related mechanisms.

## 4.2 CURE CHARACTERISTICS

The cure characteristics of RFC for various loadings of BaF/SrF and carbon black were studied using Gottfert Elastograph model 67.85. The details of the measurement are given in Chapter 2. A representative cure curve is shown in figure 4.1.

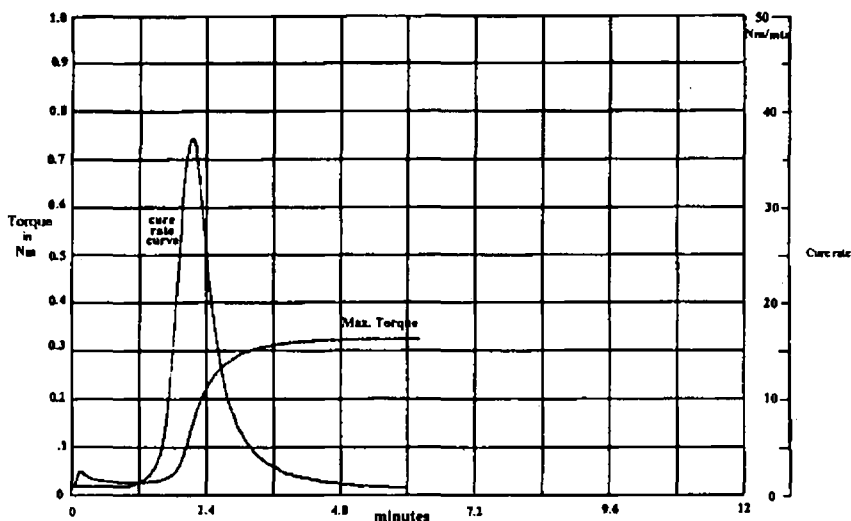
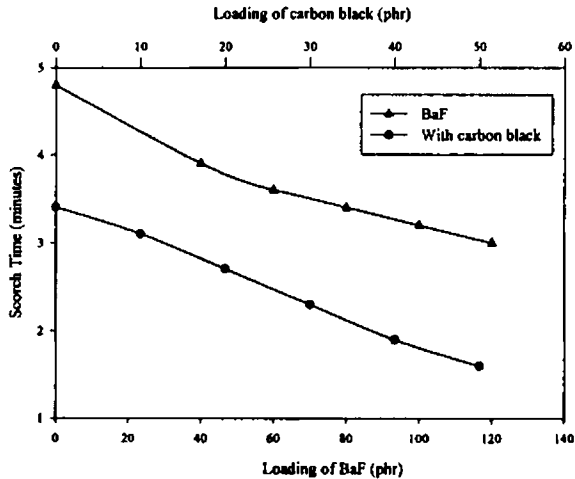


Fig 4.1 Representative Cure curve for RFC

Graphs showing the variation in scorch time and cure time with loading of barium ferrite filler and carbon black in NR are shown in figures 4.2 and 4.3 respectively. The Scorch time ( $t_{10}$ ) and cure time ( $t_{90}$ ) of these composites decreased with the addition of ferrite fillers. The addition of carbon black further

reduced both the scorch time and cure time. The scorch time decreased with the filler loading because the heat of mixing increased as the filler loading increased. The optimum cure time also decreased with the addition of fillers. The addition of carbon black further decreased the time of cure.



**Fig 4.2 Variation in scorch time with loading of barium ferrite filler and carbon black in NR**

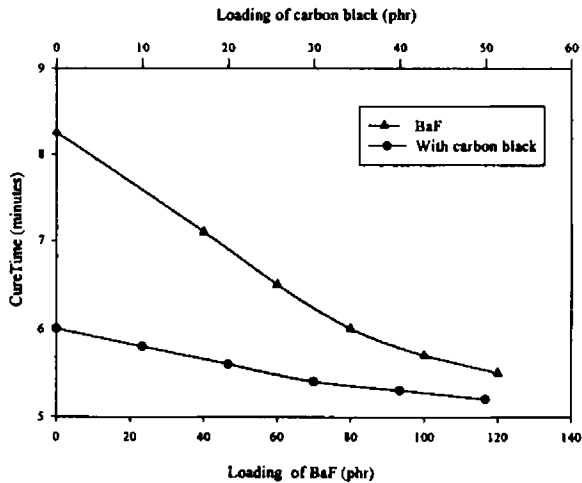


**Fig 4.3 Variation in cure time with loading of barium ferrite filler and carbon black in NR**

Similar behaviour was observed with the strontium ferrite filler, with and without carbon black in NR (Fig 4.4 and 4.5).

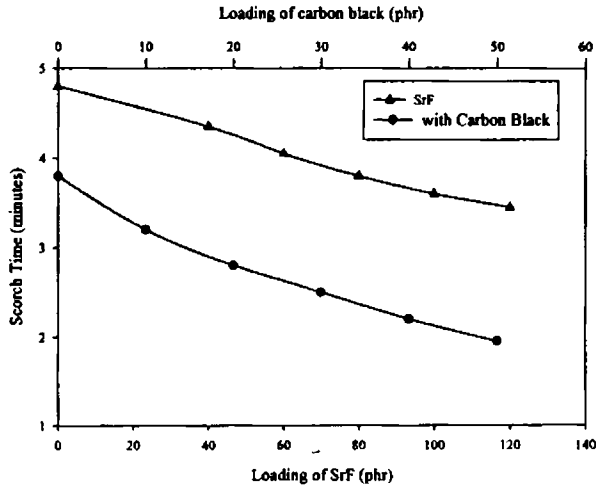


**Fig 4.4 Variation in scorch time with loading of strontium ferrite filler and carbon black in NR**

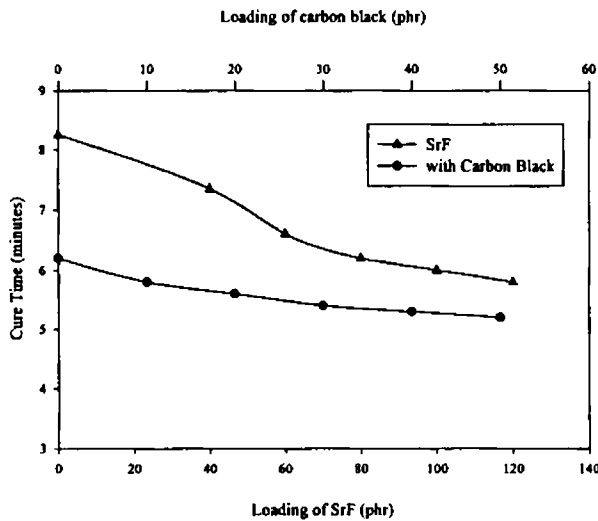


**Fig 4.5 Variation in cure time with loading of strontium ferrite filler and carbon black in NR**

In the case of NBR the variation in scorch time was almost similar to that of BaF, SrF and carbon black containing RFCs. But the cure time slightly increased with the initial addition of ferrite fillers (both BaF and SrF) and then showed a decreasing trend as in the case of NR. The cure time decreased with the addition of carbon black. Figures 4.6 and 4.7 represent the variation in scorch time and cure time with the loading of BaF and carbon black in NBR.

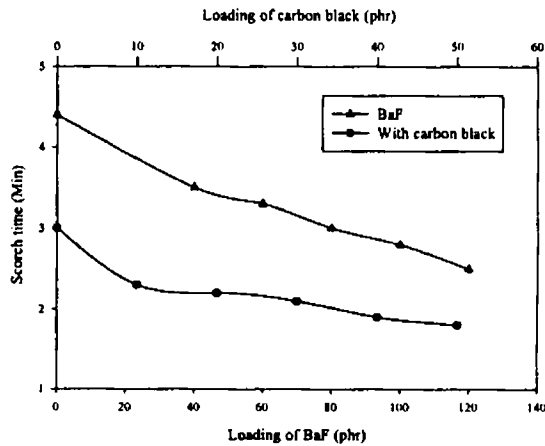


**Fig 4.6 Variation in scorch time with the loading of barium ferrite and carbon black in NBR**

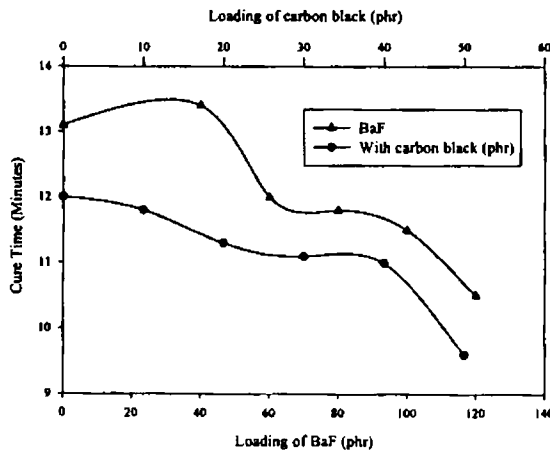


**Fig 4.7 Variation in cure time with the loading of barium ferrite and carbon black in NBR**

Similar behaviour is observed with the strontium ferrite filler. Figures 4.8 and 4.9 illustrates the variation in scorch time and cure time with loading of SrF and carbon black in NBR.

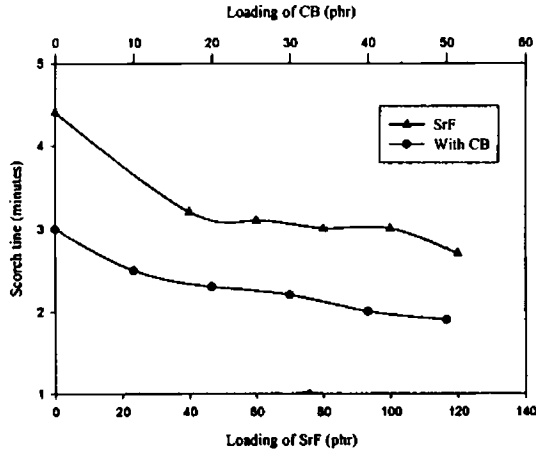


**Fig 4.8 Variation in scorch time with the loading of strontium ferrite and carbon black in NBR**

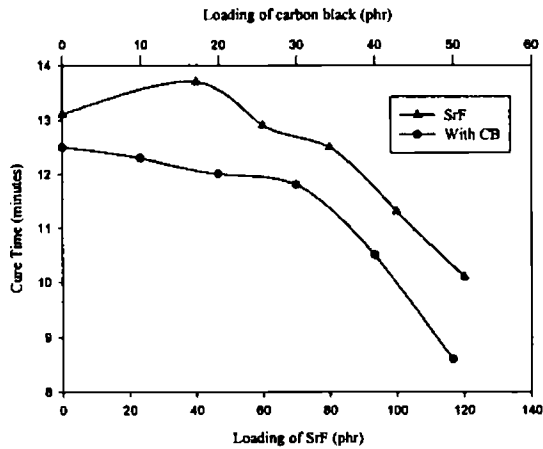


**Fig 4.9 Variation in cure time with the loading of strontium ferrite and carbon black in NBR**



Graphs showing the variation in minimum torque and maximum torque with loading of barium ferrite filler and carbon black in NR are shown in figure 4.10 and 4.11 respectively. The minimum torque ( $M_L$ ) and maximum torque ( $M_H$ ) of these composites increased with filler loading, both with ferrite and carbon black. Minimum torque is a measure of the viscosity of the compound. It can be considered as the measure of the stiffness of the unvulcanised compound. The minimum torque, increased with the loading of filler, as expected. Maximum torque gives an idea about the shear modulus of the fully vulcanised rubber at the vulcanisation temperature. The maximum torque, which is an indication of the modulus of the vulcanisates, increased with filler loading.

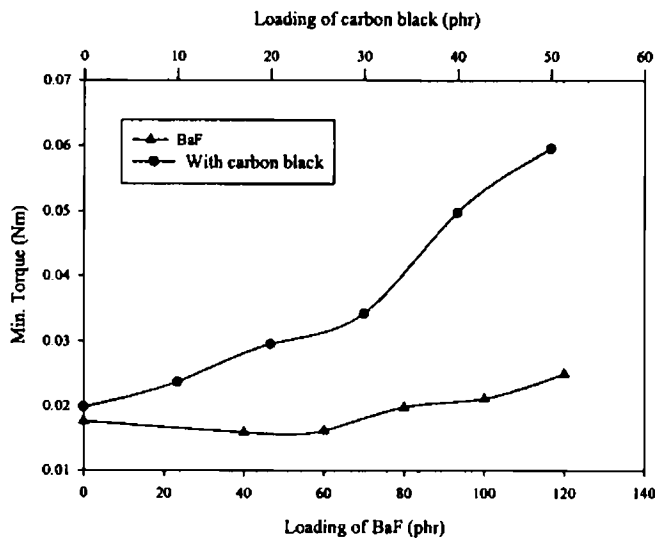


**Fig 4.10 Variation in minimum torque with loading of BaF and carbon black in NR**

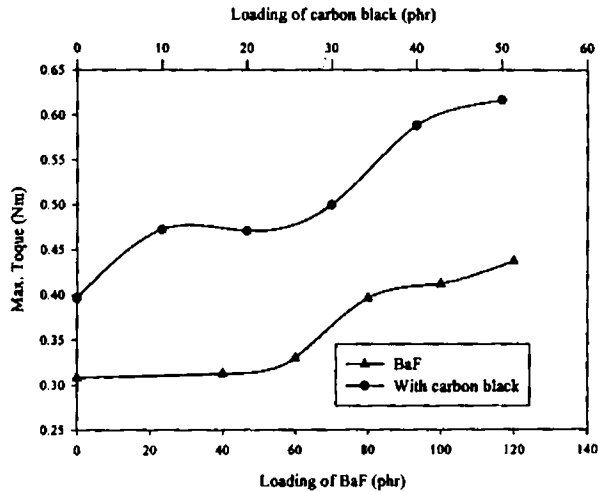


**Fig 4.11 Variation in maximum torque with loading of BaF filler and carbon black in NR**

Similar behaviour is observed in the case of NR based RFCs containing strontium ferrite filler with and without carbon black. (Figs 4.12 and 4.13).

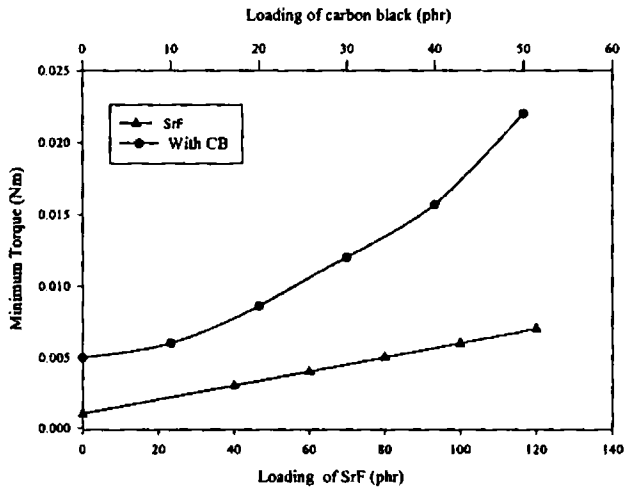


**Fig 4.12 Variation in minimum torque with loading of SrF filler and carbon black in NR**

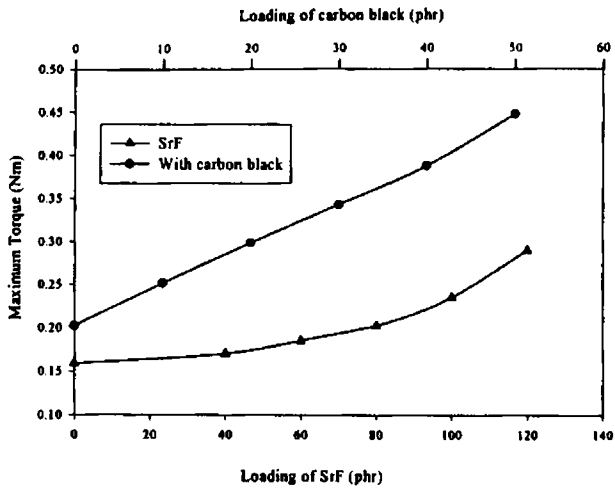


**Fig 4.13 Variation in maximum torque with loading of SrF and carbon black in NR**

As in the case of NR, the minimum and maximum torque showed an exactly similar behaviour for NBR containing BaF with and without carbon black (Figs 4.14 and 4.15).

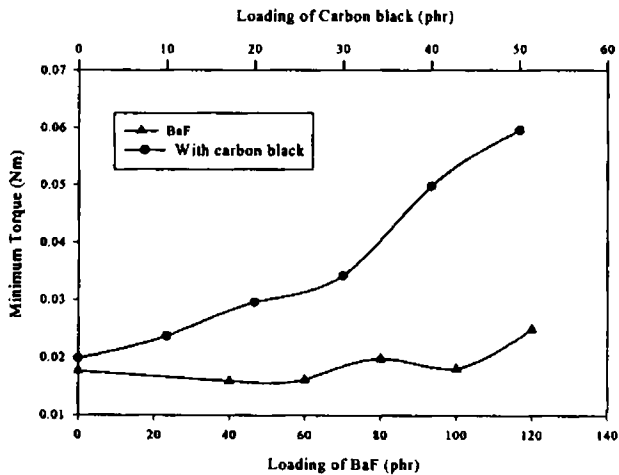


**Fig 4.14 Variation in minimum torque with loading of BaF and carbon black in NBR**

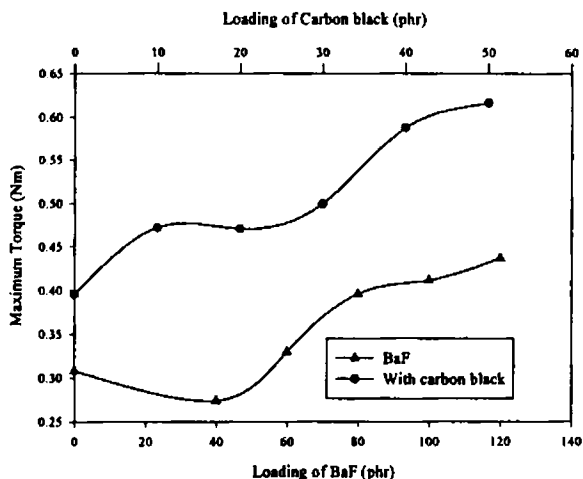


**Fig 4.15 Variation in maximum torque with loading of BaF and carbon black in NBR**

The minimum and maximum torque obtained for the RFC containing strontium ferrite in NBR, with and without carbon black is shown in figures 4.16 and 4.17 respectively. As in the case of RFCs containing BaF both with and without carbon black, the strontium ferrite filled RFCs also showed an increasing trend in torque values with the incorporation of the ferrite filler and carbon black.

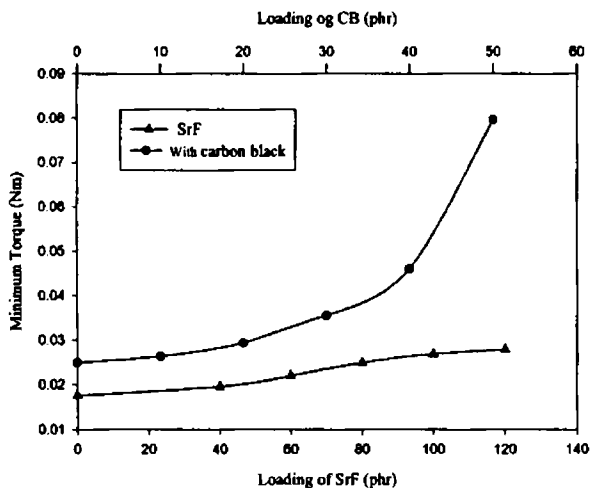


**Fig 4.16 Variation in minimum torque with loading of SrF and carbon black in NBR**

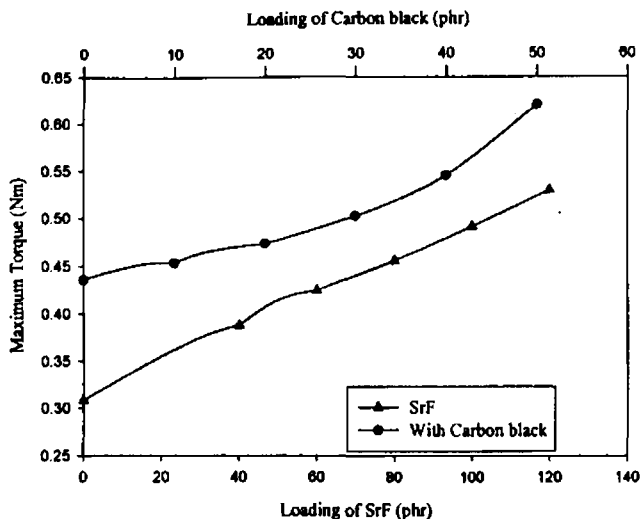


**Fig 4.17 Variation in maximum torque with loading of SrF and carbon black in NBR**

It is evident from the graphs shown in figures 4.10 to 4.17, the minimum and maximum torque increased with loading of fillers. The incorporation of BaF and SrF increased the stiffness of the compound and modulus of the vulcanisates. Evaluation of the cure parameters indicated that RFCs containing BaF and SrF with and without carbon black reduced both the scorch time and cure time. This showed that cure reaction is accelerated due to addition of these fillers and even though the scorch time decreased with the addition of these materials, the composites were still processable. These results showed that filler loading did not apparently affect the processability of the compounds.

### 4.3 MECHANICAL PROPERTIES

Mechanical properties of the RFCs were determined using an Instron Universal Testing Machine, Model 4411 Test System. The details of the measurement are cited in Chapter 2. Dumbbell shaped samples were cut from the prepared RFCs containing BaF and SrF, at loadings of 40,60,80,100 and 120 phr according to ASTM D 412 (1980). Parameters namely tensile strength, modulus at

different percentage elongations and elongation at break, which are some of the most important indications of the strength of the material<sup>9-12</sup> were determined. The effect of carbon black on the mechanical properties of these RFC were also studied using dumbbell specimens cut from the prepared RFCs containing various loadings of carbon black.

### 4.3.1 Stress strain properties of Rubber Ferrite Composites

#### 4.3.1.1 Natural Rubber based RFCs

Tensile strength is a measure of the ability of a material to withstand the forces that tend to pull it apart and to determine to what extent the material stretches before breaking. The tensile properties and hardness of the RFC containing various loadings of BaF in NR are shown in table 4.1. Table 4.2 shows the effect of carbon black on the tensile properties of RFC.

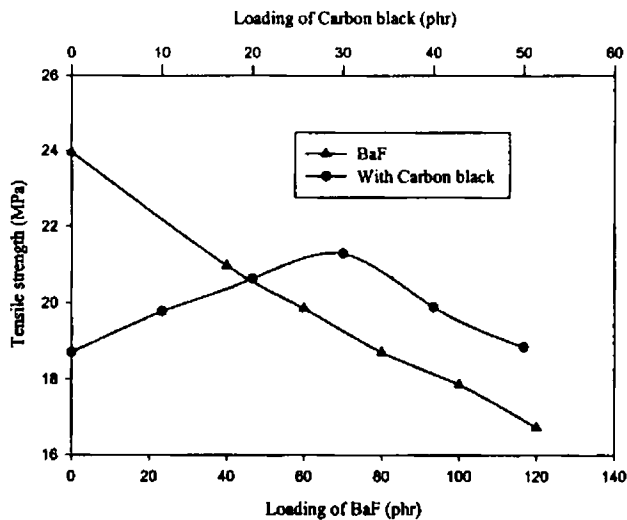
**Table 4.1 Mechanical Properties of natural rubber based RFCs containing barium ferrite**

Barium ferrite loading (phr)	Tensile Strength (MPa)	Elongation at break (%)	200 % Modulus (MPa)	300% Modulus (MPa)	Hardness (Shore A)
0	23.95	691.1	3.14	4.88	40
40	20.97	623.3	4.37	7.10	42
60	20.90	516.2	5.35	8.74	45
80	18.70	504.8	5.49	8.59	47
100	18.50	485.1	5.83	9.26	49
120	16.72	482.9	6.32	9.68	52

**Table 4.2 Mechanical properties of natural rubber based RFCs containing 80 phr of barium ferrite and various loading of carbon black**

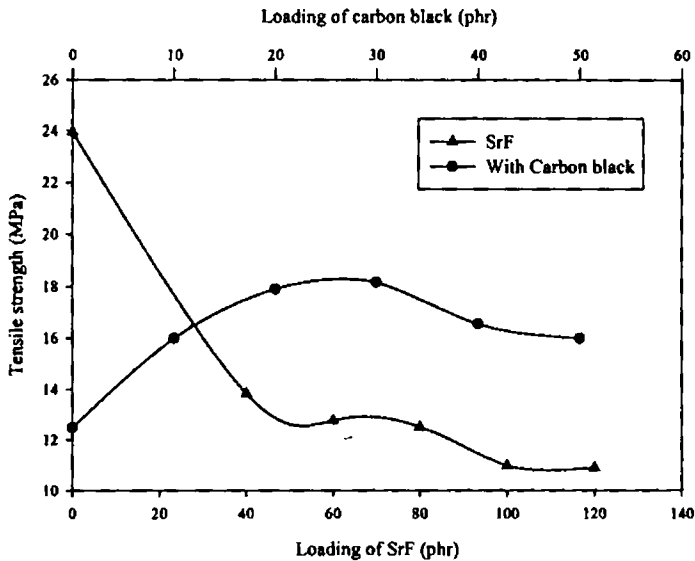
Carbon black loading (phr)	Tensile Strength (M Pa)	Elongation at break (%)	200 % Modulus (M Pa)	300 % Modulus (M Pa)	Hardness (Shore A)
0	18.70	504.9	5.49	8.59	47
10	16.88	494.6	6.17	9.48	48
20	15.83	415.9	6.52	10.42	51
30	15.29	370.1	8.51	12.75	54
40	14.89	356.5	7.89	12.39	61
50	14.84	317.1	9.43	13.96	65

Figure 4.18 shows the variation in tensile strength of NR based RFCs containing the various loadings of barium ferrite and its effect on the addition of carbon black.



**Fig.4.18 Variation in tensile strength versus loading of BaF and carbon black.**

The variation in tensile strength of NR based RFC containing the various loading of strontium ferrite and its effect on the addition of carbon black is shown in figure 4.19.



**Fig 4.19 Variation in tensile strength versus loading of SrF and carbon black.**

In both the cases the tensile strength decreased with the addition of ferrites. This is due to the poor interfacial adhesion between the ferrite filler and natural rubber. Filler reduces the effective cross section of the matrix in the RFC. This leads to an increase in internal stress, at any given external loading, compared to that of the unfilled rubber matrix. Stress concentration caused by the filler also contributes to internal stress. Micro plastic deformation occurs around the filler particles, which facilitate damage of the material at lower external load, as compared to the unfilled material<sup>13</sup>. As a consequence of the differential thermal expansion coefficient, thermally induced internal stresses also occur around the filler particles. This contributes to an increase of the dewetting stress.



Both surface area and its specific activity are important factors in reinforcement<sup>14,15</sup>. It is known that the reinforcement factor is a product of the total surface area and specific activity. The particle size contributes to reinforcement physically, while surface activity enhances the chemical contribution. However, the physical adsorption of filler is of much greater importance than its chemical nature for the mechanical properties of rubbers. The average particle size determination by employing Debye –Scherrer equation has shown that the particle sizes of these hexagonal ferrites are greater than that of N330 carbon black (20-30 nm). Particles having smaller size will have a much greater reinforcement effect than coarser ones. The total interface area between the filler and the elastomer depends upon the surface area of the filler and the amount of filler in the compound. Since the particle size of BaF and SrF are higher than that of carbon black, the extent of interface between the polymer and ferrite filler is less. Thus the RFCs with ferrite fillers showed a lower tensile strength than that containing carbon black. The mechanical properties will also be reduced at higher filler loading because of the dilution effect, which is due to the diminishing volume fraction of polymer in the composite. The addition of carbon black to RFCs containing 80 phr of BaF and SrF showed an increase in tensile strength up to a loading of 30 phr and thereafter it decreased slightly. This is because of the fact that carbon black is a good reinforcing filler and above 30 phr loading the tensile strength decreases because of the dilution effect.

The modulus of the composites increased with the incorporation of both ferrite filler and carbon black, which is characteristic of reinforcing filler. The modulus at 300 % of these rubber ferrite composites showed a steady increase with addition of BaF. Addition of 10 phr of carbon black to RFC with 80 phr of BaF showed the same modulus as that obtained by 120 phr of BaF, which indicated the reinforcing character of carbon black. Figure 4.20 depicts the variation in 300 % modulus against the loading of BaF, which shows a linear trend.

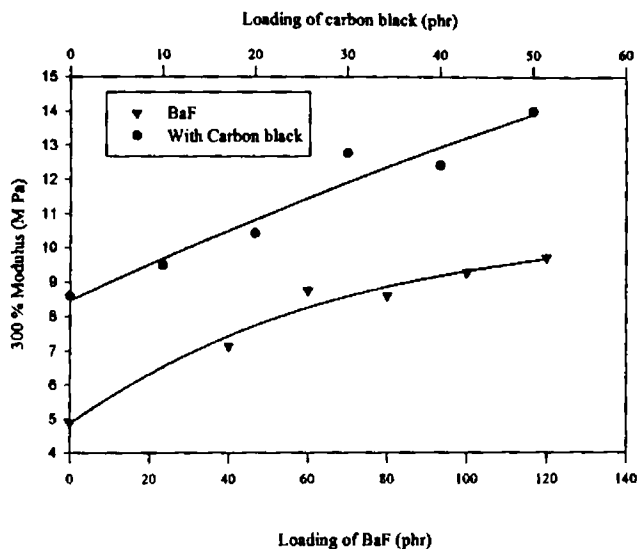


**Fig 4.20 Variation in modulus at 300 % elongation against the loading of BaF and carbon black**

The mechanical properties of the RFC containing various loadings of SrF in natural rubber are shown in table 4.3. Table 4.4 shows the effect of carbon black on the mechanical properties of RFC.

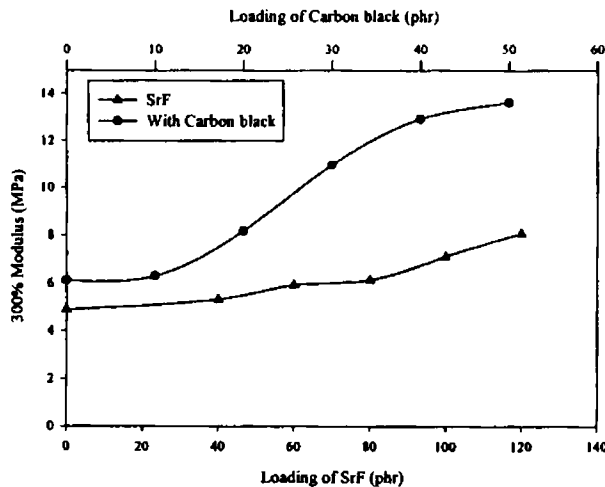
**Table 4.3 Mechanical properties of natural rubber based RFCs containing strontium ferrite**

Strontium ferrite loading (phr)	Tensile strength (MPa)	Elongation at break (%)	200 % Modulus (MPa)	300% Modulus (MPa)	Hardness (Shore A)
0	23.95	691.2	3.14	4.88	40
40	13.82	687.9	1.29	5.30	44
60	12.75	615.8	1.67	5.90	47
80	12.49	606.7	1.94	6.10	50
100	10.97	506	2.76	7.09	55
120	10.88	496	2.78	8.05	58

**Table 4.4 Mechanical properties of natural rubber based RFCs containing strontium ferrite and carbon black**

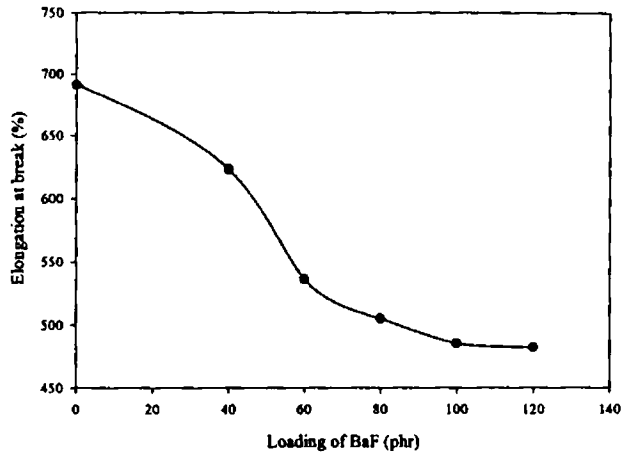
Carbon black loading (phr)	Tensile Strength (MPa)	Elongation at Break (%)	200 % Modulus (MPa)	300 % Modulus (MPa)	Hardness (Shore A)
0	12.49	606.7	1.95	6.10	50
10	15.99	481.2	3.75	6.27	53
20	17.09	463.9	4.80	8.17	57
30	18.16	425.9	6.09	10.93	60
40	16.54	357.8	7.64	12.91	64
50	15.98	356.6	7.88	13.60	67

Figure 4.21 represents the variation in modulus at 300 % elongation against the loading of SrF, which also showed an increasing trend with the filler loading. In the presence of carbon black the modulus further increased. Addition of 20 phr of carbon black to 80 phr of SrF showed almost same modulus as that obtained by 120 phr of SrF.



**Fig 4.21 Variation in modulus at 300% elongation versus loadings of SrF and carbon black**

The elongation at break of the rubber ferrite composites with the addition of barium ferrite is shown in figure 4.22.



**Fig 4.22 Variation in elongation at break with the addition of BaF.**

The elongation at break of the RFC containing SrF, with and without carbon black is shown in figure 4.23. The elongation at break showed a decreasing trend with increasing loading of ferrite fillers and carbon black in the case of natural rubber based RFCs.

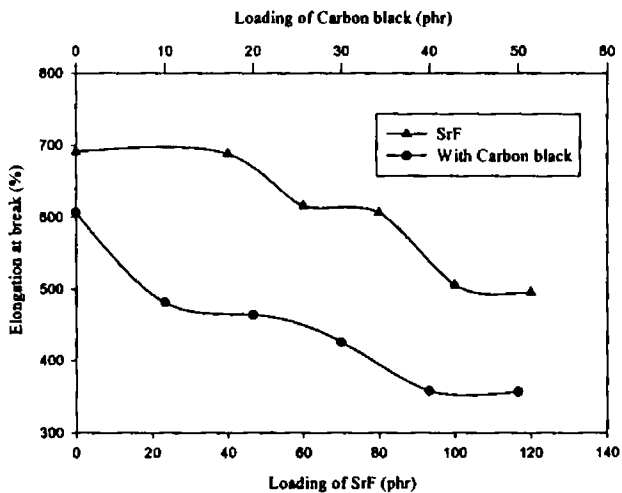


**Fig 4.23 Variation in elongation at break versus loading of SrF and carbon black.**

The hardness of these magnetic materials showed a steady increase with the filler loadings Figure 4.24 represents the variation in hardness for RFC containing BaF and carbon black in NR.

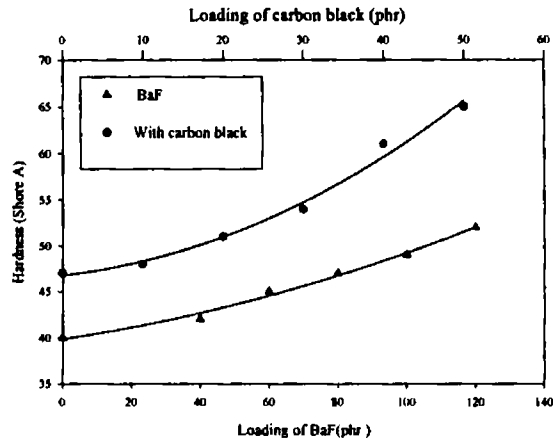


**Fig 4. 24 Variation in hardness for RFC containing BaF and carbon black in NR.**

Fig 4.25 depicts the increase in hardness of the RFC containing SrF and carbon black in NR

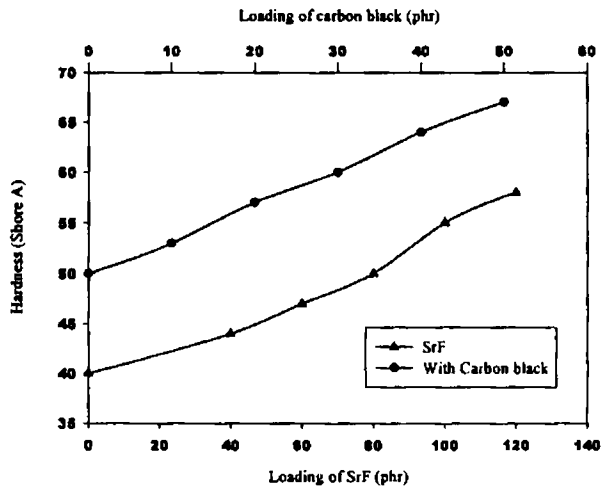


**Fig 4.25 Variation in hardness of the RFC containing SrF and carbon black in NR**

Addition of 20 phr carbon black to the RFC with 80 phr of ferrite filler showed an equivalent hardness to that containing 120 phr of BaF or SrF. This indicated that the carbon black is enhancing the hardness of the composites, which is on expected lines. Even after the addition of 50 phr of carbon black to RFCs containing 80 phr of ferrite filler, they found to be flexible and serviceable. This property can be exploited to make flexible magnets suitable for various applications.

#### 4.3.1.2 Nitrile rubber based RFCs

The mechanical properties of the RFC containing various loadings of BaF in nitrile rubber are shown in table 4.5. Table 4.6 shows the effect of carbon black on the tensile properties of RFC. Figure 4.26 shows the variation in tensile strength of RFC with the loading of barium ferrite and carbon black.

**Table 4.5 Mechanical Properties of nitrile rubber based RFCs containing barium ferrite**

Barium ferrite loading (phr)	Tensile strength (MPa)	Elongation at break (%)	200 % Modulus (MPa)	300% Modulus (MPa)	Hardness (Shore A)
0	2.13	465.9	1.74	2.09	55
40	2.93	456.0	1.78	2.10	58
60	3.12	445.0	1.79	2.11	62
80	3.29	439.9	1.83	2.14	65
100	3.44	394.0	1.87	2.14	67
120	3.26	304.7	1.90	2.24	69

**Table 4.6 Mechanical properties of nitrile rubber based RFCs containing barium ferrite and carbon black**

Carbon black loading (phr)	Tensile Strength (MPa)	Elongation at Break (%)	200 % Modulus (MPa)	300 % Modulus (MPa)	Hardness (Shore A)
0	3.29	439.9	1.83	2.14	65
10	6.35	428.2	2.29	3.56	70
20	11.59	422.3	3.03	5.48	74
30	15.26	410.1	4.99	9.60	76
40	19.02	389.7	5.88	11.68	78
50	20.76	345.3	7.80	15.39	81

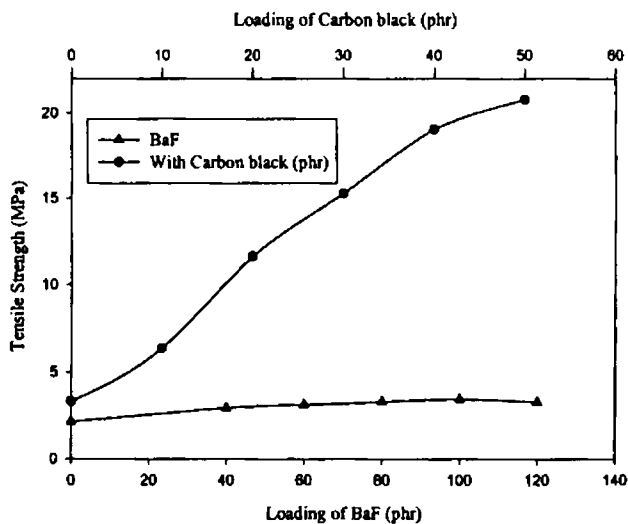


**Fig 4.26 variation in tensile strength of RFC versus loading of BaF and carbon black in NBR**

The variation in tensile strength of RFC containing the various loadings of strontium ferrite and its effect on the addition of carbon black is shown in figure 4.27.

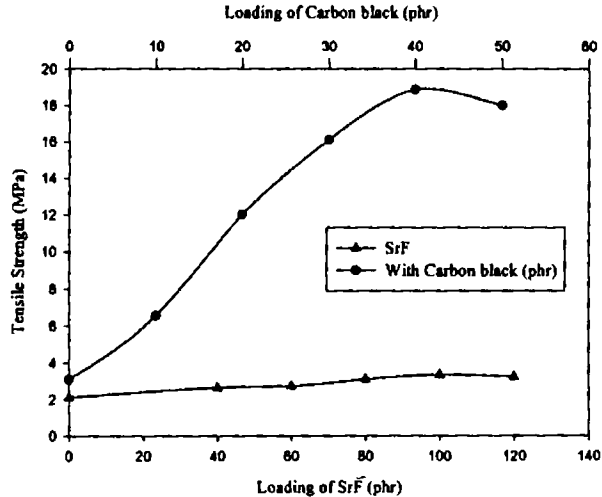
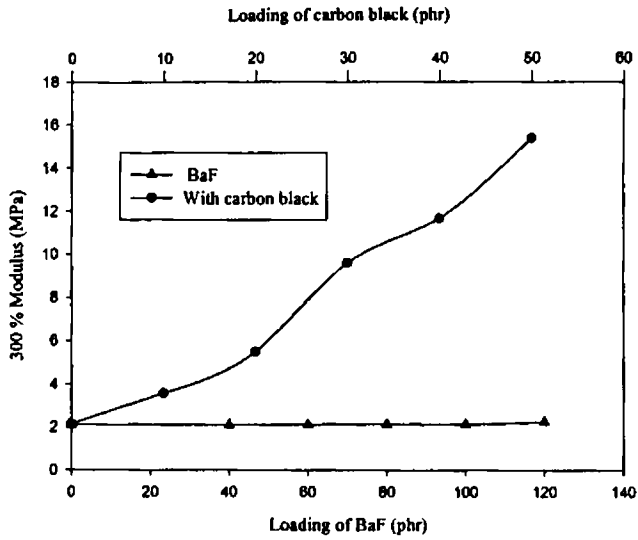


**Fig 4.27 Variation in tensile strength of RFC containing SrF with and without carbon black.**

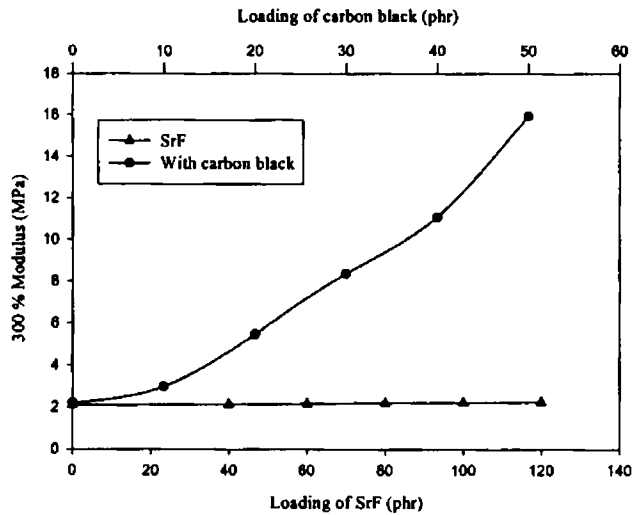
NBR gum vulcanisate has relatively low tensile strength compared to NR gum vulcanisate due to lack of stress induced crystallization. The gum NBR vulcanisate showed low tensile strength (2.13 MPa), which increased with increasing filler loading. The addition of ferrite filler reinforce the NBR matrix and showed a maximum reinforcement in the presence of carbon black. The addition of the carbon black along with ferrite filler increased the tensile strength greatly (around 20 MPa), since it act as a good reinforcing filler. The tensile strength reduced at higher filler loadings because of the dilution effect, which is due to the diminishing volume fraction of polymer in the composite.

Figure 4.28 represents the variation in modulus at 300 % elongation with the loading of BaF filler and carbon black in nitrile rubber. Figure 4.29 depicts the change in modulus with the loading of SrF and carbon black filler in nitrile rubber. The modulus increased slightly with the addition ferrite fillers, but the increase was more with the loading of carbon black



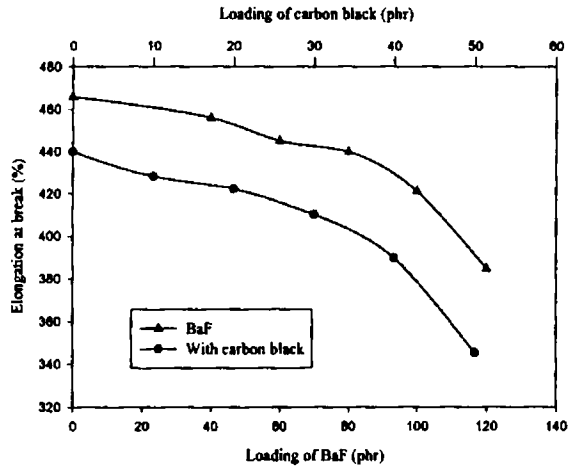


**Fig 4.28** Variation in 300 % modulus with the loading of BaF and carbon black in NBR.



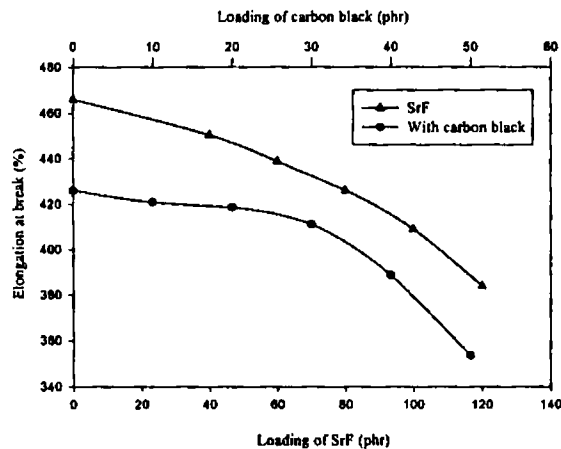
**Fig 4.29** Variation in 300 % modulus with the loading of SrF and carbon black filler in NBR.

The elongation at break of the RFC based on NBR containing BaF with and without carbon black is shown in figure 4.30.



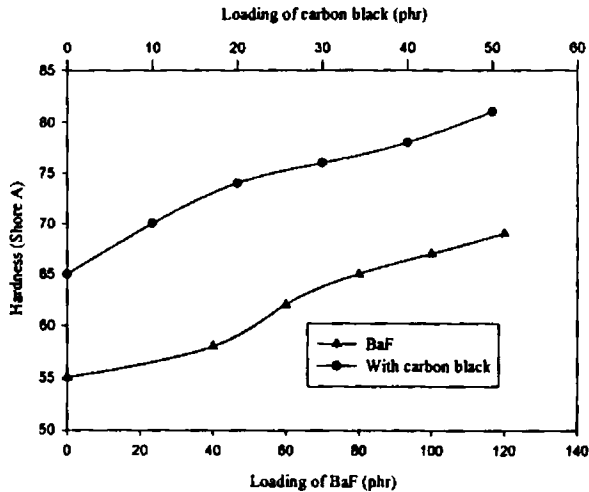
**Fig 4.30 Variation in elongation at break versus loading of BaF and carbon black.**

Figure 4.31 shows the elongation at break of the RFC containing SrF with and without carbon black. The elongation at break showed a steady decrease with increasing loading of ferrite fillers and carbon black in the case RFCs based on nitrile rubber.



**Fig 4.31 Variation in elongation at break versus loading of SrF and carbon black.**

The hardness of these magnetic composites showed a steady increase with the filler loadings Figure 4.32 shows the variation in hardness for RFC containing BaF and carbon black in NBR.



**Fig 4.32 Variation in hardness for RFC containing BaF and carbon black in NBR.**

Figure 4.33 depicts the increase in hardness with SrF and carbon black loading in NBR based composites. Addition of 10 phr carbon black to the RFC containing 80 phr of ferrite fillers almost corresponded to that produced by 120 phr of ferrite.

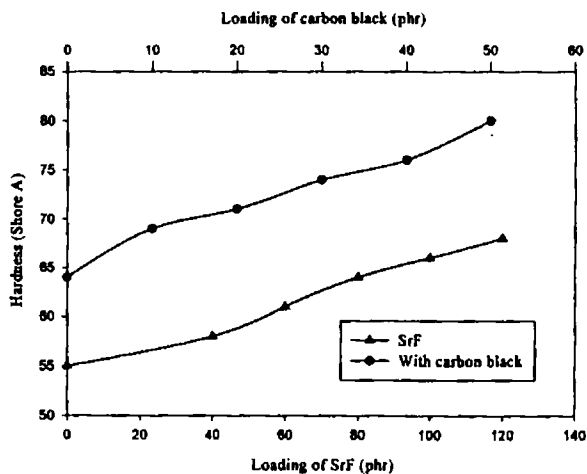


**Fig 4.33 Variation in hardness of the RFC containing SrF and carbon black in NR**

### 4.3.1.3 Abrasion Resistance

The abrasion resistance of the samples was determined using a DIN abrader (DIN 53516) as explained in the chapter 2. Figure 4.34 and 4.35 shows volume loss on abrasion of the rubber ferrite composites containing barium ferrite and strontium ferrite in nitrile rubber respectively.

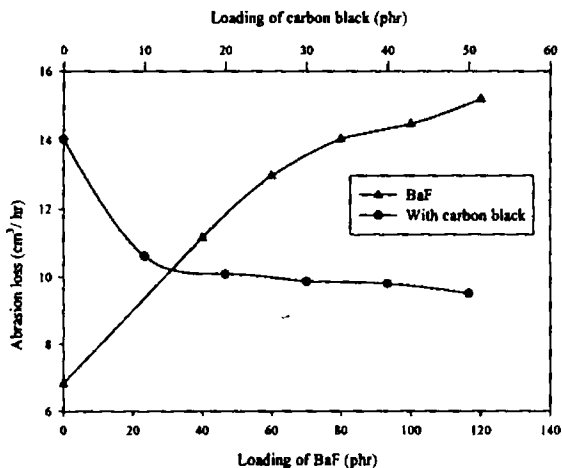


**Fig 4.34 Variation in volume loss on abrasion versus loading of BaF and carbon black in NBR**

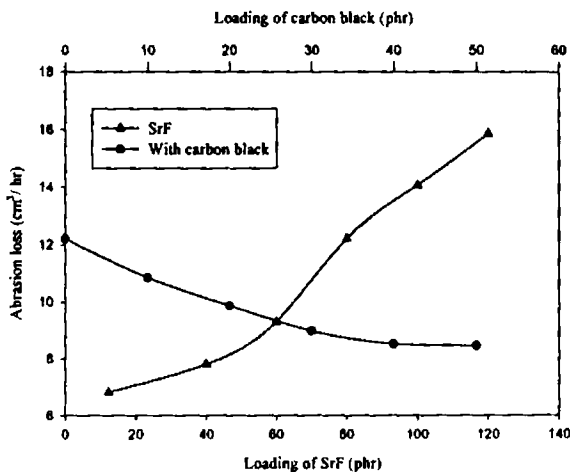


**Fig 4.35 Variation in volume loss on abrasion versus loading of SrF and carbon black in NBR**

The abrasion loss showed an increasing trend with the loading of ferrite fillers whereas in the case of rubber ferrite composites' containing various loading of carbon black it was less. This is because the particle size of carbon black is finer than that of ferrite fillers. Thus it is possible to produce flexible magnets for various applications, which requires high abrasion resistance by the incorporation of different loading of carbon black.

#### **4.4 CONCLUSION**

The studies on cure characteristics of rubber ferrite composites indicated that the addition of magnetic fillers reduces both the scorch time and cure time. The minimum and maximum torque values increased with the increasing loading of ferrite filler and carbon black. Even though the scorch time decreased and the torque values increased with the addition of these fillers, the processability of these composites were not affected. The mechanical properties of the rubber ferrite composites can be enhanced by the incorporation of appropriate amount of ferrite filler and carbon black. The evaluation of cure characteristics and mechanical properties revealed that the processability and flexibility of the matrix was not much affected even up to a loading of 120 phr of ferrite fillers.

**REFERENCES**

1. Safari Ardi M, Dick W and McQueen D.H, Plastic Rubber and Composites Processing Applications, **24** (1995) 157-164.
2. Anantharaman M. R, S. Jagatheesan, S. Sindhu, K. A. Malini, C. N. Chinnasamy, A. Narayansamy, P. Kurian and K. Vasudevan, Plastic Rubber and Composites Processing Applications, **27**, 2, (1998) 77-81.
3. Anantharaman M.R, S. Sindhu, S. Jagatheesan, K.A. Malini and Philip Kurian, Journal of Physics D Applied Physics **32** (1999) 1801-1810.
4. Mohammed E.M et al, Materials Research Bulletin **37** (2002) 753-768.
5. Katz H. S and J. V. Milewski, 'Handbook of Reinforcement of Plastics', 1978, Vannostrand Reinhold, New York.
6. Praveen Singh & T.C. Goel: Indian J. Pure and Appl Phys., **38** (2000) 213-219.
7. Anantharaman M. R, P. Kurian, B. Banerjee, E. M. Mohammed, and M. George, Kautschuk Gummi Kunststoffe, (Germany), **49**, 6/96, 424- 426.
8. Anantharaman M. R, K.A. Malini, S. Sindhu, E.M. Mohammed, S.K Date, S.D. Kulkarni, P.A. Joy, and Philip Kurian, Bull. Mater. Sci., **24**,6 (2001) 623-631.
9. Steven Blow. Handbook of Rubber Technology, Galgotia Publishing Pvt. Ltd. 1998.
10. Allen. W, Natural Rubber and the Synthetics, Granada Publishing Ltd. 1972.
11. Vishu Shah, Handbook of plastic testing technology, John Wiley and sons Inc., USA 1998.
12. Charles A Harper, Handbook of Plastic, Elastomers and Composites (2<sup>nd</sup> Edition) McGraw Hill Inc.1992.
13. Vollenberg. P, D.Heikens and H.C.B.Laden: Polymer Composites, **9** (1988) 382.
14. Blow C.M. and C.Hepburn, 'Rubber Technology and Manufacture', 2<sup>nd</sup> edition, (1985), Butterworths Publishers, London
15. Roberts. A.D, Natural Rubber Science and Technology, 1998, Oxford University Press, New York 556.

# Chapter 5

---

## DIELECTRIC PROPERTIES OF RUBBER FERRITE COMPOSITES

### 5.1 INTRODUCTION

Rubber ferrite composites are composite magnetic materials, which have the unique advantage of being modified so as to tailor make materials for specific applications. Generally composites can offer a combination of properties and a diversity of applications to produce materials that surpasses the performance of the individual components. Thus the composites can be designed to exploit the best properties of the constituents. Rubber ferrite composites prepared by incorporating ferrites in rubber matrixes are increasingly being used as microwave absorbers and in other devices where flexibility and mouldability is an important criterion. RFC utilises this property of the polymer matrix along with the dielectric properties of the magnetic fillers to obtain a combination of predetermined dielectric and mechanical properties required for definite applications. The dielectric and mechanical properties can be enhanced by the addition of required amount of carbon black. Dielectric measurements on materials provide valuable information about the matrix filler interaction, dispersion of filler and percolation threshold<sup>1-3</sup>, which are important designing parameters for application such as electromagnetic wave absorbers, EMI shielding materials<sup>4,5</sup> and many electronic applications<sup>6-10</sup>.

It has been known that the dielectric properties of polycrystalline materials are influenced by factors like preparative techniques, cation distribution, grain size,

the ratio of  $\text{Fe}^{3+}/\text{Fe}^{2+}$  ions, ac conductivity and sintering temperature <sup>11,12</sup>. The dielectric properties of ceramic ferrite samples are also influenced by various factors like method of preparation, sintering conditions, ionic charge, chemical composition and grain size. The dependence of these factors on the dielectric properties of ceramic fillers will have a profound influence on the overall physical properties of the composites <sup>13,14</sup>. When ferrites are fired at higher temperature it is possible that films of high resistivity over the constituent grains are formed. Such materials in which the individual grains are separated either by air gaps or by low conducting layers behave as a heterogeneous dielectric material.

The evaluation of dielectric, structural and magnetic properties of the ceramic BaF, SrF and RFCs are important since the interrelationship of the properties of the filler and the matrix will help in the design of devices for various applications.

RFCs containing BaF and SrF in natural and nitrile rubber matrix were prepared and their dielectric properties were evaluated. The ceramic ferrite samples were prepared by conventional solid-state reactions. Their incorporation in natural and nitrile rubber matrix was achieved according to a specific recipe. The details of preparation are cited in chapter 3. The variation in dielectric constant with frequency for the ceramic ferrite and RFCs were studied. The effect of loading of ferrite fillers and temperature on the dielectric constant of the composites was also studied and the results were correlated in this chapter.

The effect of carbon black on the dielectric properties of the rubber ferrite composites containing 80 phr of ferrite filler was also studied.

## **5.2 DIELECTRIC MEASUREMENTS**

The dielectric constants of both ceramic and composite samples were evaluated using a dielectric cell and an impedance analyser (Model: HP 4285A). The dielectric measurements were carried out at different frequencies ranging from 100 KHz to 8 MHz. This was repeated for different temperatures ranging from 303K to 393K.



### 5.2.1 Ceramic samples

The dielectric constant of BaF and SrF samples were determined using an experimental set up as described in chapter 2. The samples were made in the form of pellets using a hydraulic press by exerting a pressure of 9 tons. These circular disc pellets having a diameter of 10mm was loaded into the dielectric cell. The lead and fringe capacitance was eliminated by a method described by Ramasastry and Syamasundara Rao <sup>15</sup>. The capacitances at 303K were measured in the frequency range 100KHz to 8 MHz. This was repeated at different temperatures of 313K, 333K, 353K, 373K, and 393K. The dielectric constant,  $\epsilon_r$  was calculated using the formula

$$C = \epsilon_0 \epsilon_r A/d \quad (5.1)$$

Where A is area of sample piece used, d is the thickness of the sample,  $\epsilon_r$  is the dielectric constant of the medium and  $\epsilon_0$  is the dielectric constant of air and C is the observed capacitance of the sample. Dielectric constants at various temperatures and frequencies were also determined. Knowledge of dielectric properties of the ceramic samples at various frequencies and temperatures was considered as a prerequisite, since the same material has to be incorporated in the rubber matrix.

#### 5.2.1.1 Effect of frequency on dielectric properties

In ferrite materials, very high dielectric constant at very low frequencies, have been reported by various researchers <sup>16-20</sup>. The reported values for dielectric constant of ceramic samples show that the dielectric constant fall from a dc value of several thousands to the normal values of the order of tens for a frequency of around 100 KHz. These results have been explained by Koops phenomenological theory and Maxwell-Wagner interfacial polarization <sup>16,21</sup>.

The dielectric constants of the ceramic samples of BaF and SrF versus frequency were plotted at different temperatures and are shown in figures 5.1 and 5.2. A decrease in dielectric constant with increase of frequency was observed in this case also. This decrease was rapid at lower frequencies (up to 2MHz) and slower at higher frequencies. The dielectric constant measurements were made up to a maximum frequency of 8 MHz. The variation pattern remained the same for both BaF and SrF. The dielectric constant of BaF decreased from 25.85 at 100 KHz

to 7.92 at 8 MHz whereas that of SrF decreased from 21.5 to 9.26 in the same frequency range.

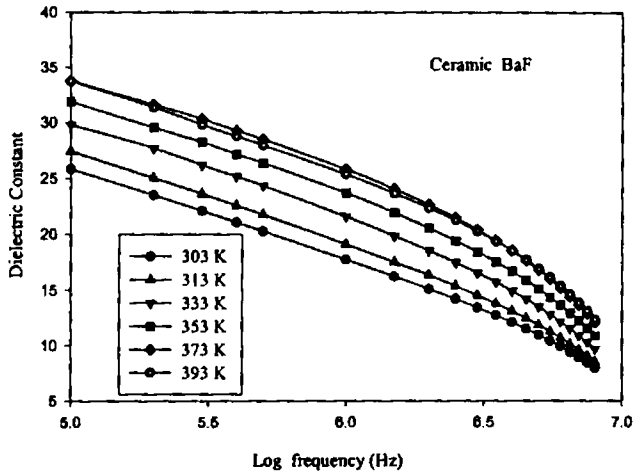


**Fig 5.1 Dielectric constant ( $\epsilon$ ) of ceramic BaF versus log frequency (Hz) at different temperatures**

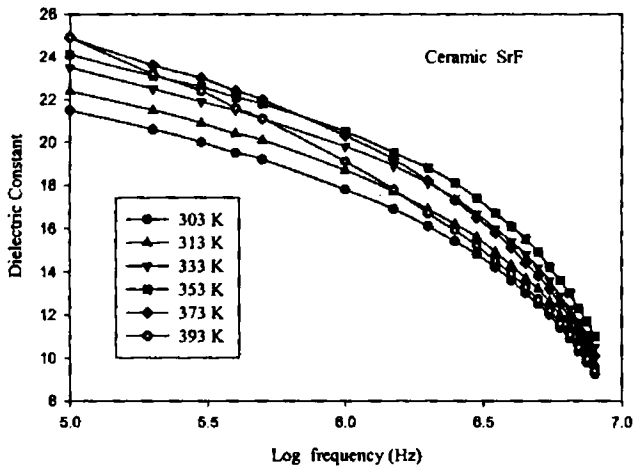


**Fig 5.2 Dielectric constant ( $\epsilon$ ) of ceramic SrF versus log frequency (Hz) at different temperatures.**

The observed decrease in dielectric constant with increase in frequency can be explained using Koop's phenomenological theory of dispersion<sup>21</sup>, which is based on Maxwell Wagner theory of interfacial polarization. It is assumed that the

dielectric structure of ferrites is formed in two layers, namely, the well conducting grains and poorly conducting grain boundaries. At very low frequencies the oxide grain boundaries are more active and this contributes to the very high dielectric constant at low frequencies. A general relation of the following form explains the variation of dielectric constant with frequency.

$$\epsilon'' = (\sigma - \sigma') / (\epsilon' \times \omega) \quad (5.2)$$

where  $\epsilon'$  and  $\epsilon''$  are the real and imaginary part of the dielectric constant,  $\sigma$  and  $\sigma'$  are the ac and dc conductivities respectively, and  $\omega$  is the angular frequency which is equal to  $2\pi f$ , where  $f$  is frequency of the applied field.

### 5.2.1.2 Effect of temperature on dielectric properties

The effect of temperature on the dielectric constant for the ceramic samples was studied in the temperature ranging from 303K to 393K. At this temperature range the permittivity value of BaF increased from 25.85 to 33.76 at 1KHz and that of SRF increased from 21.50 to 24.90. The variation in dielectric constant with temperature for ceramic BaF and SrF are shown in figures 5.1 and 5.2 respectively. It was observed that the dielectric constant of ceramic samples increased with increase of temperature. In dielectrics, the dielectric constant increases with temperature because of the increase in ionic polarization<sup>19</sup>. The high dielectric constants at low frequencies and high temperatures can be explained by the presence of permanent dipole moments indicating a small effective charge separation. Such a small separation must be due to asymmetry in the fields experienced by either oxygen or metallic ions. In most cases, the atoms or molecules in the samples cannot orient themselves at low temperature region. When temperature rises the orientation of these dipoles is facilitated and this increases the dielectric polarization. But at very high temperature the chaotic thermal oscillations of molecules are intensified and the degree of orderliness of their orientation is diminished and thus the permittivity passes through a maximum value. In the present study the maximum temperature of measurement was only 393K and no decrease in dielectric constant was observed. Higher temperatures were not considered in these experiments, since the upper service temperature

required for most of the RFC based products is below 373K. More over the polymer matrix degrades at higher temperatures. The variation in dielectric constant with temperature at low frequencies (100 KHz) was much more pronounced than at higher frequencies. For both the samples similar behaviour was observed. At higher frequencies temperature has little effect on the dielectric constant<sup>22,23</sup>.

### 5.2.2 Dielectric properties of gum natural rubber vulcanisate

The dielectric constant at different temperatures and frequencies of the gum natural rubber vulcanisate was evaluated. The dielectric constant of unvulcanised natural rubber is reported to be in the range 2.6 to 3.0. A dielectric constant of 3.22 was obtained for gum NR vulcanisate. A decrease in dielectric constant with increase in temperature was observed for natural rubber. The variation pattern is shown in figure 5.3. This is because as temperature increases the mobility of the polymer chain increases and hence density decreases<sup>21</sup>. The reduction in polymer density will cause a decrease in dielectric constant.

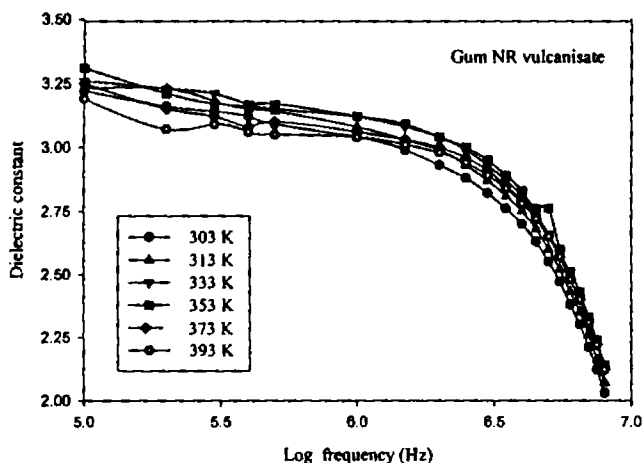


**Fig 5.3 Dielectric constant versus log frequency of gum NR vulcanisate at different temperatures.**

### 5.2.3. Dielectric Properties of gum nitrile rubber vulcanisate

The dielectric properties of gum nitrile rubber vulcanisate were also evaluated. A dielectric constant of 13.7 was observed for nitrile rubber vulcanisate at low frequencies and it decreased with increase in frequency. The high dielectric constant of the nitrile rubber, compared to the natural rubber indicates that it is superior in dielectric properties, compared to NR. The temperature dependence of dielectric constant for the nitrile rubber matrix was also carried out. It showed a slight increase in dielectric constant at low temperatures (13.9 at 313K) and then decreased with increase in temperature. The increasing trend in dielectric values was more pronounced at higher frequencies. At 2 MHz the dielectric value increased with temperature up to 373K and then decreased slightly. The variation pattern is shown in figure 5.4.

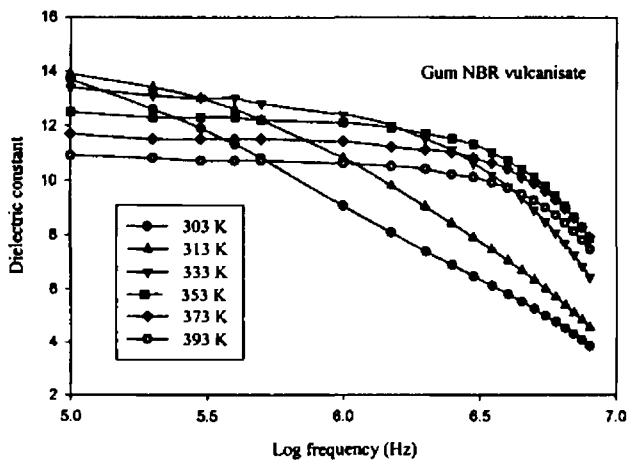


**Fig 5.4 Dielectric constant versus log frequency of gum NBR vulcanisate at different temperatures**

### 5.3. DIELECTRIC STUDIES OF NATURAL RUBBER BASED RUBBER FERRITE COMPOSITES

The dielectric properties of RFCs based on natural rubber were carried out at different frequencies and temperatures. The dependence of dielectric constant on various factors like frequency, temperature and loading of ferrite fillers and carbon black were studied.

### 5.3.1 Rubber Ferrite Composites containing barium ferrite

The RFCs containing BaF in natural rubber was prepared as cited in chapter 3. The dielectric properties of these RFCs and the effect of the addition of carbon black were studied in detail.

#### 5.3.1.1 Effect of frequency on dielectric properties of RFC

The dielectric properties of natural rubber based RFCs with change in frequency at different temperatures were carried out in detail. Almost similar behaviour as that of the ceramic component present in the matrix was obtained in the case of RFCs. The absolute values of the dielectric constant of the composites were found to be greater than that of the gum NR vulcanisate, but less than that of the ceramic BaF. It can be seen that the dielectric constant decreased with frequency for composites containing different loadings of BaF. This behaviour is in accordance with the Maxwell Wagner theory of interfacial polarization. Figures 5.5a to 5.5e shows the variation in dielectric constant of RFC with frequency at different temperatures.

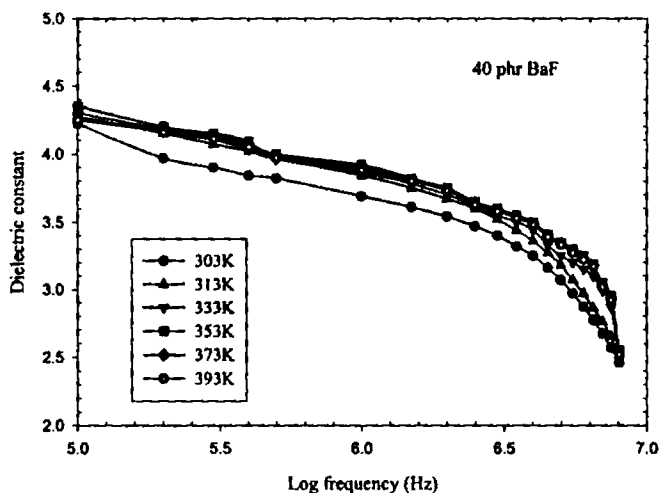


**Fig 5.5a Dielectric constant versus log frequency of NR based RFC containing 40 phr BaF at different temperatures**

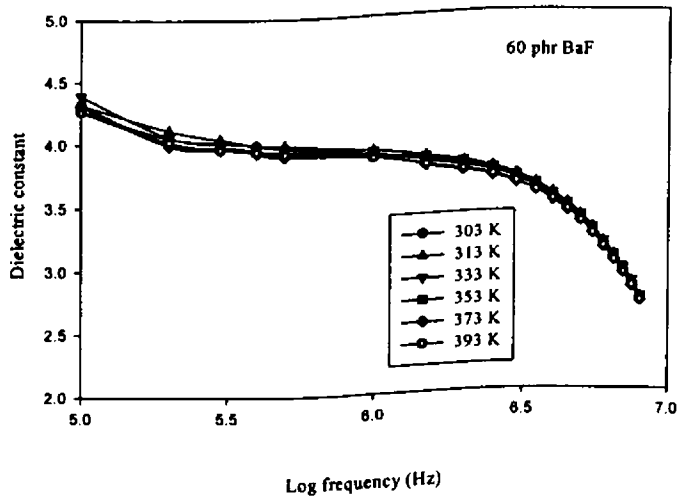


**Fig 5.5b Dielectric constant versus log frequency of NR based RFC containing 60 phr of BaF at different temperatures**

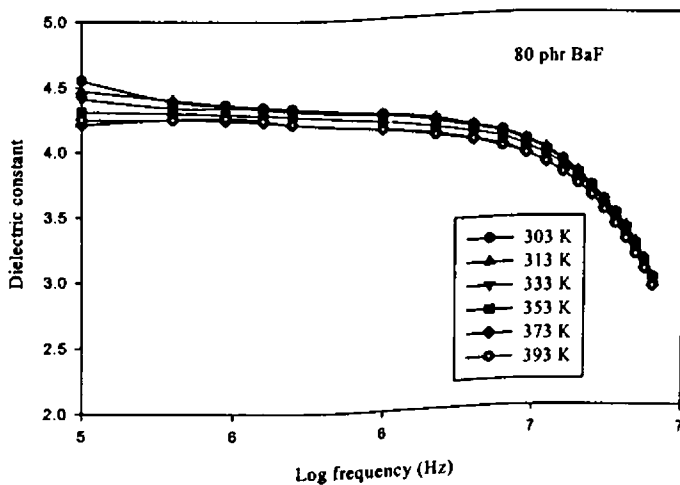


**Fig 5.5c Dielectric constant versus log frequency of NR based RFC containing 80 phr of BaF at different temperatures**

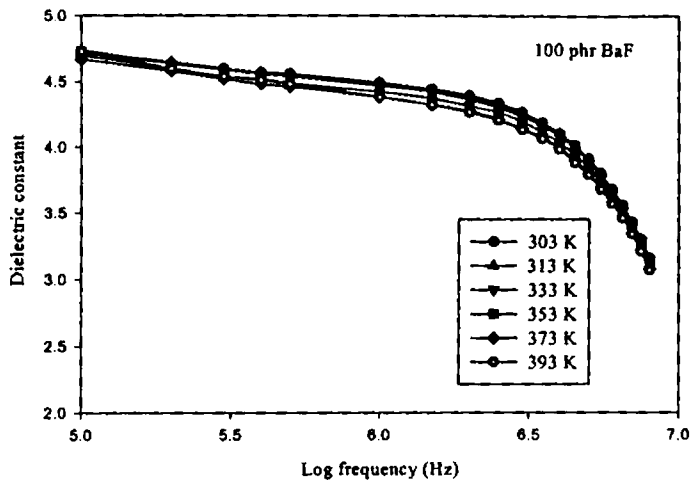


**Fig 5.5d Dielectric constant versus log frequency of NR based RFC containing 100 phr of BaF at different temperatures**

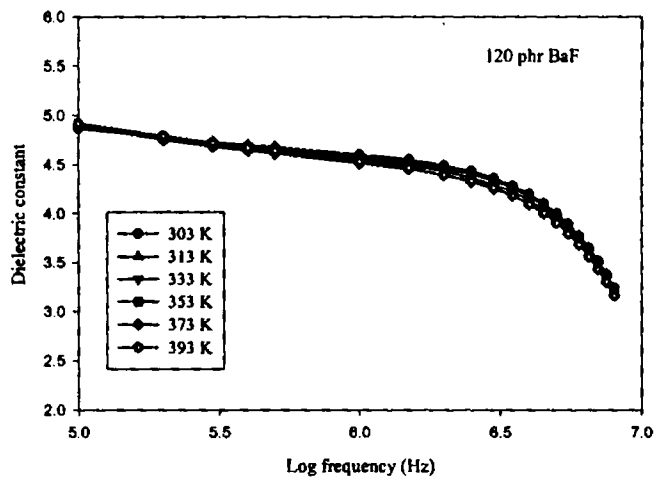


**Fig 5.5e Dielectric Constant versus log frequency of NR based RFC containing 120 phr of BaF at different temperatures**



Figures 5.6a and 5.6b represents the variation in dielectric constant with frequency for different loading of BaF at 303K and 393 K respectively.

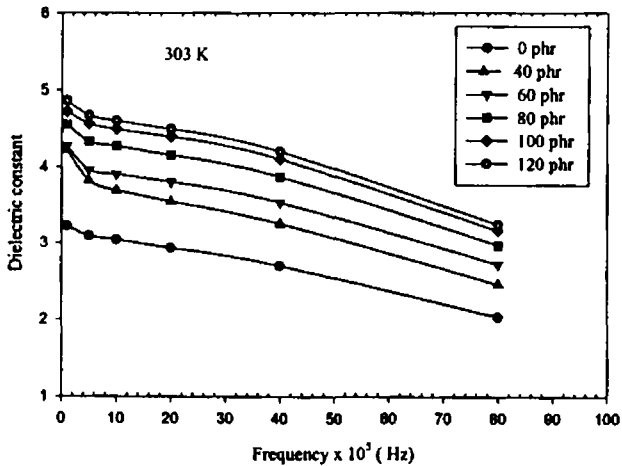


**Fig 5.6a Dielectric constant versus frequency of NR based RFC for different loading of BaF at 303K**

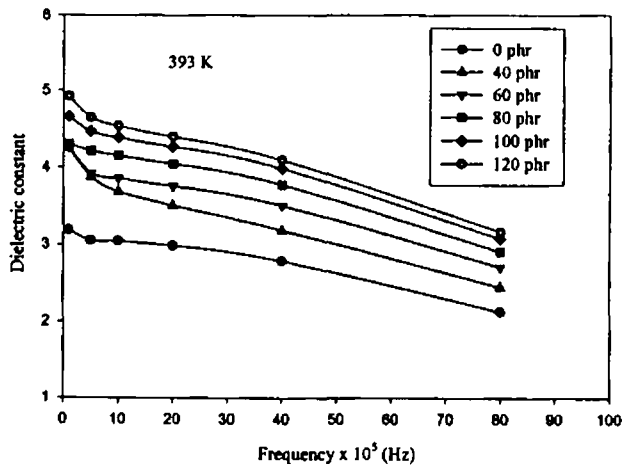


**Fig 5.6b Dielectric constant versus frequency of NR based RFC for different loading of BaF at 393 K**

Figures 5.7a and 5.7b depicts the variation in dielectric constant with frequency for different loadings of carbon black at 303K and 393 K respectively. It was observed that the variation in dielectric constant with frequency was more pronounced at higher loadings of carbon black.

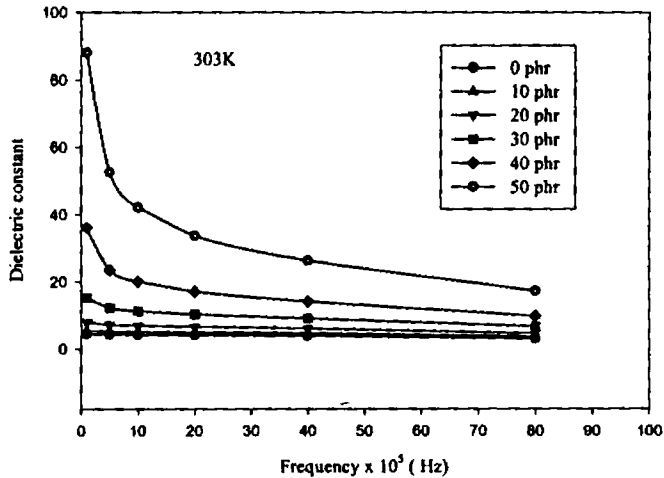


**Fig 5.7a Dielectric constant versus frequency of NR based RFC containing 80 phr of BaF and various loadings of carbon black at 303K**

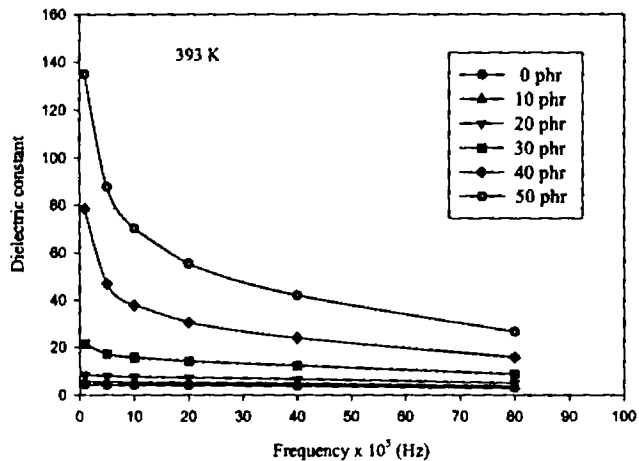


**Fig 5.7b Dielectric constant versus frequency of NR based RFC containing 80 phr of BaF and various loadings of carbon black at 393K**

### 5.3.1.2 Effect of temperature on dielectric properties of RFC

The effects of temperature on the dielectric properties of natural rubber based RFCs containing BaF at various frequencies were studied. The dielectric constant of rubber ferrite composites increased with increase in temperature. In these composites the increase in dielectric constant with temperature was not so prominent as in the case of ceramic samples. Representative graphs showing the variation in dielectric constant with temperature for different loadings of BaF at selected frequencies are shown in figures 5.8a to 5.8c.

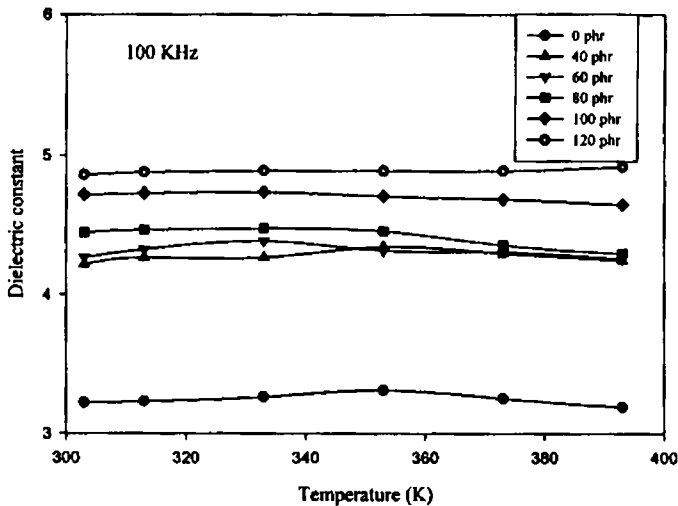


**Fig 5.8a Dielectric constant versus temperature of NR based RFC for different loadings of BaF at 100 KHz**

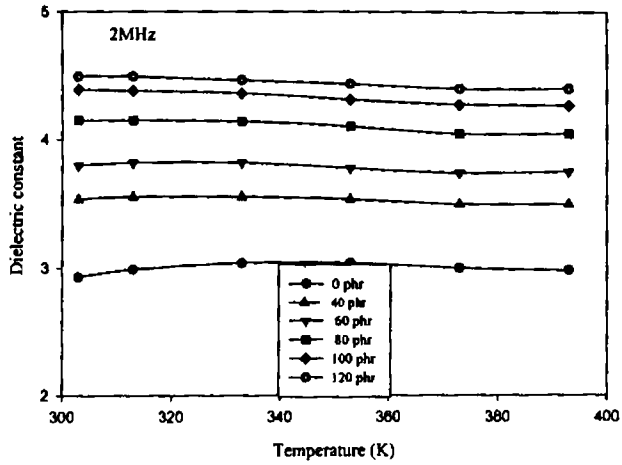


**Fig 5.8b Dielectric constant versus temperature of NR based RFC for different loadings of BaF at 2 MHz**

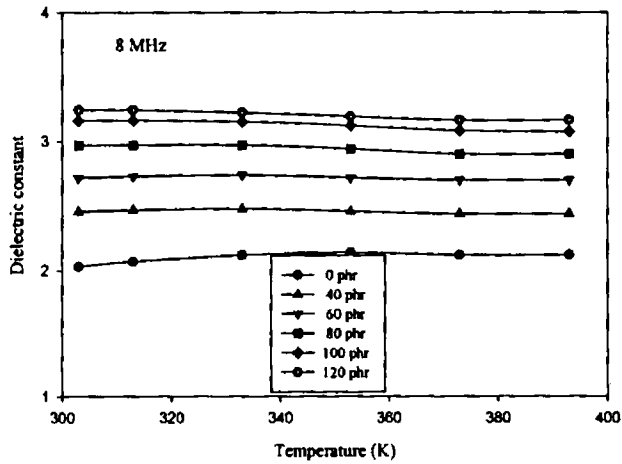


**Fig 5.8c Dielectric constant versus temperature of NR based RFC for different loadings of BaF at 8 MHz**

But the RFC containing carbon black showed large increase in the permittivity values, which is evident from the figures 5.9a to 5.9c. It was also observed that the variation of dielectric constant with temperature was more at higher loading of carbon black.

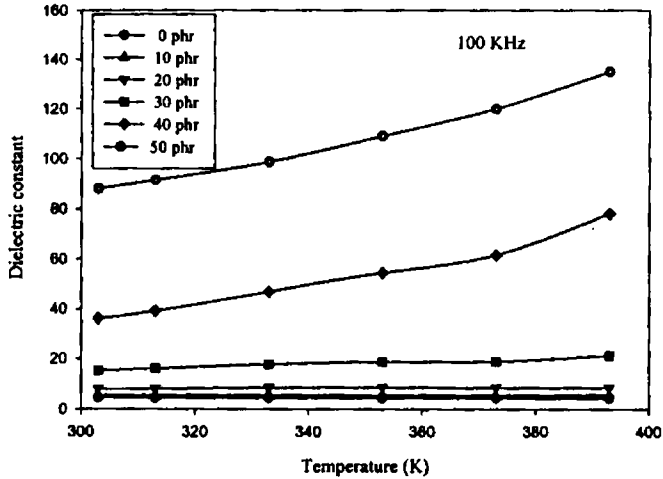


**Fig 5.9a Dielectric constant versus temperature of NR based RFC containing 80 phr of BaF and various loading of carbon black at 100 KHz.**

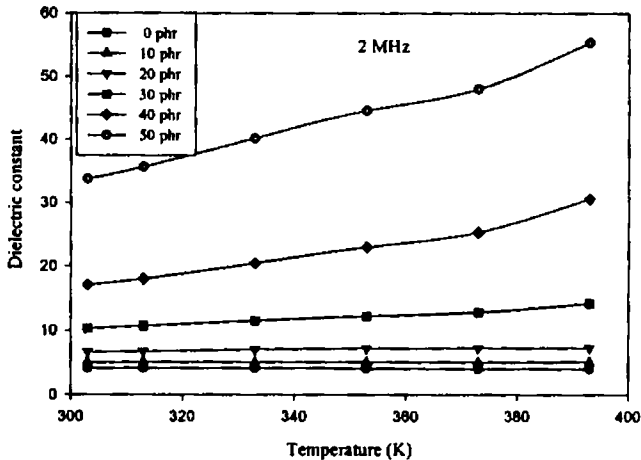


**Fig 5.9b Dielectric constant versus temperature of NR based RFC containing 80 phr of BaF and various loading of carbon black at 2 MHz**

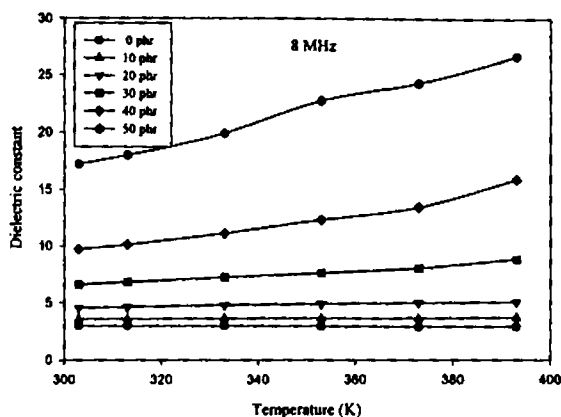


**Fig 5.9c Dielectric constant versus temperature of NR based RFC containing 80 phr of BaF and different loadings of carbon black at 8 MHz**

### 5.3.1.3 Effect of loading on dielectric properties of RFC

Variation in dielectric constant with the loading of BaF was also studied. Figures 5.10a to 5.10f shows the variation in dielectric constant with loading of BaF at different frequencies and temperatures. The dielectric constant was found to increase with increase in weight fraction of the ferrite material. Dielectric constant was found to be maximum for a loading of 120phr of BaF. It increased from 3.22 in the case of NR gum vulcanisate to 4.86 for composite containing 120 phr of BaF at 100 KHz. As the frequency increased from 100 KHz to 8MHz the dielectric constant decreased from 4.86 to 3.24.

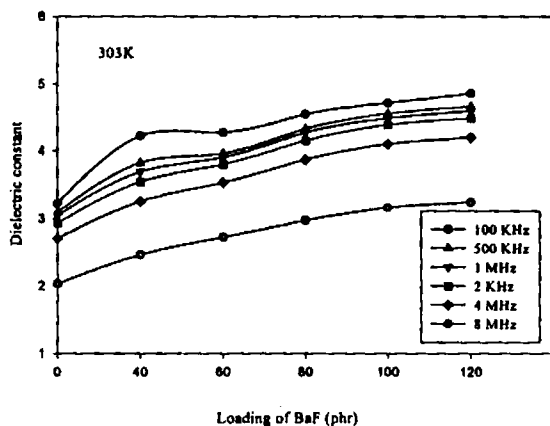


**Fig 5.10a Dielectric constant versus loading of BaF in NR for different frequencies at 303K**

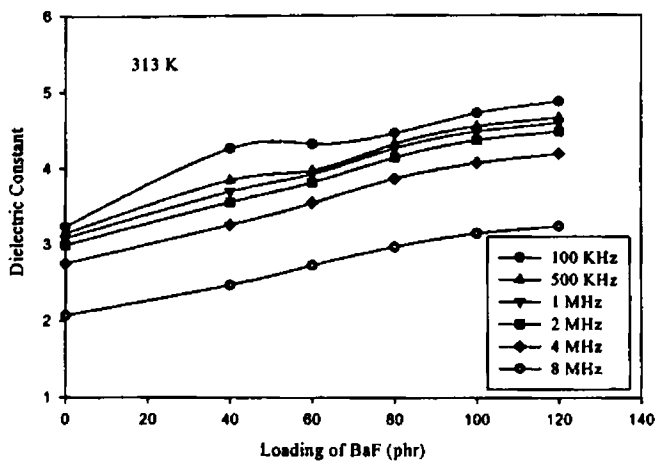


**Fig 5.10b Dielectric constant versus loading of BaF in NR for different frequencies at 313K**

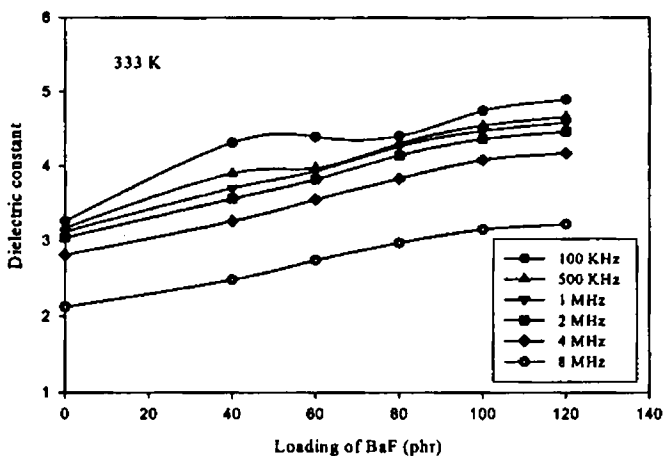


**Fig 5.10c Dielectric constant versus loading of BaF in NR for different frequencies at 333K**

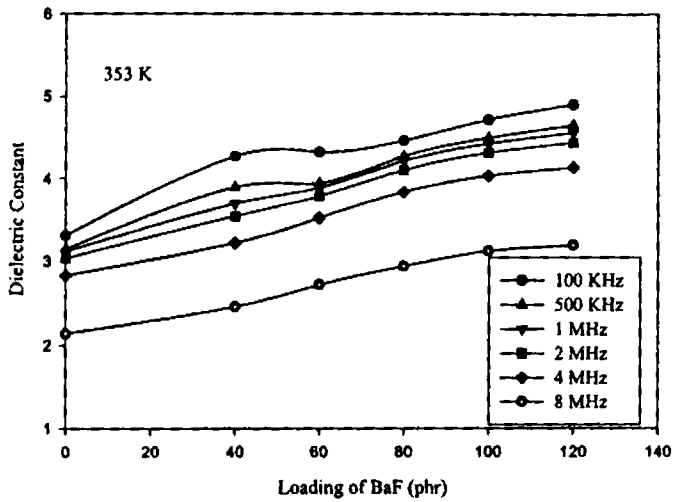


**Fig 5.10d Dielectric constant versus loading of BaF in NR for different frequencies at 353K**

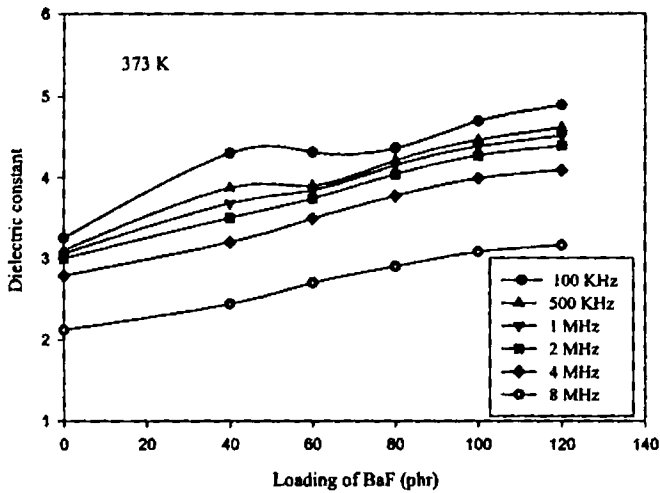


**Fig 5.10e Dielectric constant versus loading of BaF in NR for different frequencies at 373K**



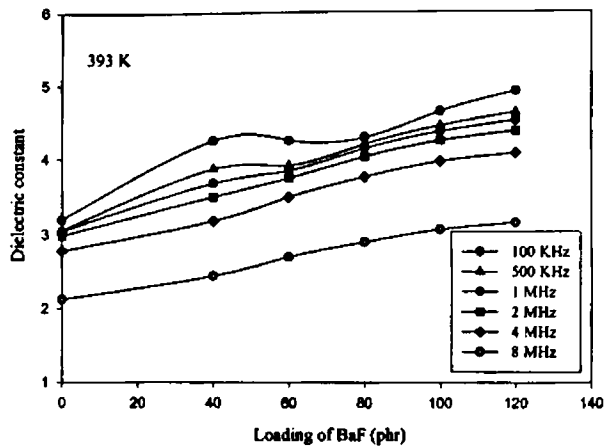


**Fig 5.10 f Dielectric constant versus loading of BaF in NR for different frequencies at 393K**

Moreover the addition of carbon black increased the dielectric constant greatly. The variation pattern remains the same for all loadings of carbon black. The RFC containing 80 phr of BaF, which has a dielectric constant of 4.55, increased to 5.51 by the addition of 10 phr carbon black and it increased to 88.00 for a carbon black loading of 50 phr. Figures 5.11a to 5.11f depicts the variation in dielectric constant with the loading of carbon black at different frequencies and temperatures. The variation in dielectric constant with loading of carbon black was more pronounced at lower frequencies than at higher frequencies.

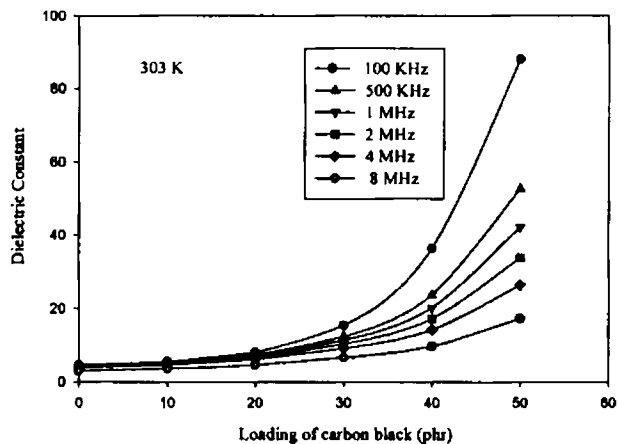


**Fig 5.11 a Dielectric constant versus loading of carbon black in NR based RFC containing 80 phr of BaF at various frequencies and 303K**

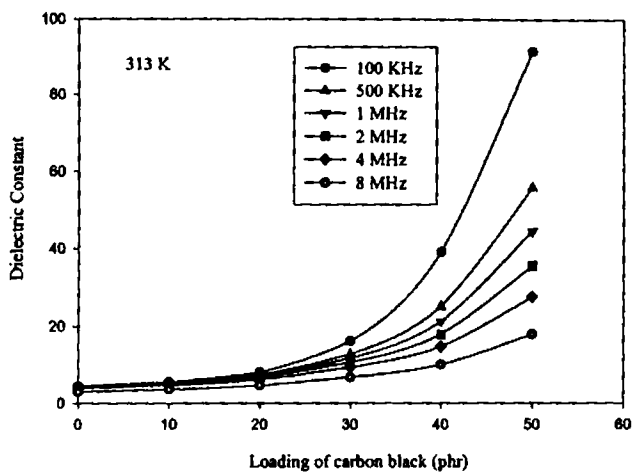


**Fig 5.11b Dielectric constant versus loading of carbon black in NR based RFC containing 80 phr of BaF at various frequencies and 313K**

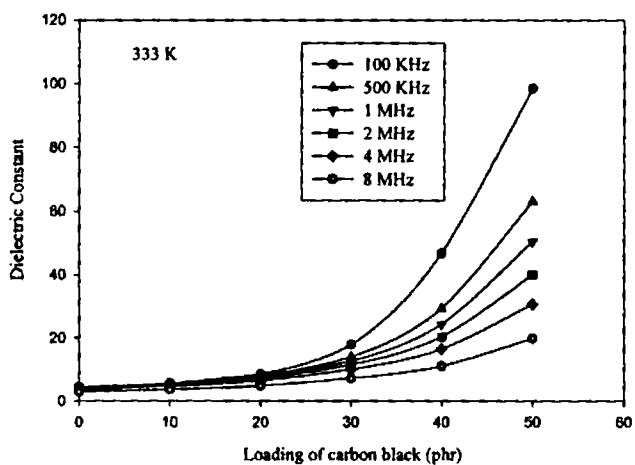


**Fig 5.11c Dielectric constant versus loading of carbon black in NR based RFC containing 80 phr of BaF at various frequencies and 333K**

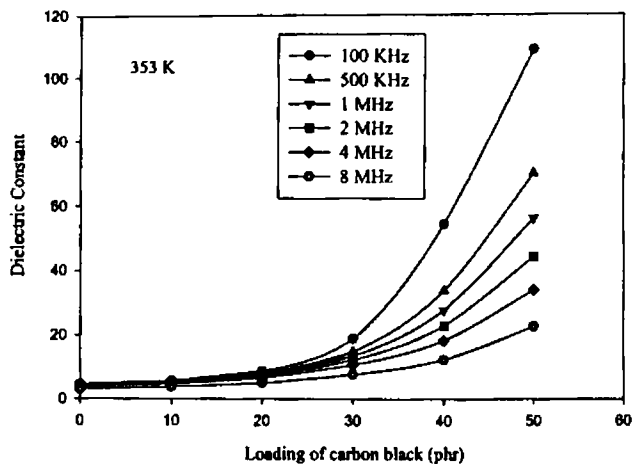


**Fig 5.11d Dielectric constant versus loading of carbon black in NR based RFC containing 80 phr of BaF at various frequencies and 353K**

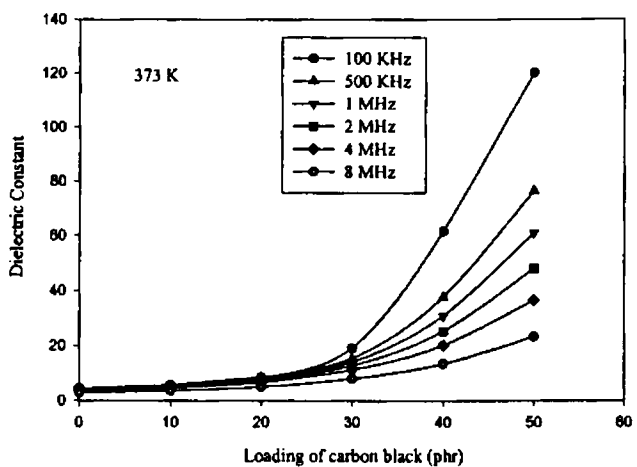


**Fig 5.11e Dielectric constant versus loading of carbon black in NR based RFC containing 80 phr of BaF at various frequencies and 373K**

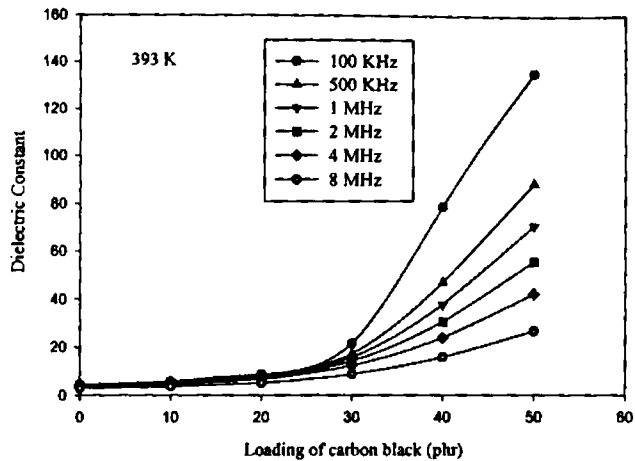


**Fig 5.11f Dielectric constant versus loading of carbon black in NR based RFC containing 80 phr of BaF at various frequencies and 393K**

The variation in dielectric constant with the loading of BaF at different temperatures is shown in figures 5.12a to 5.12f, which showed that the dielectric constant values increase with the filler loading. The dielectric constant increased from 4.86 to 4.92 in the temperature range of 303K to 393K for composites containing 120 phr of BaF at 1MHz. At 8 MHz it decreased from 3.24 to 3.16 for the same temperature range. Hence at higher loading of BaF the effect of temperature and frequency on dielectric constant was negligible.

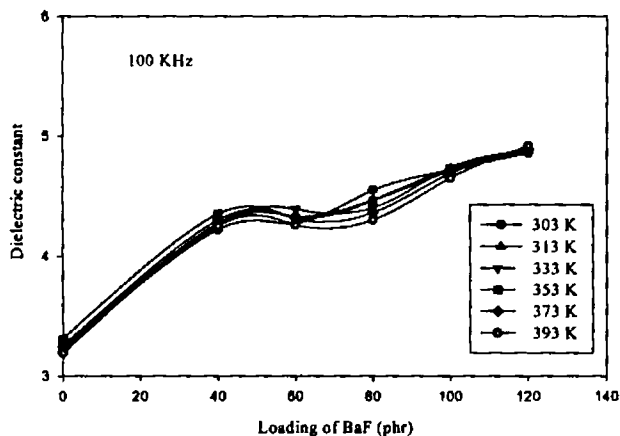


**Fig 5.12a Dielectric constant versus loading of BaF in NR for different temperatures at 100 KHz**

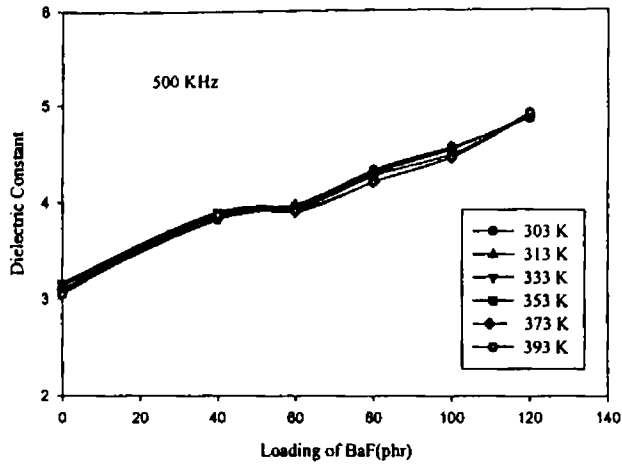


**Fig 5.12b Dielectric constant versus loading of BaF in NR for different temperatures at 500 KHz**

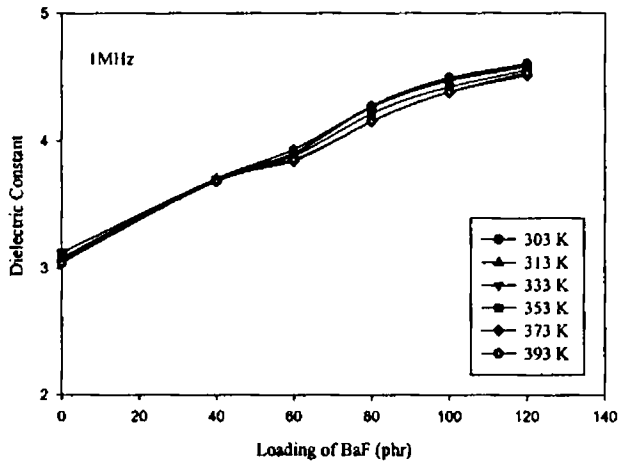


**Fig 5.12c Dielectric constant versus loading of BaF in NR for different temperatures at 1 MHz**

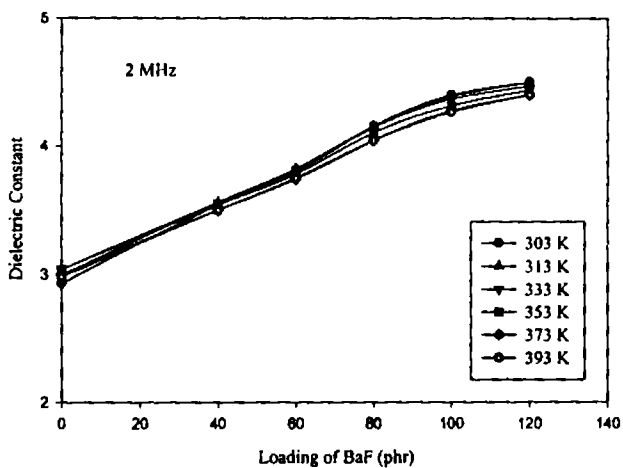


**Fig 5.12d Dielectric constant versus loading of BaF in NR for different temperatures at 2 MHz**

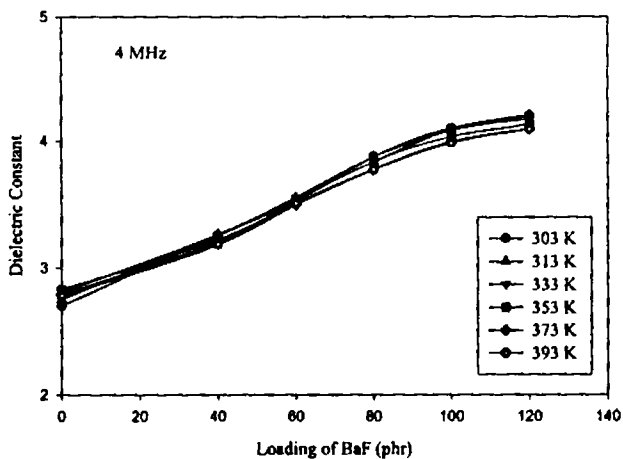


**Fig 5.12e Dielectric constant versus loading of BaF in NR for different temperatures at 4 MHz**

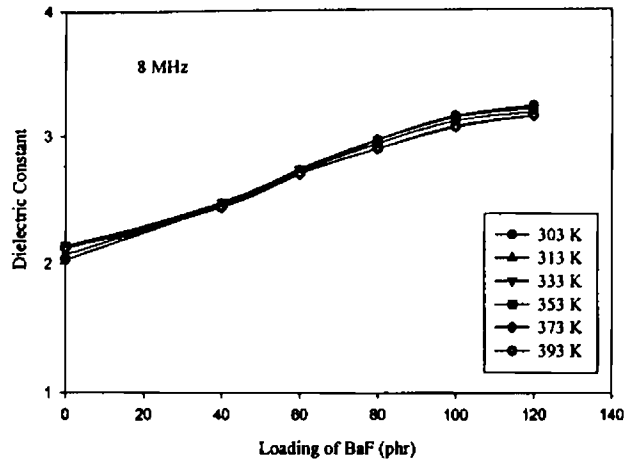


**Fig 5.12f Dielectric constant versus loading of BaF in NR for different temperatures at 8 MHz**

In the case of RFC containing 50 phr of carbon black the dielectric constant increased from 88.00 to 135 in the temperature range of 303K to 393K at 100 KHz, whereas at higher frequency of 8MHz the dielectric constant increased from 17.20 to 26.60. Figures 5.13a to 5.13f represent the variation in dielectric constant with the loading of carbon black at different frequencies.

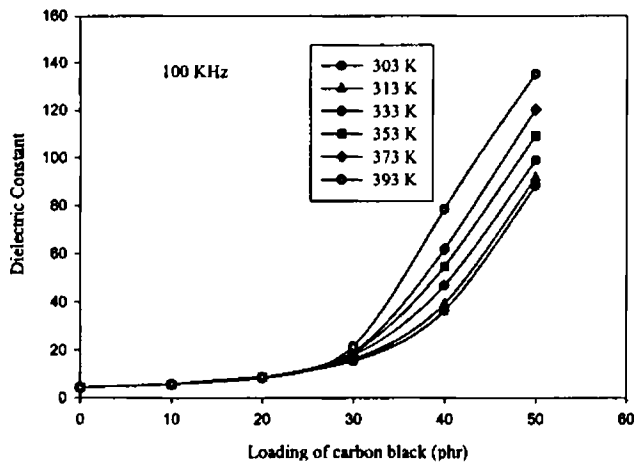


**Fig 5.13a Dielectric constant versus loading of carbon black in NR based RFC containing 80 phr of BaF for various temperatures at 100 KHz**

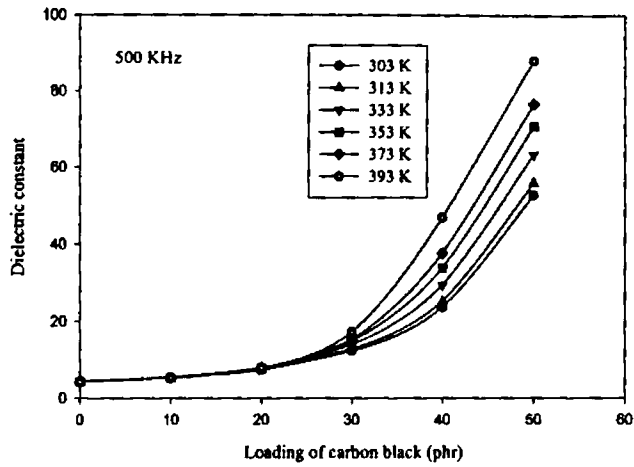


**Fig 5.13b Dielectric constant versus loading of carbon black in NR based RFC containing 80 phr of BaF for various temperatures at 500 KHz**

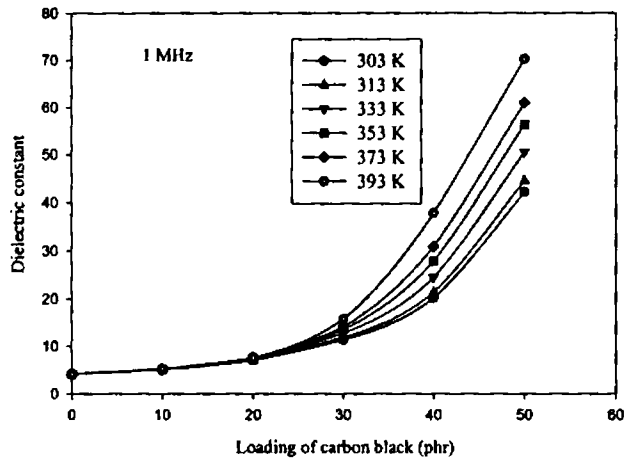


**Fig 5.13c Dielectric constant versus loading of carbon black in NR based RFC containing 80 phr of BaF for various temperatures at 1MHz**



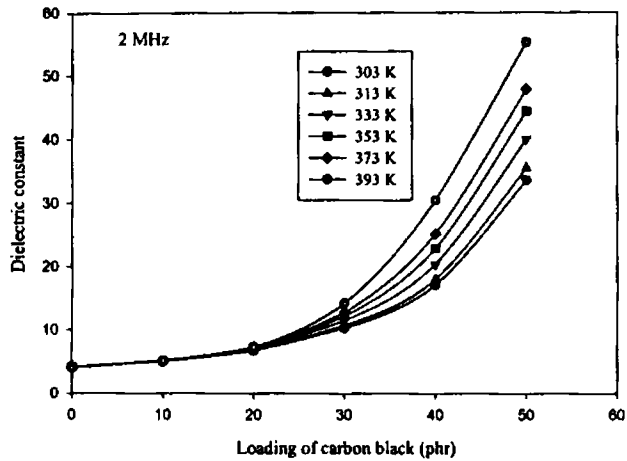


**Fig 5.13d Dielectric constant versus loading of carbon black in NR based RFC containing 80 phr of BaF for various temperatures at 2 MHz**

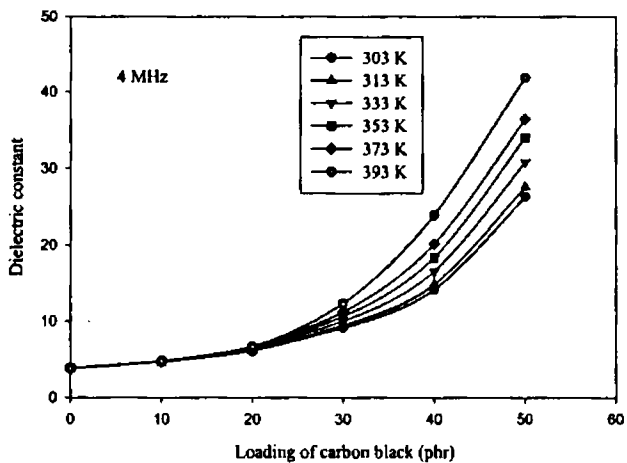


**Fig 5.13e Dielectric constant versus loading of carbon black in NR based RFC containing 80 phr of BaF for various temperatures at 4 MHz**

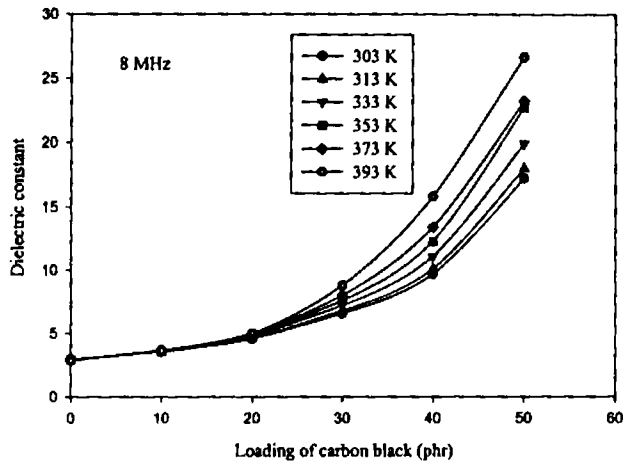


**Fig 5.13f Dielectric constant versus loading of carbon black in NR based RFC containing 80 phr of BaF for various temperatures at 8 MHz**

### 5.3.2 Rubber Ferrite Composites containing strontium ferrite

The RFCs based on natural rubber and strontium ferrite was prepared as explained in chapter 3. The dielectric properties of these RFCs and its effect on the addition of carbon black were studied in detail.

#### 5.3.2.1 Effect of frequency on dielectric properties of RFC

The variation in dielectric constant of the natural rubber based RFCs containing strontium ferrite with frequency at different temperatures was studied. Figure 5.14a represents the variation in dielectric constant with frequency for different loadings of SrF at 393K, whereas figure 5.14b shows the variation in dielectric constant with frequency of RFC containing 80 phr of SrF and different loadings of carbon black at 393K. In this case also a similar behaviour as that of the natural rubber based RFC containing BaF both with and with out carbon black was observed in the temperature range of 303K to 393K.

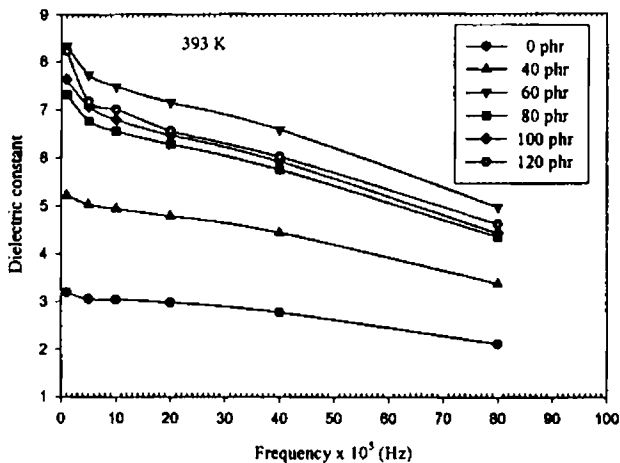


**Fig 5.14a Dielectric constant versus frequency of NR based RFC containing different loadings of SrF at 393K**

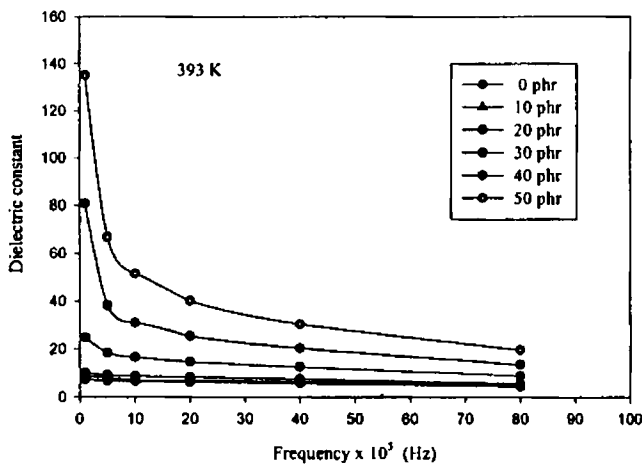


**Fig 5.14b Dielectric constant versus frequency of NR based RFC containing 80 phr of SrF and different loadings of carbon black at 393K.**

### 5.3.2.2 Effect of temperature on dielectric properties of RFC

The temperature dependence on the dielectric properties of natural rubber based rubber ferrite composites containing strontium ferrite at various frequencies was studied. The effect of temperature on rubber ferrite composites containing 80phr of SrF and various loading of carbon black on RFC was also studied. Figure 5.15a shows the variation in dielectric constant with temperature for different loadings of strontium ferrite at 100 KHz.

The dielectric constant of rubber ferrite composites containing strontium ferrite increased with increase in temperature. The addition of carbon black showed considerable increase in the dielectric constant values, which is clear from the figure 5.15b.

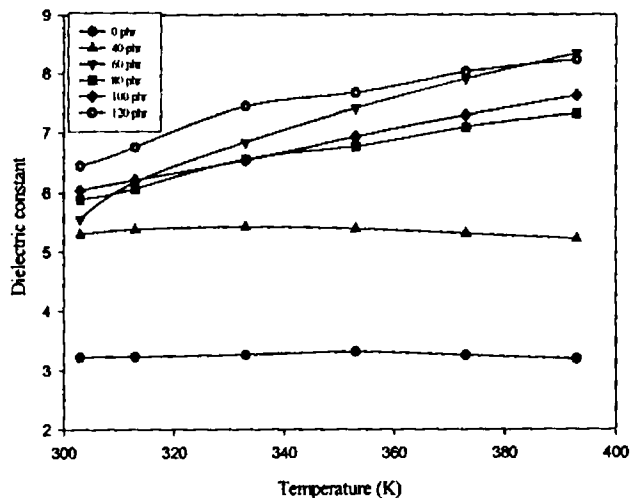


**Fig 5.15 a Dielectric constant versus temperature of NR based RFC for different loadings of SrF at 100 KHz**

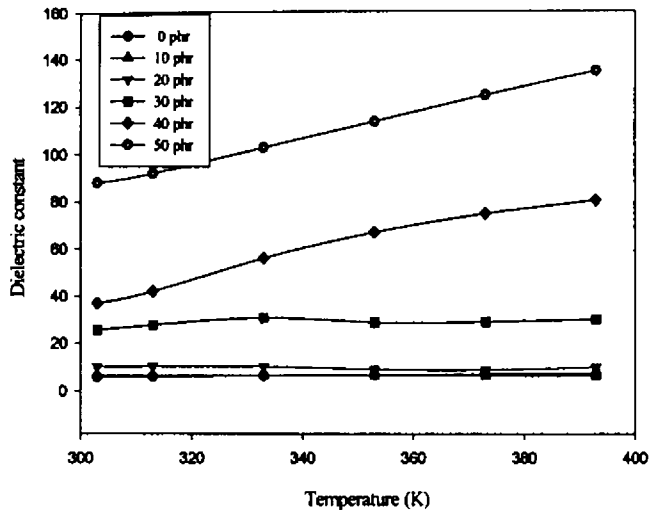


**Fig 5.15b Dielectric constant versus temperature of NR based RFC containing 80 phr of SrF and different loadings of carbon black at 100 KHz**

### 5.3.2.3 Effect of loading of ferrite on dielectric properties of RFC

Variations in dielectric constant with loading of SrF in NR based RFCs were also studied. Figures 5.16a and 5.16b shows the variation in dielectric constant with loading of SrF and carbon black respectively at different frequencies and 303K. The variation pattern was similar to that of the RFC containing BaF. Maximum value of dielectric constant was observed for the loading of 120phr of SrF. The addition of carbon black increased the dielectric constant to a greater extent. The variation pattern remained the same for all loading of carbon black. The RFC containing 80 phr of SrF had a dielectric constant of 5.89, which increased to 6.52 by the addition of 10 phr carbon black. The carbon black is added up to 50 phr in steps of 10. The resulting dielectric values at a frequency of 100 KHz were 10.2, 25.6, 70.5 and 88.0 respectively. Thus it is evident that the addition of 10 phr of carbon black to RFC containing 80 phr of SrF can enhance the dielectric constant that is obtained by the incorporation of 120 phr of ferrite filler. It was also observed that the addition of 50 phr of carbon black to the RFC containing 80 phr of SrF gave the same dielectric constant of 88.0 as that obtained by the incorporation of 50 phr of carbon black in RFC containing 80 phr of BaF.

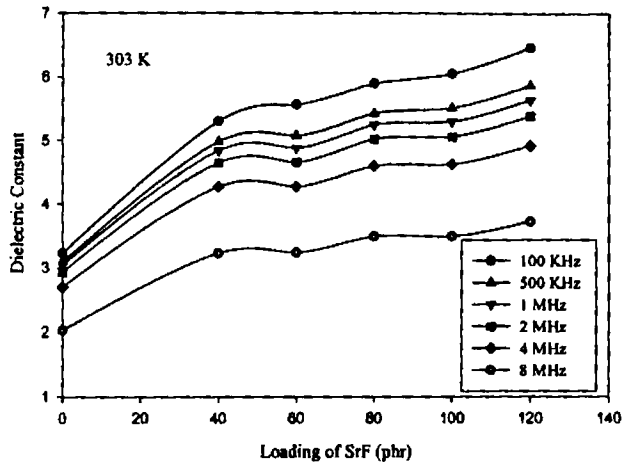


**Fig 5.16a Dielectric constant versus loading of SrF in NR for different frequencies at 303K.**

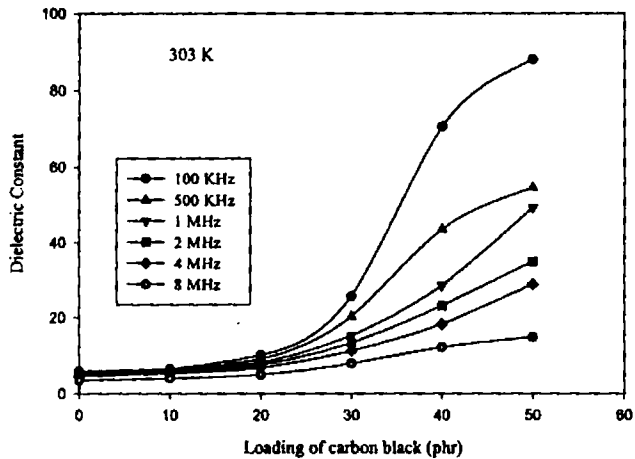


**Fig 5.16b Dielectric constant versus loading of carbon black in NR based RFC containing SrF for various frequencies at 303K**

The variation in dielectric constant with the loading of SrF and carbon black at different temperatures indicated that the permittivity values increased with the filler loading. The dielectric constant increased from 6.45 at 303K to 8.22 at 393K for 120 phr loading of SrF at a frequency of 100 KHz. At 8 MHz the value increased from 3.71 to 4.62. The dielectric constant increased from 88.00 at 303K to 135 at 393K with the addition of 50 phr carbon black to RFC containing 80 phr of SrF at 100 KHz, whereas at a frequency of 8MHz the value increased from 17.7 to 19.60.

#### **5.4 DIELECTRIC STUDIES OF NITRILE RUBBER BASED RUBBER FERRITE COMPOSITES**

The dielectric properties of nitrile rubber based RFCs were carried out at different frequencies and temperatures. The effect of dielectric constant on various parameters such as frequency, temperature and loading of ferrite fillers and carbon black were studied.

##### **5.4.1 Nitrile rubber based RFCs containing barium ferrite**

The rubber ferrite composites containing BaF in NBR was prepared as explained in chapter 3. The effect of the incorporation of carbon black on the dielectric properties of RFCs was also studied in detail.

##### **5.4.1.1 Frequency dependence on dielectric constant of RFCs**

The dielectric behaviour of NBR based RFCs containing BaF with change in frequency at different temperatures was studied. Figure 5.17a represent the variation in dielectric constant with frequency for different loadings of BaF in NBR at 393K. The absolute values of the dielectric constant of the composites were found to be greater than that of the gum NBR vulcanisates but less than that of the ceramic component. The dielectric constant decreased with increasing frequency for composites containing different loadings of BaF, which is in accordance with the Maxwell Wagner theory of interfacial polarization. Almost a similar behaviour as that of the RFCs containing BaF in NR was obtained in this case also.

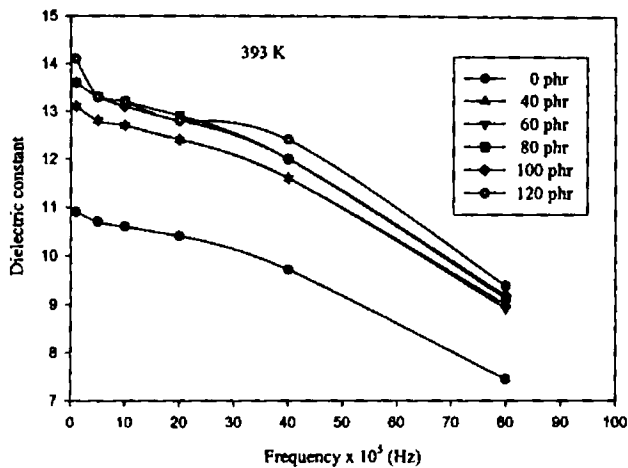


**Fig 5.17a Dielectric constant versus frequency of NBR based RFC with different loading of BaF at 393K**

Figure 5.17b depicts the variation in dielectric constant with frequency for different loadings of carbon black at 393K. It was observed that the variation in dielectric constant with frequency was more at higher loadings of the carbon black.

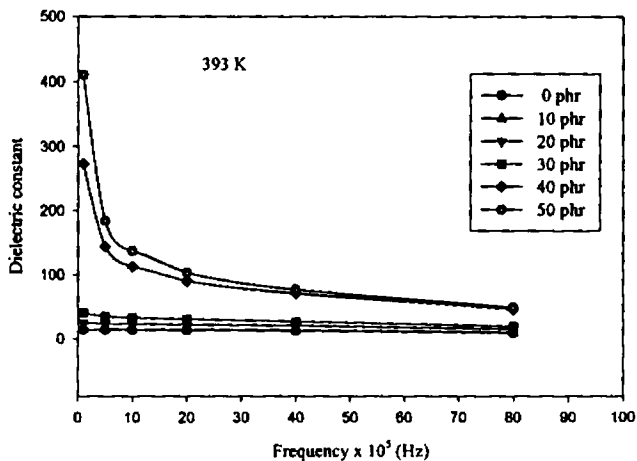


**Fig 5.17b Dielectric constant versus frequency for NBR based RFC containing BaF and different loadings of carbon black at 393K.**



### 5.4.1.2 Temperature dependence on dielectric constant of RFCs

The effect of temperature on the dielectric constant of rubber ferrite composites at various frequencies and different loading of barium ferrite and carbon black was studied. The dielectric constant of rubber ferrite composites containing barium ferrite in nitrile rubber increased initially with increase of temperature and then decreased. This behaviour is different from that of the natural rubber based RFCs, since nitrile rubber is a polar polymer and the mobility of the dipole increases with temperature. Figure 5.18a illustrates the variation in dielectric constant with temperature for different loadings of barium ferrite at 100 KHz. The behaviour was similar for RFC containing carbon black at lower loadings but at higher loading it showed an appreciable increase in the permittivity values. Figure 5.18b represents the variation in dielectric constant with the loading of carbon black.

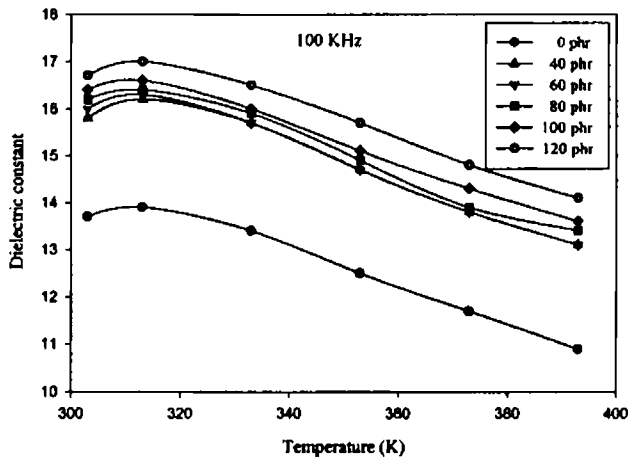


**Fig 5.18a Dielectric constant versus temperature for different loadings of BaF in NBR at 100 KHz**

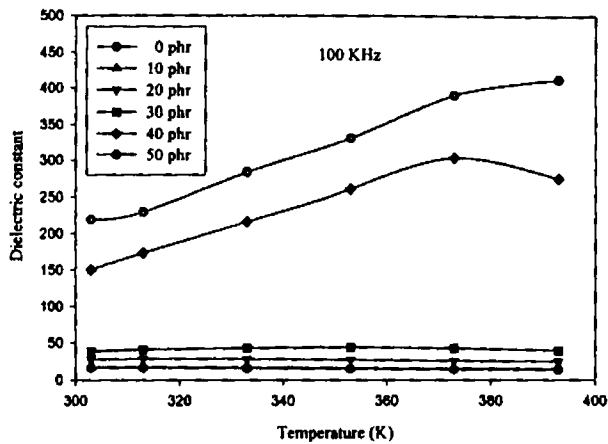


**Fig 5.18b Dielectric constant versus temperature of NBR based RFCs containing BaF and different loadings of carbon black at 100 KHz**

#### 5.4.1.3 Dependence of BaF loading on dielectric constant of RFCs

Variations in dielectric constant with the loading of barium ferrite and carbon black were also studied. Figure 5.19a shows the variation in dielectric constant with loading of BaF at different frequencies. The dielectric constant was found to increase with the addition of the ferrite filler. As expected the maximum value of dielectric constant was observed for a loading of 120phr of BaF. Dielectric constant increased from 13.7 for NBR gum vulcanisate to 16.7 with 120 phr of BaF at 303K and a frequency of 100 KHz.

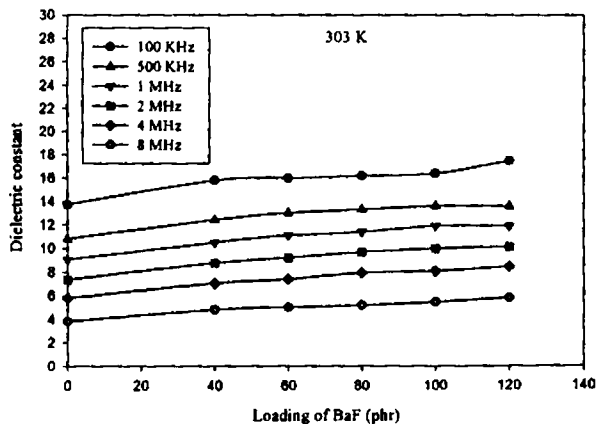


**Fig 5.19a Dielectric constant versus loading of BaF in NBR for different frequencies at 303K**

The incorporation of carbon black into RFC increased the dielectric constant greatly. The variation pattern remained the same for all the loading of carbon black. The RFC containing 80 phr of BaF had a dielectric constant of 16.2, which increased to 17 by the addition of 10 phr carbon black at 303K and a frequency of 100 KHz. The dielectric constant of these composites increased from 27.3 for a loading of 20 phr of carbon black to 219 for a loading of 50 phr of carbon black. Figure 5.19b depicts the variation in dielectric constant with the loading of carbon black at different frequencies. The variation in dielectric constant with loading of carbon black was more pronounced at lower frequencies than at higher frequencies.

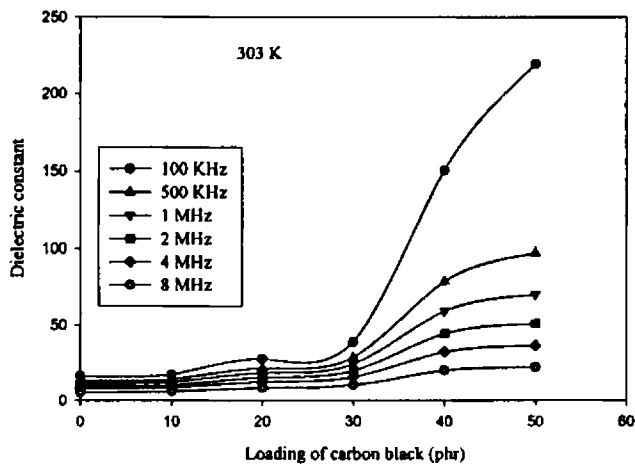


**Fig 5.19b Dielectric constant versus loading of carbon black in NBR based RFC containing BaF at 303K**

#### 5.4.2 Nitrile rubber based RFCs containing strontium ferrite

The rubber ferrite composites containing strontium ferrite and carbon black in nitrile rubber was prepared as explained in chapter 3 and the dielectric studies were carried out. The dependence on the dielectric constant of RFCs on various factors like frequency, temperature and loading of SrF and carbon black were studied.

### 5.4.2.1 Frequency dependence on dielectric constant of RFCs

The variation in dielectric constant of NBR based RFCs containing strontium ferrite with frequency at different temperatures was studied. It can be seen that the dielectric constant decreased with frequency for different loadings of SrF. The absolute values of the dielectric constant of the composites were found to be in between that of the gum NBR vulcanisate and the ceramic SrF. Figure 5.20a represent the variation in dielectric constant with frequency for different loadings of strontium ferrite at 393 K. This behaviour was similar to that of the NBR based RFCs containing BaF.

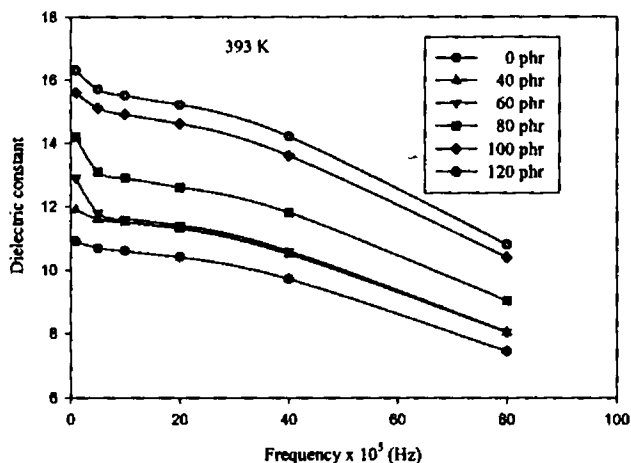


**Fig 5.20a Dielectric constant versus frequency for various loadings of SrF in NBR at 393K.**

Figure 5.20b represent the variation in dielectric constant with frequency for different loadings of SrF at 393K. For higher loadings of SrF the decrease in dielectric constant was more pronounced at lower frequency range than at higher frequency range.

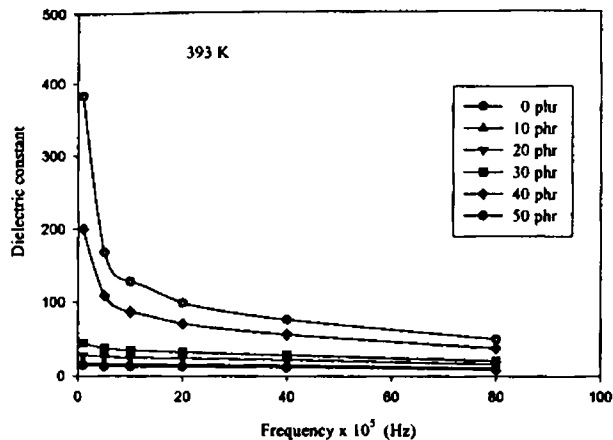


**Fig 5.20b Dielectric constant versus frequency for different loadings of carbon black containing 80 phr SrF in NBR at 393K.**

#### 5.4.2.2 Temperature dependence on dielectric constant of RFC

The effect of temperature on the dielectric properties of nitrile rubber based rubber ferrite composites containing strontium ferrite and carbon black was studied. The dielectric constant of rubber ferrite composites containing strontium ferrite increased initially with increase in temperature and then decreased. Figure 5.21a illustrates the variation in dielectric constant with temperature for different loadings of strontium ferrite at 100 KHz. This behaviour was similar to that of the nitrile rubber based rubber ferrite composites containing barium ferrite.

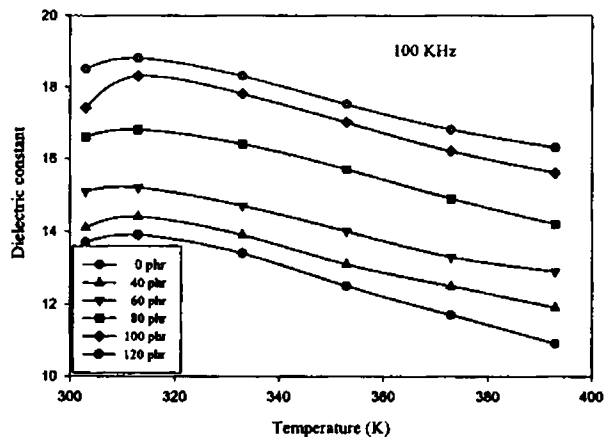


**Fig 5.21a Dielectric constant versus temperature for various loadings of SrF in NBR at 100 KHz**

The addition of carbon black caused appreciable increase in the dielectric constant. Figure 5.21b represents the variation in dielectric constant with temperature for various loading of carbon black. It was observed that the increase in dielectric constant with temperature was more at higher loadings of the carbon black.

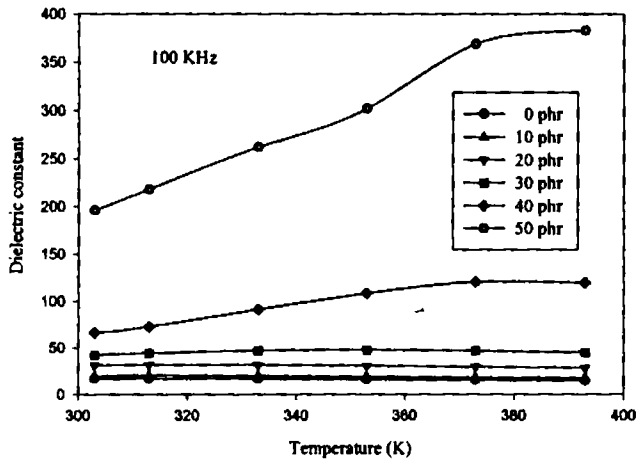


**Fig 5.21b Dielectric constant versus temperature for NBR based RFCs containing 80 phr SrF and various loadings of carbon black.**

#### 5.4.2.3 Dependence of SrF loading on dielectric constant of RFC

Studies on the variation in dielectric constant with the addition of strontium ferrite were also carried out. It was observed that the dielectric constant increases with increase of volume fraction of the ferrite material. Dielectric constant was maximum for a loading of 120phr of strontium ferrite. At 303K the dielectric constant of the nitrile rubber gum vulcanisate increased from 13.7 to 18.5 for a loading of 120 phr of SrF at 100 KHz. The dielectric constant of these rubber ferrite composites decreased as the frequency increases. Figure 5.22a shows the variation in dielectric constant with loading of strontium ferrite for different frequencies at 303K.

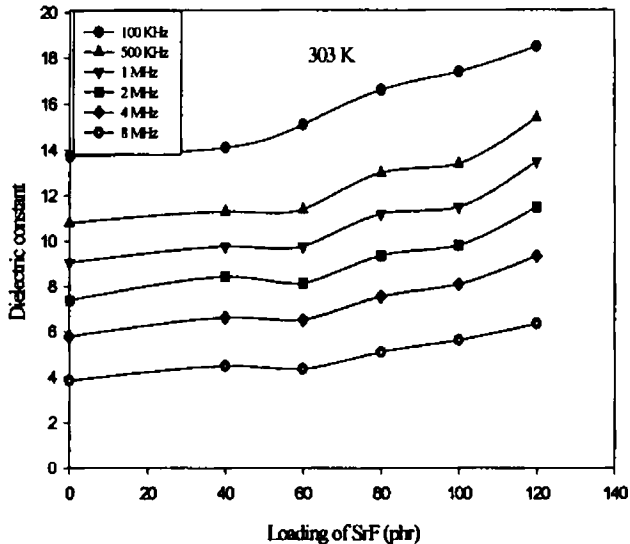


**Fig 5.22a Dielectric constant versus loading of SrF in NBR for various frequencies at 303K**

The addition of carbon black significantly increased the dielectric constant. The RFC containing 80 phr of SrF showed a dielectric constant of 16.6, which increased to 19.5 by the addition of 10 phr carbon black at 100KHz. Further addition of carbon black in steps of 10 up to 50 phr, the dielectric constant increased to 31, 42, 106 and 196 respectively. Figure 5.22b represent the variation in dielectric constant with the loading of carbon black on NBR based RFCs containing 80 phr of strontium ferrite at different frequencies and 303K. The increase in dielectric constant with loading of carbon black was more pronounced at lower frequencies than at higher frequencies.

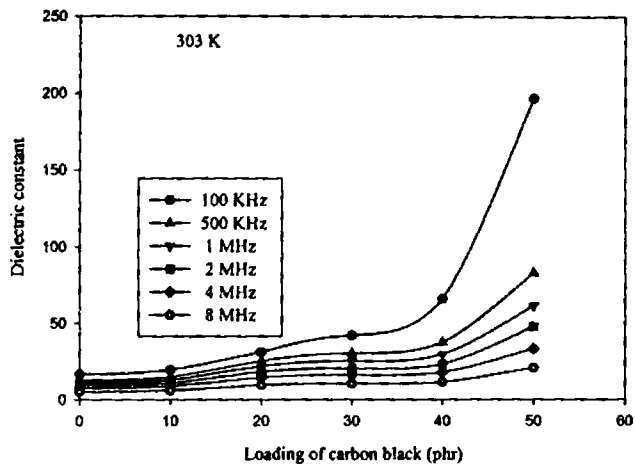


**Fig 5.22b Dielectric constant versus loading of carbon black in NBR based RFC containing 80 phr of SrF for different frequencies at 303K**

## 5.5 AC CONDUCTIVITY STUDIES

The ac conductivity of the ceramic BaF and SrF, NR and NBR gum vulcanisates and composites containing these ferrites are evaluated using the data obtained from the dielectric measurements.

### 5.5.1 Introduction

Every materials conduct electricity to a greater or lesser extent. Ferrites are an important group of magnetic materials with a wide range of applications due to their magnetic properties and low dielectric loss. The electrical properties are significant for ferrites and composites containing these ferrites. The study of ac electrical conductivity gives an idea about the behaviour of charge carriers under an ac field, their mobility and the mechanism of conduction<sup>24-31</sup>.

Rubber ferrite composites are important class of materials made by incorporating ferrite filler in natural rubber or synthetic rubber. Their applications range from electronic and electric industries, motor stators and rotors, information



technology, printing and decoration. The size, shape and magnetisation pattern can be designed according to user's need. Though literature on the ac conductivity of ceramic ferrite fillers exists, data on rubber ferrite composites are rather scarce. RFCs are essentially dielectric materials and their electrical properties are very important from the application point of view. Hence studies on ac conductivity on RFC and the correlation with that of the corresponding fillers assumes significance.

It was reported that the electron hopping between  $Fe^{2+}$  and  $Fe^{3+}$  is responsible for conduction in ferrites. The conductivity studies on ferrites carried out by various researchers proved its semiconducting behaviour and also proved the dependence of electrical conductivity on preparation condition, sintering time, temperature and the types of impurities<sup>32-37</sup>.

The evaluation of ac electrical conductivity of ceramic BaF and SrF, NR and NBR gum vulcanisate, as well as the rubber ferrite composites was calculated using the data obtained from the dielectric measurements as explained in chapter 2. Their dielectric constant and dielectric loss were evaluated by parallel plate capacitor method by using a dielectric cell and an Impedance analyzer (HP 4285A). The acquisition of  $\tan\delta$  values from dielectric permittivity measurements and subsequent evaluation of ac conductivity have been made automatic.

From the dielectric loss and dielectric constant, ac conductivity of these samples were evaluated using the relation

$$\sigma_{ac} = 2\pi f \tan\delta \epsilon_0 \epsilon_r \quad (5.3)$$

where  $f$  is the frequency of the applied field,  $\epsilon_0$  is the absolute permittivity,  $\epsilon_r$  is the relative permittivity and  $\tan\delta$  is the loss factor.

AC conductivity of the ceramic samples, NR and NBR gum vulcanisates and RFCs were evaluated in the frequency range from 100KHz to 8MHz. The measurements were done at different temperatures of 303, 313, 333, 353, 373 and 393K. The RFCs studied were based on NR containing various loading of SrF and carbon black.

## 5.5.2 Effect of frequency on ac conductivity

The frequency dependence on the ac conductivity of the ceramic ferrites, NR and NBR gum vulcanisate were evaluated from the dielectric measurement data employing the equation 5.3.

### 5.5.2.1 Ceramic samples

The ac electrical conductivity of both ceramic BaF and SrF were calculated from the dielectric constant and dielectric loss values at different frequencies. The ac conductivity increased with frequency for both samples.

In ferrites the low conductivity is associated with the simultaneous presence of ferrous and ferric ions on equivalent lattice sites (usually octahedral sites). In such a situation the mechanism of conduction that comes into play is the Verwey type conduction or hopping conduction. The electrical conduction in BaF and SrF with the structural formula  $\text{BaFe}_{12}\text{O}_{19}$  and  $\text{SrFe}_{12}\text{O}_{19}$  respectively is explained by the hopping mechanism. The extra electron on a ferrous ion requires only very small energy to move to a similarly situated ferric ion. The valence states of the two ions are interchanged. Under the influence of an electric field these extra electrons can be considered to constitute the conduction current by hopping or jumping from one 'iron' ion to the other. Depending on the sintering conditions such ions with different valence states can be produced during preparation of ferrite samples. Also a partial reduction of  $\text{Fe}^{3+}$  to  $\text{Fe}^{2+}$  ions is possible at elevated firing temperatures of the order of 1000K.

The variation in ac conductivity with frequency at 303K for the ceramic BaF and SrF samples are given in figures 5.23 and 5.24 respectively. The ac conductivity showed an increasing trend with increase in frequency for both the samples. But at frequencies above 5MHz the ac conductivity values showed a decreasing trend. This behaviour can be explained as follows.

The dielectric structure of ferrites is given by Koops Phenomenological theory and Maxell-Wagner theory. According to this theory dielectric structure was formed by a first layer of fairly well conducting ferrous ions, which is separated by a thin layer of poorly conducting grain boundary formed by oxygen ions. At lower frequencies these grain boundaries are more active and hence hopping of  $\text{Fe}^{2+}$  and

$\text{Fe}^{3+}$  ion is less. As the frequency of the applied field increases the conductive grains become more active by promoting the hopping between  $\text{Fe}^{2+}$  and  $\text{Fe}^{3+}$  ions, there by increasing the hopping conduction. Thus a gradual increase in conductivity with frequency is observed. At higher frequencies the frequency of the hopping ions could not follow the frequency of the applied field and it lags behind it. This causes a dip in conductivity at higher frequencies.

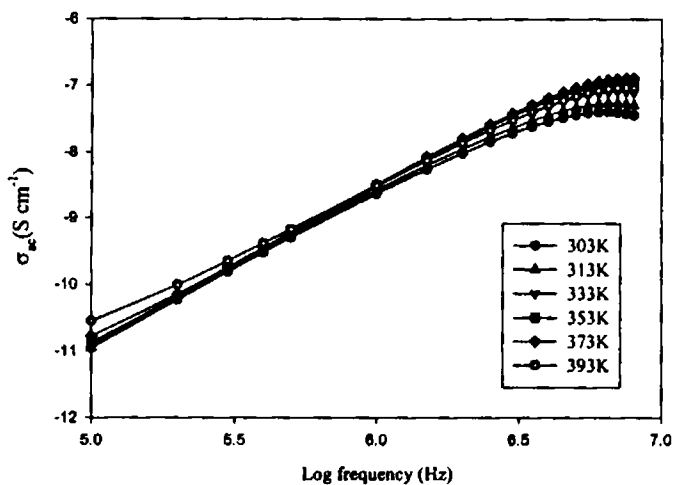


**Fig 5.23** Variation in ac conductivity of ceramic BaF versus log frequency at various temperatures

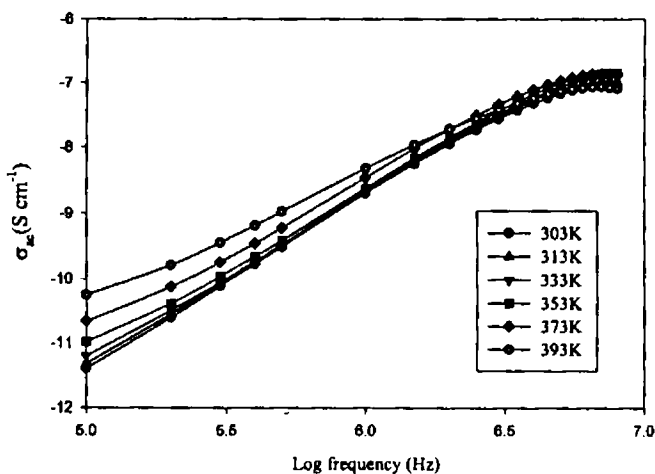


**Fig 5.24** Variation in ac conductivity of ceramic SrF versus log frequency at various temperatures

### 5.5.2.2 Natural rubber gum vulcanisate

In most polymers it is difficult to detect any electrical conductivity and most of the conductivities observed is due to the presence of non rubber constituents like ions from impurities such as catalyst residues, dissociable end groups and degradable products. Unvulcanised natural rubber is nonconducting and the vulcanised rubber contains different compounding ingredients which may act as carriers for conduction. Also polymers are known to be semicrystalline and natural rubber can be thought of as a continuous matrix of an amorphous polymer in which properties are modified by the crystalline regions that act as the reinforcing centres. As far as the electrical properties are considered the crystalline centres lower the conductivity. If the conduction is ionic, ion mobility through the crystalline region will be low and in the case of electronic conduction the crystalline amorphous interface may act as a trapping region. Thus it can be considered similar to Maxwell-Wagner two layer model<sup>40-42</sup>.

The variation in ac conductivity with frequency for NR gum vulcanisate is given in figure 5.25. It can be observed that the ac conductivity increases with increase in frequency and drops after reaching a maximum at higher frequencies. At lower frequencies the crystalline-amorphous interface may be more active and as the frequency increases the ions are able to move across this interface, which in turn will increase the conductivity. High frequency limit is reached when applied frequency is greater than maximum hopping rate.

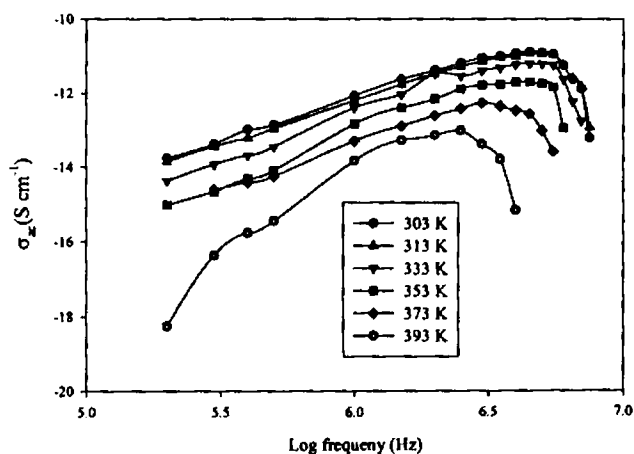


**Fig 5.25 Variation in ac conductivity versus log frequency of NR gum vulcanisate at various temperatures**

### 5.5.2.3 Nitrile rubber gum vulcanisate

The ac conductivity of the NBR gum vulcanisate has been obtained from the dielectric measurements. The variation in ac conductivity with frequency for NBR gum vulcanisate is given in figure 5.26. It can be observed that the ac conductivity increases with increase in frequency and drops after reaching a maximum at higher frequencies, especially at high temperatures.

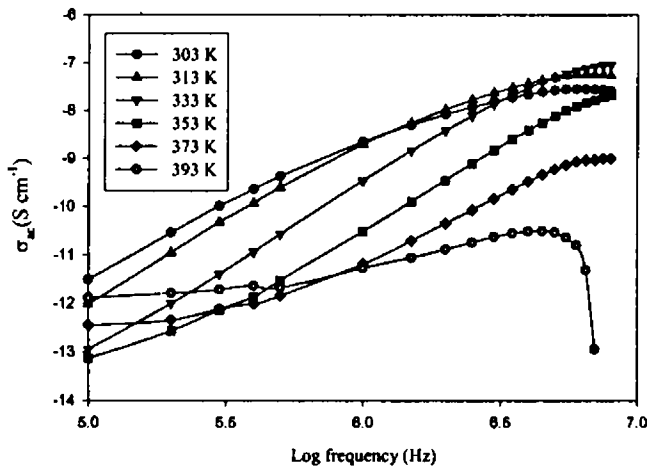


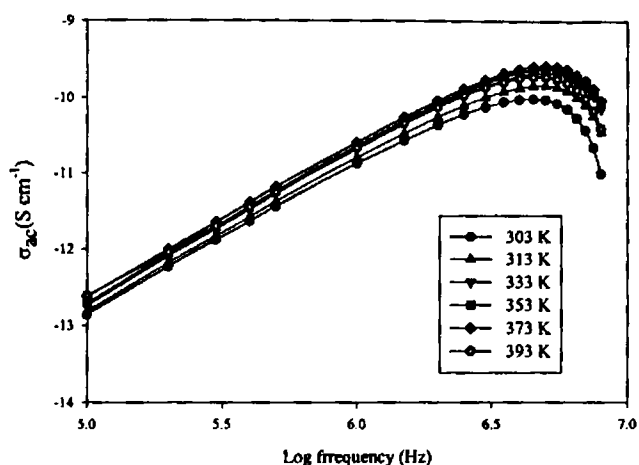
**Fig 5.26 Variation in ac conductivity versus log frequency of NBR gum vulcanisate at various temperatures**

### 5.5.3 AC conductivity studies of NR based rubber ferrite composites

Using the data obtained from the dielectric measurements, the ac conductivity of the NR based RFCs containing 40, 60, 80, 100 and 120 phr of SrF were calculated. The effect of carbon black on the ac conductivity of RFCs containing 80 phr of SrF and 10, 20, 30, 40 and 50 phr of carbon black was also studied.

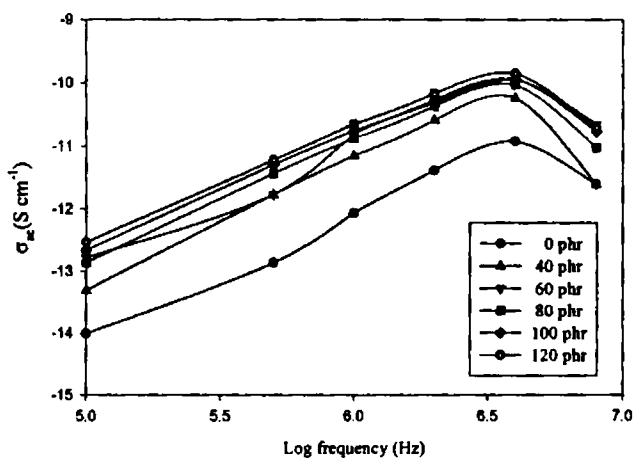
#### 5.5.3.1 Frequency dependence on AC conductivity of RFCs

The ac conductivity of the NR based RFC containing SrF was done at different temperatures and frequencies. The RFCs also showed the same trend as that of the ceramic ferrites. The figure 5.27 depicts a representative graph showing the variation in ac conductivity versus log frequency of the RFCs.



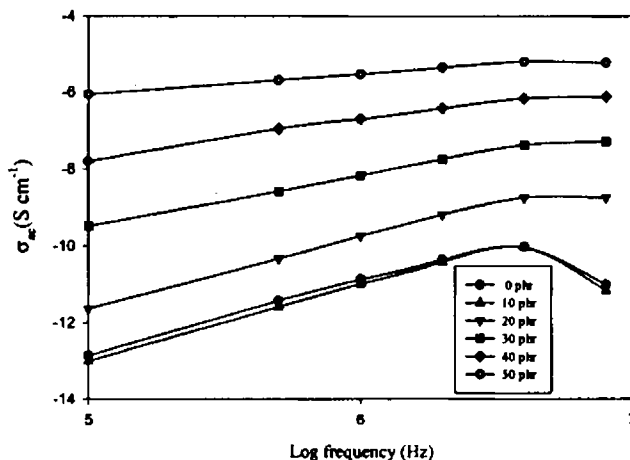
**Fig 5.27** Variation in ac conductivity versus log frequency of NR based RFC containing 60 phr of SrF at various temperatures.

Figure 5.28 depicts the variation in ac conductivity versus log frequency of NR based RFCs containing various loading of SrF at 303K. The ac conductivity increased with frequency for all the samples including the NR gum vulcanisate and then showed a dip at higher frequencies. The decrease in conductivity at high frequencies is due to the lag in hopping of the charge carriers with the applied field frequency.



**Fig 5.28** Variation in ac conductivity versus log frequency of NR based RFC containing various loading of SrF at 303K

Since the incorporation of carbon black is found to enhance the micro wave absorbing properties, the NR based RFCs containing 80 phr of SrF and various loading of carbon black were prepared and the ac conductivity was studied. Figure 5.29 shows the variation in ac conductivity of these RFCs with frequency for various loading of carbon black. The ac conductivity increased with increasing frequency and showed a slight dip at higher frequencies. More over the ac conductivities increased with the loading of carbon black. This is because carbon black acts as semiconducting materials.



**Fig 5.29** Variation in ac conductivity with log frequency of NR based RFC containing 80 phr of SrF and various loading of carbon black.

### 5.5.3.2 Temperature dependence on AC conductivity of RFCs

The temperature dependence on the NR based RFC containing 40,60, 80, 100 and 120 phr of SrF was evaluated at a frequency of 1MHz. The figure 5.30 depicts a representative graph showing the variation in ac conductivity of RFCs with temperature.

The ac conductivity of the RFCs showed a slight increase with increase in temperature. This is due to increase in hopping between  $Fe^{2+}$  and  $Fe^{3+}$  ions at higher temperatures. In the case of NR gum vulcanisate a decrease in conductivity is noticed due to its nonconductive nature.

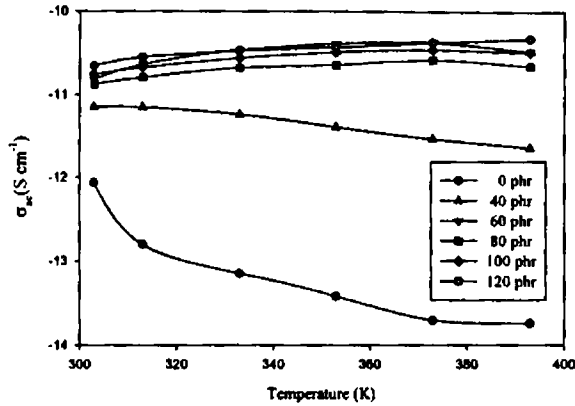


**Fig 5.30 Variation in ac conductivity versus temperature of NR based RFC containing different loading of SrF at 1MHz.**

The temperature dependence on the ac conductivity of the RFCs containing carbon black was studied using the dielectric parameters. Figure 5.31 shows the variation in ac conductivity of these composites with temperature at 1MHz. The addition of carbon black into the RFCs slightly enhanced the ac conductivity with increase in temperature up to 353K. At lower loading of carbon black the increase in ac conductivity with temperature was not so prominent.

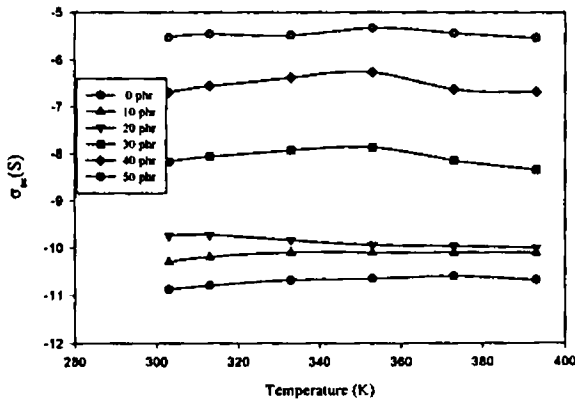


**Fig 5.31 Variation in ac conductivity versus temperature of NR based RFC containing 80 phr of SrF and various loading of carbon black at 1MHz**



### 5.5.3.3 Dependence of filler loading on ac conductivity

The effect of loading of SrF on ac conductivity NR based RFCs was also carried out within the frequency range of 100 KHz to 8 MHz at 303K. The figure 5.32 depicts the variation in ac conductivity versus temperature of the RFCs containing various loading of SrF at 303K. The ac conductivity of the RFCs increased with the increasing loading of SrF, which is due to the increase in weight fraction of the ferrite filler in the composites. The ac conductivity of these composites increased with the increase in frequency.

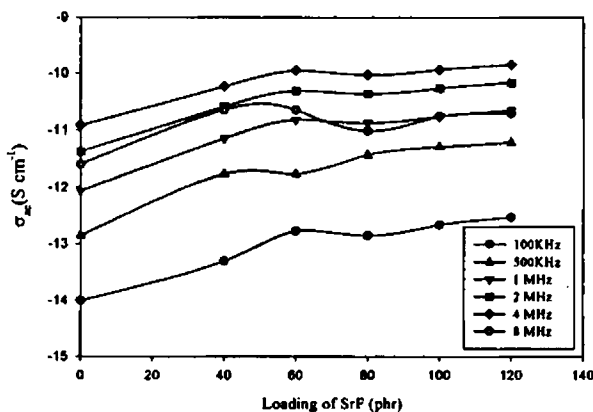


**Fig 5.32 Variation in ac conductivity versus loading of SrF in NR for different frequencies at 303K.**

The effect of loading of carbon black on the NR based RFCs containing 80 phr of SRF was also studied. Figure 5.33 depicts the variation in ac conductivity versus loading of carbon black in NR based RFCs containing 80 phr of SrF at 303K.

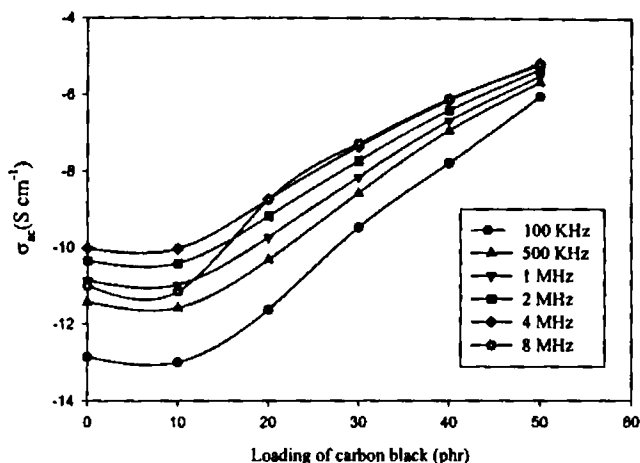


**Fig 5.33 Variation in ac conductivity versus loading of carbon black in NR based RFC containing 80 phr of SrF at different frequencies and 303K**

The ac conductivity of the carbon black containing RFCs steadily increased with the increasing loading of carbon black. The conductivity values showed an increase with increasing frequency due to the higher hopping conduction at higher frequencies.

## 5.6 CONCLUSION

The rubber ferrite composites intended for microwave applications warrants appropriate dielectric and mechanical properties. For applications involving RFCs at high frequencies it is necessary to modify the magnetic and dielectric properties.

The dielectric constant decreased with increase of frequency for ceramic samples of BaF and SrF, natural rubber and nitrile rubber gum vulcanisate and for the RFC samples, both with and without carbon black. The dielectric constant of these materials increased with increase in temperature. But for composites containing BaF and SrF the increase in dielectric constant with temperature was not so prominent as in the case of ceramic samples, whereas in the case of RFCs containing carbon black it showed an appreciable increase with the temperature. The dielectric constant of NBR gum vulcanisate was found to be greater than that

of NR gum vulcanisate, which indicated that that NBR is superior in dielectric properties compared to NR.

The addition of ferrite fillers to both natural and nitrile rubber increased the dielectric constant. It was observed that the dielectric constant increases with increase in volume fraction of the ferrite material. Maximum value of dielectric constant was observed for a loading of 120phr of ferrite filler. The incorporation of carbon black into these RFCs increased the dielectric constant values to a greater extent. The dielectric constant increased substantially even with addition of 10 phr of carbon black into RFCs containing 80 phr of ferrite fillers. The RFCs containing BaF/SrF in NBR along with carbon black is superior when compared to RFCs based on NR for dielectric applications

The ac conductivity increased with frequency for ceramic samples, NR and NBR gum vulcanisates and rubber ferrite composites containing SrF with and without carbon black. For the ceramic BaF and SrF the ac conductivity were found to be almost the same. NBR gum vulcanisate showed high ac conductivity than that of NR gum vulcanisate. The ac conductivity of the RFCs increased with the increasing loading of SrF. In the case of carbon black containing RFCs the ac conductivity steadily increased with the increasing loading of carbon black.

Thus addition of ferrite fillers and appropriate loading of carbon black into natural and nitrile rubber matrix can modify the dielectric property of the composites. Microwave absorbers with optimum dielectric and mechanical properties can be prepared by incorporating BaF and SrF, along with suitable loading of carbon black in both natural and nitrile rubber matrix.

**REFERENCES**

1. Safari. A.M, W.Dick, D.H.McQueen, *Plastics Rubber and Composites Processing Appl.* **24** (1995) 157.
2. Slama. JR. Vicen, P. Krivosik, A. Grusova, R. Dosoudil, J. Magn. and Magn. Mater. **196/197** (1999) 359.
3. Arcos. D, R. Valenzeula, M. Vazquez, M. Vallet-Regi, J. *Solid State Chem.* **141** (1998) 10.
4. Gigbi. Z. and L.Jilken, J. Magn. Mater. **37** (1983) 267.
5. Saini D.R, A.V. Sheony and V.M. Nadkarni, J. *Appl. Polym. Sci.* **29** (1983) 4123.
6. Kuar B K, Singh P K, Kishan P, Kumar N, Rao S L N, Prabhat K Singh, Srivastava G P, J. *Appl. Phys.* **63** (8) (1988) 3780-3782.
7. El Hiti M A, J. *Mag. and Mag. Mat.* **164** (1996) 187-196.
8. Josyulu O and Sobhanadri J, *Phys. Status Solid i(a)* **59** (1980) 323.
9. Ahmed M A, El Hiti M A, Mosaad M. M and Attia S M, J. *Magn. Magn Mater.* **146** (1995) 84.
10. Murthy V R K and Sobhanadri J, *Phys. Status Solid i(a)* **36** (1976) 133.
11. Reddy P V and Rao T S, J. *Less. Common. Met.* **86** (1982) 255.
12. Charles Phelps Smyth, *Dielectric Behaviour and Structure*, Mc Graw-Hill Book Company, Inc., 1955.
13. M.R. Anantharaman, S. Sindhu, S. Jagatheesan, K.A. Malini and Philip Kurian, *Journal of Physics D Applied Physics* **32** (1999) 1801-1810.
14. M. R. Anantharaman, K.A. Malini, S. Sindhu, E.M. Mohammed, S.K Date, S.D. Kulkarni, P.A. Joy, and Philip Kurian, *Bull. Mater. Sci.*, **24,6**, (2001) 623-631.
15. Ramasastry C and Syamasundara Rao. Y, J. *Phys. E: Sci. Instrum.* **12** (1979) 1023-4.

16. Standley K. J, 'Oxide Magnetic Materials', 2<sup>nd</sup> edition, (1972), 36, Clarendon Press, Oxford.
17. Charles Phelps Smyth, Dielectric Behaviour and Structure, Mc Graw-Hill Book Company, Inc., 1955.
18. M.A. Abdeen, die. Beh. In NZF, J of MMM, **192**, (1999) 121-129.
19. V.P. Miroshkin, Ya. P. Panova and V.V. Passynkov, Phys. Stat. Sol.(a) **66**, 779 (1981).
20. S.A. Mazen M.H. Abdallah, M.A. Elghandoor and H.A. Hashem, Phys. Stat. Sol. (a) **144**, (1994) 461.
21. C.G. Koops, Phys. Rev. **83** (1951) p 121-124.
22. Tareev B 1979 Physics of Dielectric Materials (Mir Publishers) Moscow.
23. Frank E Karasz 1972 Dielectric Properties of Polymers (Plenum Press) New York.
24. J.P. Suchet, Electrical Conduction In Solid Materials, Pergamon Press, 1975.
25. Andrej Znidarsie and Miha Drofenik J. Ame. Ceram. Soc. **82** (1999) 359.
26. Ahmed M.A. and Elhiti M.A, Journal de Physique III **5** (1995) 775- 781.
27. Abdeen A.M, J. Magn. Magn. Mater. **192** (1999) 121 – 129.
28. Pal M, Brahma P and Chakravorty D, J. Phys. Soc. Jap. **63**, 9 (1994) 3356-3360.
29. Brockman F.G and White R.P, J. Amer. Ceram. Soc. **54** (1971) 183
30. Abdeen A.M, J. Magn. Magn. Mater. **185** (1998) 199 – 206.
31. Elhiti M.A, J. Magn. Magn. Mater. **164** (1996) 187 – 196.
32. C. Prakash, J.S. Bijal, P. Kishan, J. Less- common Met. **106** (1985) 243
33. A.B. Naik, J.J. Powar, Ind. J. Pure Appl. Phys. **239** (1985) 436.
34. R. Satyanarayana, S.R. Murthy, Crystal Res. Technol. **20** (1985) 701.
35. S. Jankowski, J. Amer. Ceram. Soc., **71** (1988) C-176.
36. P.V. Reddy, R. Satyanarayana, T.S. Rao, Phys. Stat. Sol. (a) **78** (1983) 109

37. F. Haberey, H.J.P.Wijn, Phys. Stat. Sol. (a) **26** (1968) 231.
38. D.A. Seanor (edt.) Electrical properties of Polymers, Academic press New York, 1982.
39. Ya. M. Paushkin, T.P. Vishnyakova, A.F. Lunin, S.A. Nizova, Organic Polymeric Semiconductors, Keter Publishing House Jerusalem Ltd, 1974.
40. James M. Margolis, (Edt), Conductive Polymers and Plastic, Chapman and Hall, New York, 1989.

# Chapter 6

---

## **MAGNETIC PROPERTIES OF RUBBER FERRITE COMPOSITES**

### **6.1 INTRODUCTION**

It is well known that polycrystalline ferrite ceramic powders can be incorporated in various elastomer matrixes to produce rubber ferrite composites<sup>1-7</sup>. The incorporation of these ferrite powders can be carried out both in natural and synthetic rubber matrix to produce flexible magnets. They have the special advantage of easy processability into complex shapes, which is not possible with conventional ceramic materials. The impregnation of magnetic fillers in the polymer matrixes can, not only bring economy but also imparts magnetic properties to the matrix. They also modify the dielectric and mechanical properties of the composites<sup>8,9</sup>. These flexible elastomer magnets find extensive applications in microwave absorbers and other devices, where flexibility and mouldability are important criteria. For applications involving microwave absorption it is essential that the materials warrant an appropriate permittivity and a desirable magnetic property<sup>8-13</sup>. This can be achieved in single step by synthesising rubber ferrite composites.

Rubber ferrite composites can be synthesised by the incorporation of ferrite powders in natural or synthetic rubber matrixes. Both the soft and hard ferrites can be embedded in the rubber matrix. It has been reported that flexible magnets with appropriate magnetic properties can be made by judicious choice of soft ferrites like

nickel zinc ferrite and manganese zinc ferrite in both natural and butyl rubber matrix<sup>14,15</sup>. The incorporation of hard ferrites in the elastomer matrix can produce flexible permanent magnets, which find widespread applications. The preparation of RFCs and evaluation of various properties such as magnetic, dielectric and mechanical assumes significance not only in tailor making composites but also in understanding the fundamental aspects that govern these properties. The results of investigation on the magnetic properties of ceramic barium ferrite and strontium ferrite and RFCs containing these ferrites are discussed in this chapter.

Hard ferrites namely barium ferrite and strontium ferrite have been prepared using ceramic processing techniques. The details are described in chapter 3. These hexagonal ferrites were then incorporated in natural rubber and nitrile rubber matrix at different loadings according to a specific recipe as cited in chapter 3. The RFCs containing various loading of carbon black were also prepared. Magnetic properties were evaluated for BaF, SrF and rubber ferrite composites with and without carbon black. From the magnetic data obtained for the ceramic fillers and RFCs, the variation in magnetic properties with loading of ferrite filler and carbon black were studied. A general relationship connecting the magnetic property of the ceramic filler and the composites were correlated using equation 6.1. The validity of the equation was then checked using observed data and the calculated values of magnetisation.

## **6.2 MAGNETIC MEASUREMENTS**

Magnetic measurements of the ceramic barium ferrite, strontium ferrite and rubber ferrite composites with and without carbon black were carried out using Vibrating Sample Magnetometer (VSM) model:4500 (EG&G PARC) at room temperature, as explained in chapter2. The hysteresis loop parameters namely saturation magnetisation ( $M_s$ ), magnetic remanence or retentivity ( $M_r$ ) and coercivity ( $H_c$ ) were evaluated.

### **6.2.1 Ceramic samples.**

Magnetic properties of the ceramic barium ferrite and strontium ferrite were evaluated at room temperature (303K). Figures 6.1 and 6.2 shows the hysteresis loop for the ceramic barium ferrite and strontium ferrite respectively.



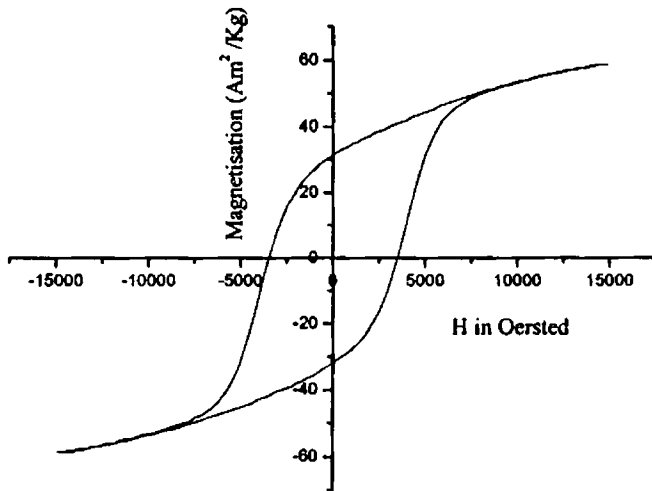


**Fig 6.1 Hysteresis loop of ceramic BaF**

The hysteresis loop parameters of the ceramic ferrites have confirmed the magnetic character. The saturation magnetisation ( $M_s$ ) and coercivity ( $H_c$ ) of BaF is slightly higher than that of the SrF, whereas the magnetic remanence ( $M_r$ ) of BaF is slightly lower than that of SrF. The measured values of saturation magnetisation of these ceramic ferrites matched well with that of the reported values.

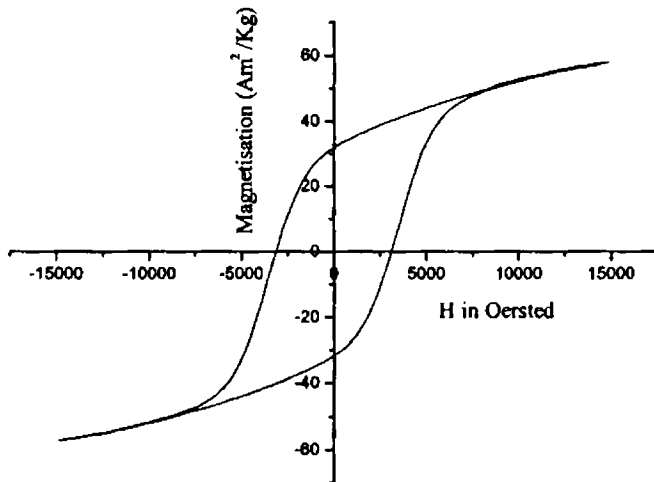


**Fig 6.2 Hysteresis loop of ceramic SrF**

## 6.2.2 Magnetic measurements of rubber ferrite composites based on natural rubber.

The hysteresis loops and magnetic parameters of NR based rubber ferrite composites containing various loading of barium ferrite and strontium ferrite were studied. The effect of carbon black on the magnetic properties of these RFCs was also studied.

### 6.2.2.1 Rubber ferrite composites containing barium ferrite

The rubber ferrite composites containing 40,60,80,100 and 120 phr of BaF in natural rubber were prepared as explained in chapter 3. The magnetic parameters of these RFCs have shown that they are magnetic in nature. The table 6.1 shows the hysteresis loop parameters of natural rubber based RFCs containing barium ferrite. Hysteresis loop for rubber ferrite composites containing 120 phr of BaF is shown in figure 6.3.

**Table 6.1. Hysteresis loop parameters of NR based RFCs containing BaF**

Barium ferrite loading (phr)	Coercivity, $H_c$ (A/m)	Magnetic remanence, $M_r$ ( $\text{Am}^2/\text{Kg}$ )	Saturation magnetisation, $M_s$ ( $\text{Am}^2/\text{Kg}$ )	$M_r/M_s$
40	3458	8.10	14.94	0.54
60	3468	11.57	21.01	0.55
80	3468	13.68	24.81	0.55
100	3468	15.49	28.25	0.55
120	3468	17.44	31.71	0.55
Ceramic BaF	3468	30.52	58.83	0.52

From the table 6.1 it is clear that the magnetic properties increased with the loading of BaF filler. The saturation magnetisation and the magnetic remanence values increased steadily with the filler loading.

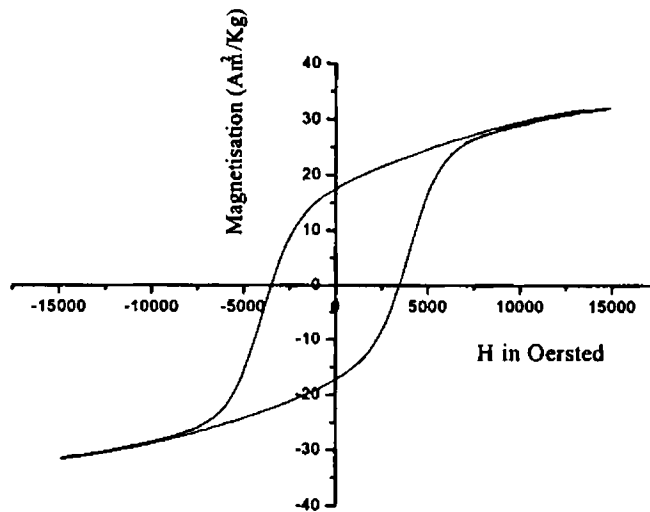


**Fig 6.3 Hysteresis loop of natural rubber based RFC containing 120 phr of BaF**

The variation in magnetic remanence with loading of BaF in NR based RFCs is shown in figure 6.4. It increased with the loading of ferrite filler.

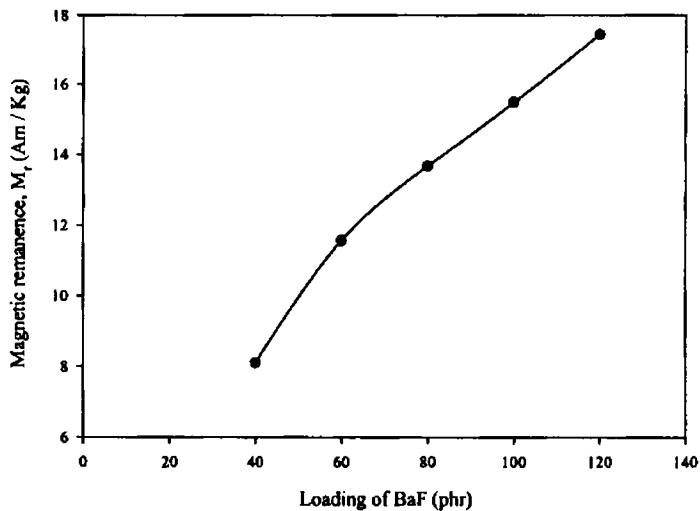


**Fig 6.4 Variation in magnetic remanence versus loading of BaF in NR**

The variation in coercivity with loading of BaF in natural rubber is shown in figure 6.5. It showed almost same value as that of the ceramic component. It is reported that the coercivity of ceramic samples mainly depend on parameters like sintering conditions and particle size <sup>2,16</sup>. The slight variations in coercivity between the ceramic and composites can occur due to the particle size reduction that takes place during compounding and mixing. However this variation is negligible. From this observation it can be concluded that loading of BaF has no effect on coercivity of RFCs.

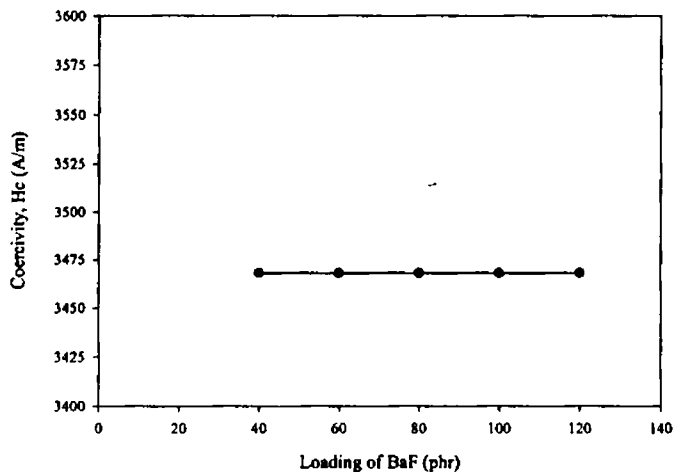


**Fig 6.5 Variation in coercivity with loading of BaF in natural rubber**

#### **6.2.2.2 Effect of carbon black on the magnetic properties of RFC containing barium ferrite**

Carbon black was incorporated into NR based RFC containing 80 phr of BaF and its magnetic properties were evaluated. The table 6.2 shows the hysteresis loop parameters of these rubber ferrite composites. It indicated that the saturation magnetisation and the magnetic remanence decreased with increase in the loading of carbon black. The decrease in the magnetic properties with the incorporation of carbon black is due to the reduction in the weight fraction of the magnetic component in the RFCs. However the coercivity values did not show much variation with the addition of carbon black.

**Table 6.2 Magnetic properties of NR based RFCs containing 80 phr of BaF and various loading of carbon black**

Carbon black loading (phr)	Coercivity, $H_c$ (A/m)	Magnetic remanence, $M_r$ ( $\text{Am}^2/\text{Kg}$ )	Saturation magnetisation, $M_s$ ( $\text{Am}^2/\text{Kg}$ )	$M_r / M_s$
0	3468	13.68	24.81	0.55
10	3509	13.08	23.98	0.55
20	3509	12.48	22.79	0.55
30	3509	11.65	21.56	0.54
40	3509	11.07	20.18	0.55
50	3509	10.41	18.76	0.56

Even though the saturation magnetisation and magnetic remanence decreased, the RFCs containing carbon black still possessed appreciable magnetisation values. This can be utilised for the preparation of RFCs intended for microwave applications, which warrants an appropriate magnetic and dielectric properties. Figure 6.6 depicts the hysteresis loop of NR based rubber ferrite composites containing 80 phr BaF and 50 phr of carbon black.

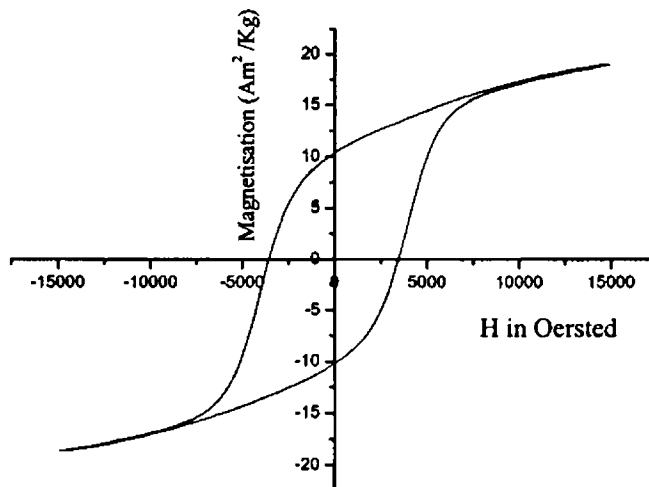


**Fig 6.6 Hysteresis loop of NR based rubber ferrite composites containing 80 phr BaF and 50 phr of carbon black.**

### 6.2.2.3 Rubber ferrite composites containing strontium ferrite

The natural rubber based RFCs containing 40,60,80,100 and 120 phr of SrF were prepared as explained in chapter 3. The magnetic measurements at room temperature were studied using VSM. The table 6.3 shows the magnetisation parameters of natural rubber containing strontium ferrite.

**Table 6.3 Magnetisation parameters of natural rubber based RFCs containing various loading of SrF**

Strontium ferrite loading (phr)	Coercivity, $H_c$ (A/m)	Magnetic remanence, $M_r$ ( $\text{Am}^2/\text{Kg}$ )	Saturation magnetisation, $M_s$ ( $\text{Am}^2/\text{Kg}$ )	$M_r/M_s$
40	3054	10.03	17.82	0.56
60	3054	12.82	22.24	0.58
80	3054	15.06	26.83	0.56
100	3054	17.21	30.90	0.56
120	3054	18.57	33.44	0.56
Ceramic SrF	3059	32.17	58.04	0.55

From tables 6.1 and 6.3 it can be observed that the ceramic SrF shows a lower coercivity value than the ceramic BaF. The saturation magnetisation and the magnetic remanence of these ceramic ferrites are found to be almost same. The hysteresis loop of rubber ferrite composites containing 40 phr of SrF is shown in figure 6.7.

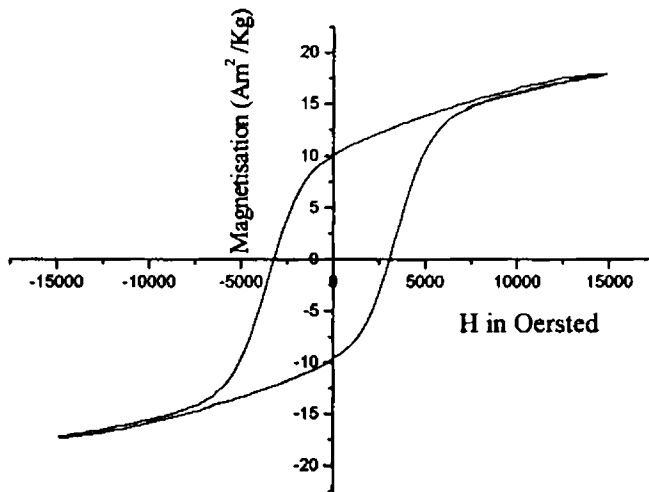


**Fig 6.7 Hysteresis loop of NR based rubber ferrite composites containing 40 phr of SrF**

The table 6.3 shows that the magnetic properties of these composites increase with the loading of SrF filler. The saturation magnetisation and the magnetic remanence values increased steadily with the loading of SrF. The variation of  $M_s$  and  $M_r$  for different loading of SrF is shown in figures 6.8 and 6.9 respectively.

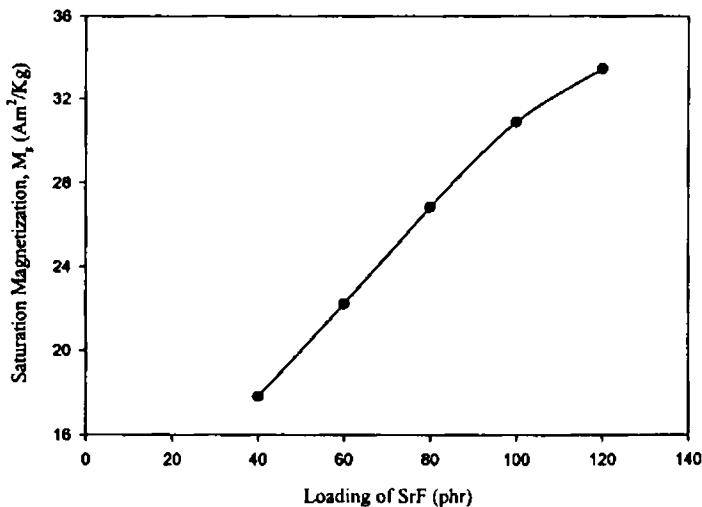


**Fig 6.8 Variation in saturation magnetisation with loading of SrF in NR based RFCs**

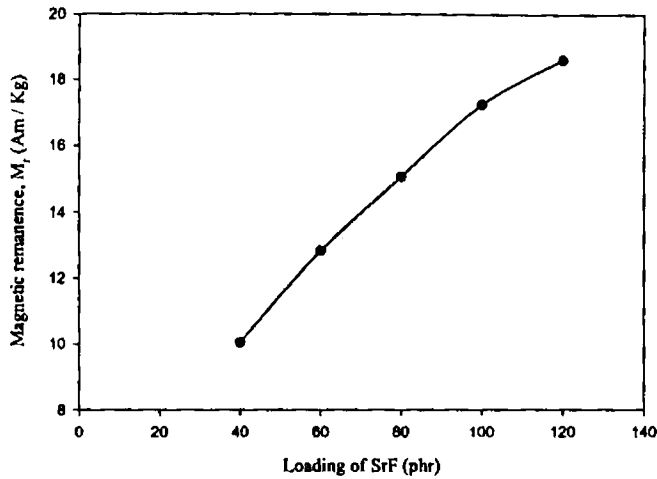


**Fig 6.9 Variation in magnetic remanence with loading of SrF in NR based RFCs**

The coercivity values of the RFCs containing SrF also showed a similar behaviour as that of the ceramic component. The variation in coercivity of NR based RFCs with loading of SrF is shown in fig. 6.10.

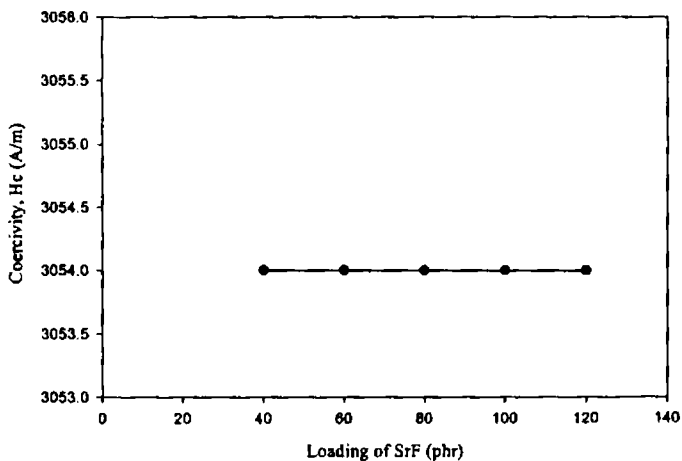


**Fig 6.10 Variation in coercivity with loading of SrF in natural rubber based RFCs**



The magnetic property measurements of NR based composites indicated that the SrF filled materials are having a higher  $M_s$  and  $M_r$  value than that of the RFCs based on BaF.

#### 6.2.2.4 Effect of carbon black on the magnetic properties of RFCs containing strontium ferrite

The NR based RFCs with 80 phr of SrF and 10, 20, 30, 40 and 50 phr loading of carbon black were prepared as explained in chapter 3. The VSM studies indicated that the saturation magnetisation and the magnetic remanence decreased with the loading of carbon black. As in the case of RFC containing BaF, the decrease in the magnetic properties is due the decrease in weight fraction of the magnetic component in the rubber ferrite composites. The coercivity values do not vary with the increase in loading of carbon black.

The variation in saturation magnetisation and magnetic remanence for different loading of carbon black in NR containing 80phr of SrF is shown in figures 6.11 and 6.12 respectively.

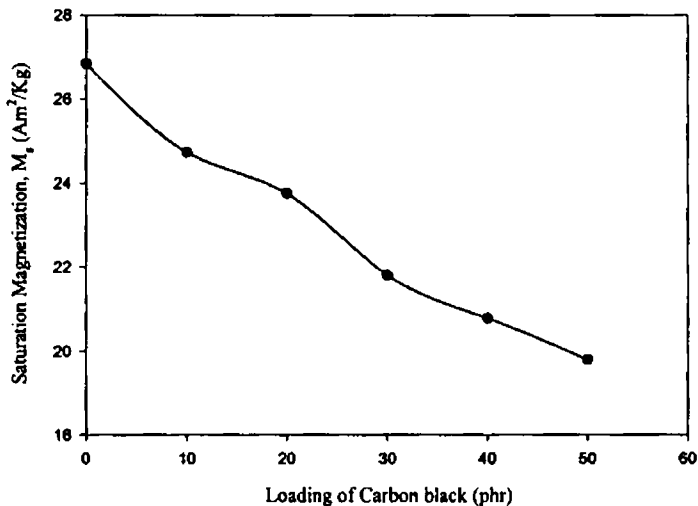


**Fig 6.11** Variation in saturation magnetisation with the loading of carbon black in NR containing 80phr of SrF

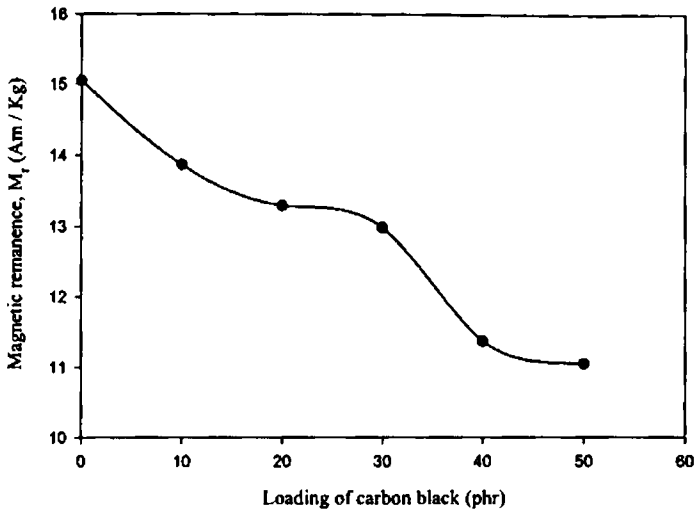


**Fig 6.12 Variation in magnetic remanence with the loading of carbon black in NR containing 80phr of SrF**

Figure 6.13 shows the hysteresis loop of NR based rubber ferrite composites containing 80 phr of SrF and 50 phr of carbon black.

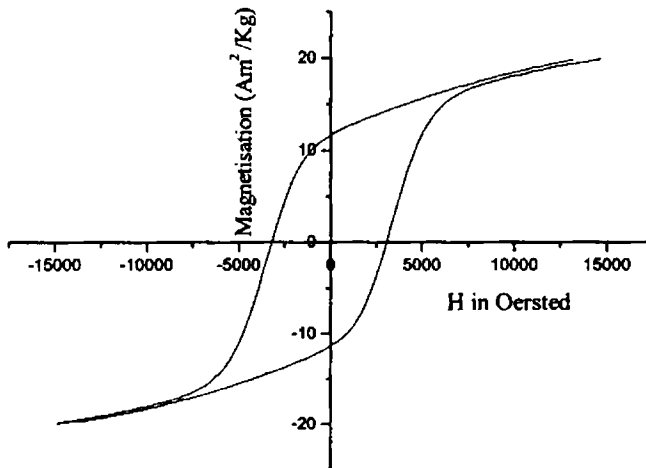


**Fig 6.13 Hysteresis loop of NR based RFCs containing 80 phr SrF and 50 phr of carbon black**

### 6.2.3 Magnetic measurements of nitrile rubber based RFCs.

The nitrile rubber based RFCs containing various loading of ferrite fillers and carbon black were prepared as per the procedure explained in chapter 3. The hysteresis loops and the magnetic parameters of these composites were measured using the Vibrating Sample Magnetometer at room temperature.

#### 6.2.3.1 Rubber ferrite composites containing barium ferrite

The rubber ferrite composites based on NBR containing 40,60,80,100 and 120 phr of BaF were prepared and magnetic measurements were carried out as explained in chapter 2. Table 6.4 shows the hysteresis loop parameters of these nitrile rubber based RFCs.

**Table 6.4. Hysteresis loop parameters of nitrile rubber based RFCs containing BaF**

Barium ferrite loading (phr)	Coercivity, $H_c$ (A/m)	Magnetic remanence, $M_r$ ( $\text{Am}^2/\text{Kg}$ )	Saturation magnetisation, $M_s$ ( $\text{Am}^2/\text{Kg}$ )	$M_r / M_s$
40	2933	8.75	16.89	0.52
60	2943	11.45	23.15	0.50
80	2933	14.74	28.22	0.52
100	2943	15.55	30.31	0.51
120	2943	16.56	33.08	0.50

The table 6.4 indicated that the saturation magnetisation and the magnetic remanence values of RFCs increased with the loading of BaF filler. The coercivity values of RFCs were less than that of the ceramic BaF, but did not vary with the different loading of BaF. Hysteresis loop of the NBR based rubber ferrite composite containing 40 phr of BaF is shown in figure 6.14.

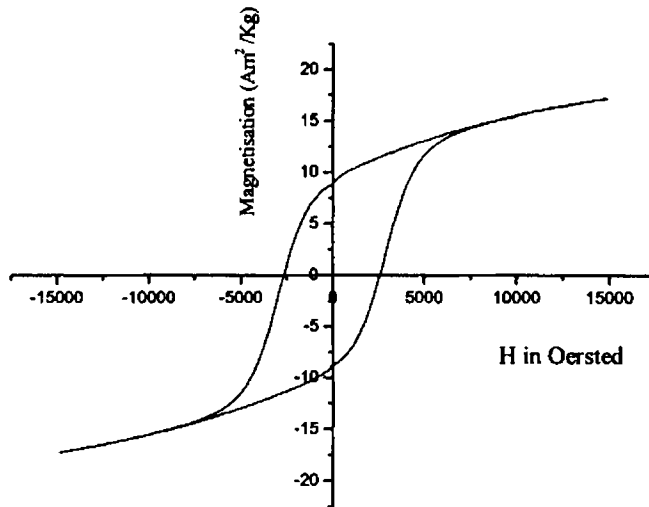


**Fig 6.14 Hysteresis loop of the NBR based RFC containing 40 phr of BaF**

The variation in saturation magnetisation and magnetic remanence with loading of BaF in NBR is shown in figures 6.15 and 6.16 respectively.

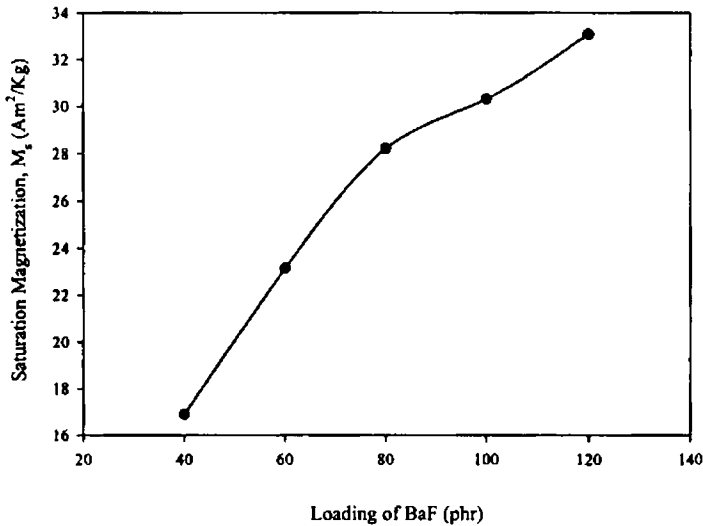


**Fig 6.15 Variation in saturation magnetisation with the loading of BaF in NBR**

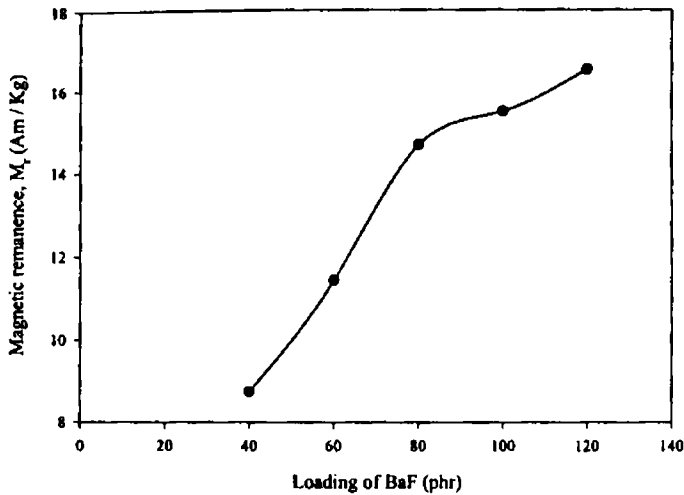


**Fig 6.16** Variation in magnetic remanence with the loading of BaF in NBR

### 6.2.3.2 Effect of carbon black on the magnetic properties of RFCs containing barium ferrite

The RFCs containing 80 phr of BaF and various loading of carbon black in NBR was prepared and the magnetic properties were studied as explained in chapter 2. The table 6.5 shows the hysteresis loop parameters of these rubber ferrite composites.

**Table 6.5** Hysteresis loop parameters of NBR based RFC containing 80 phr BaF and different loading of carbon black.

Carbon black loading (phr)	Coercivity, $H_c$ (A/m)	Magnetic remanence, $M_r$ ( $\text{Am}^2/\text{Kg}$ )	Saturation magnetisation, $M_s$ ( $\text{Am}^2/\text{Kg}$ )	$M_r/M_s$
0	2933	14.74	28.22	0.52
10	2934	13.85	26.12	0.53
20	2934	12.08	24.19	0.50
30	2933	11.66	23.15	0.54
40	2933	11.45	22.39	0.51
50	2933	11.23	22.16	0.51

Table 6.5 indicated that the saturation magnetisation and the magnetic remanence values decreased with the loading of carbon black. However the coercivity values remained the same for these composites. Even though the RFCs containing carbon black shows slightly lower magnetisation values they are useful in making devices, which requires good mechanical and dielectric properties. Figure 6.17 depicts the hysteresis loop for NBR based rubber ferrite composites containing 80 phr BaF and 50 phr of carbon black.

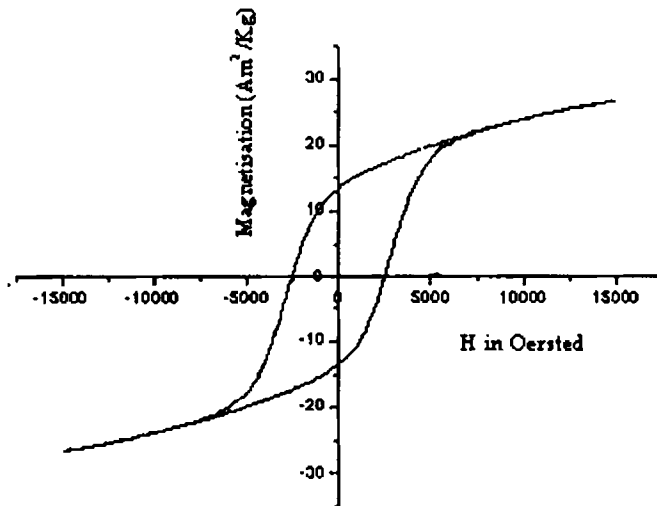


**Fig 6.17 Hysteresis loop for NBR based RFCs containing 80 phr BaF and 50 phr of carbon black.**

### 6.2.3.3 Rubber ferrite composites containing strontium ferrite

The NBR based rubber ferrite composites containing 40,60,80,100 and 120 phr of SrF were prepared as explained in chapter 3. The magnetic measurements at room temperature were studied using VSM. The table 6.6 shows the magnetic properties of RFCs containing various loading of SrF.

**Table 6.6. Magnetic properties of nitrile rubber based RFCs containing SrF.**

Strontium ferrite loading (phr)	Coercivity, $H_c$ (A/m)	Magnetic remanence, $M_r$ ( $\text{Am}^2/\text{Kg}$ )	Saturation magnetisation, $M_s$ ( $\text{Am}^2/\text{Kg}$ )	$M_r/M_s$
40	2653	7.93	17.51	0.45
60	2663	10.37	22.76	0.46
80	2663	13.51	27.47	0.49
100	2665	15.18	30.61	0.50
120	2664	16.49	33.53	0.49

The variation in saturation magnetisation and magnetic remanence for different loading of SrF in nitrile rubber is shown in figures 6.18 and 6.19 respectively. It can be observed that the saturation magnetisation and magnetic remanence increases with the loading of strontium ferrite.

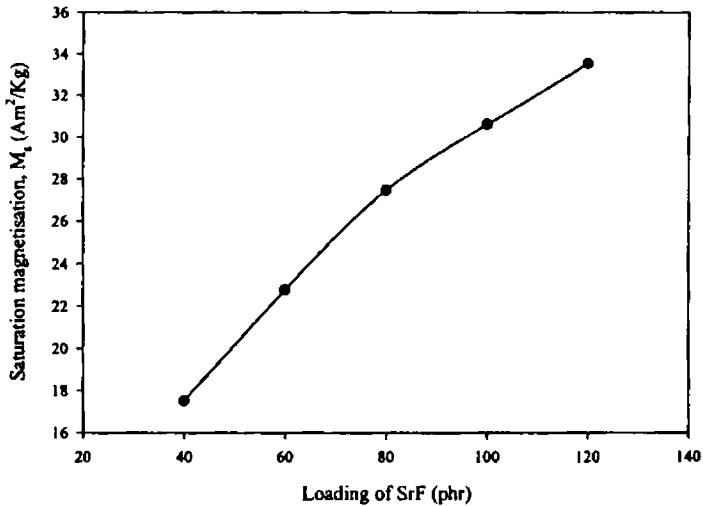


**Fig 6.18 Variation in saturation magnetisation with the loading of SrF in NBR**

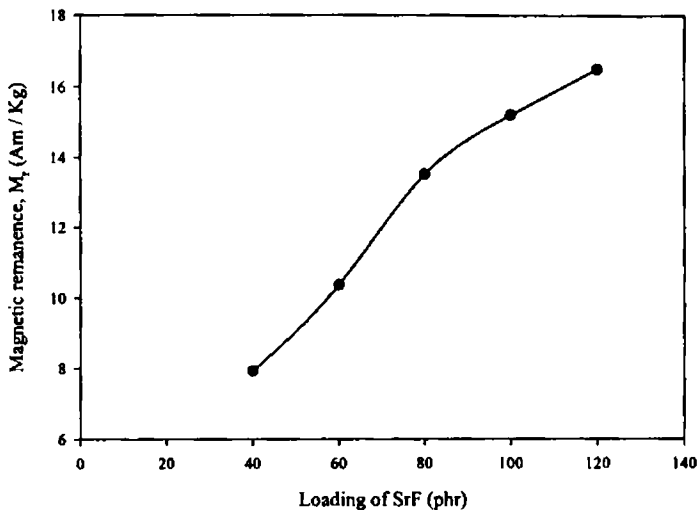


**Fig 6.19 Variation in magnetic remanence with the loading of SrF in NBR based RFCs**

#### **6.2.3.4 Effect of carbon black on the magnetic properties of RFCs containing strontium ferrite**

The rubber ferrite composites containing 10, 20, 30, 40 and 50 phr loading of carbon black along with 80 phr of strontium ferrite in nitrile rubber were prepared as explained in chapter 3. The VSM studies indicated that the saturation magnetisation and the magnetic remanence values decreased with the loading of carbon black, which can be explained by the decrease in the weight fraction of the ferrite material in the composites. The coercivity values remained constant for the increase in loading of carbon black. The table 6.7 shows the hysteresis loop parameters of nitrile rubber containing strontium ferrite and various loading of carbon black. From tables 6.1 to 6.7, it can be observed that the  $M_r/M_s$  values of the rubber ferrite composites both with and without carbon black remains almost the same as that of the ceramic ferrites.



**Table 6.7. Magnetic properties of nitrile rubber based RFCs containing 80 phr of SrF and various loading of carbon black.**

Carbon black loading (phr)	Coercivity, $H_c$ (A/m)	Magnetic remanence, $M_r$ ( $\text{Am}^2/\text{Kg}$ )	Saturation magnetisation, $M_s$ ( $\text{Am}^2/\text{Kg}$ )	$M_r/M_s$
0	2663	13.51	27.47	0.49
10	2653	13.26	26.55	0.50
20	2655	12.76	24.95	0.51
30	2655	12.60	23.56	0.54
40	2653	11.98	22.14	0.54
50	2653	11.19	21.35	0.52

The variation in saturation magnetisation and magnetic remanence for different loadings of carbon black in nitrile rubber with 80 phr of SrF and various loading of carbon black is shown in figures 6.20 and 6.21 respectively.

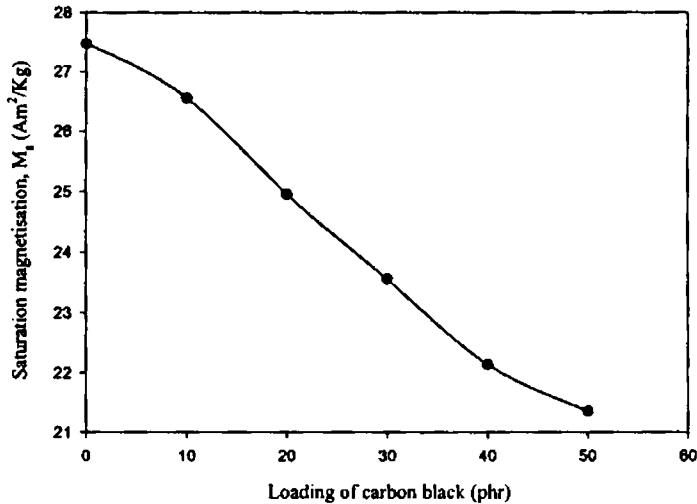


**Fig 6.20 Variation in saturation magnetisation with loading of carbon black in NBR based RFCs containing 80 phr SrF.**

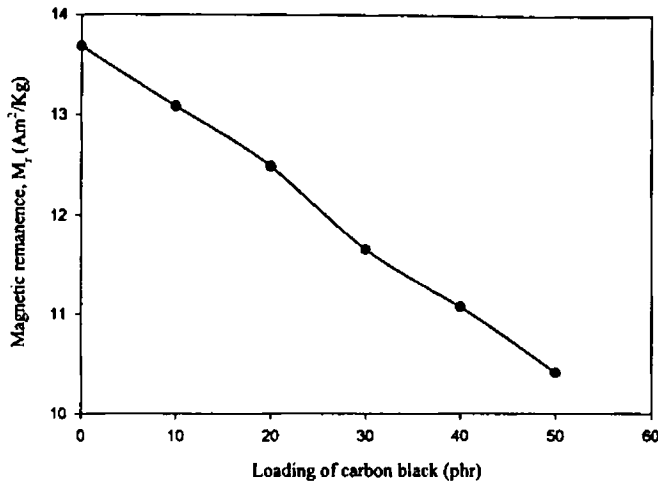


**Fig 6.21 Variation in magnetic remanence with loading of carbon black in NBR based RFCs containing 80 phr SrF.**

### 6.3 TAILORING OF MAGNETIC PROPERTIES OF RUBBER FERRITE COMPOSITES (SATURATION MAGNETISATION)

Rubber ferrite composites with predetermined properties are mandatory when designing RFCs for special purpose applications. Hence attempts were made to tailor the magnetic properties of the composites from the known values of the saturation magnetisation ( $M_s$ ) of the ceramic fillers. If the  $M_s$  values of the ceramic fillers are known a simple mixture equation of the general form (equation 6.1) involving the weight fractions of the filler can be employed for estimating the  $M_s$  of the composite samples.

$$M_{rfc} = W_1 M_1 + W_2 M_2 \quad (6.1)$$

where  $W_1$  is the weight fraction of filler,  $M_1$  is the saturation magnetisation of the filler,  $W_2$  is the weight fraction of the polymer matrix and  $M_2$  is the saturation magnetisation of the matrix. Since the matrix namely NR and NBR is nonmagnetic this equation can be reduced to the following form

$$M_{rfc} = W_1 M_1 \quad (6.2)$$

The variation in saturation magnetisation of the NR based RFCs with the loading of the barium ferrite was studied. Figure 6.22 shows the variation in magnetisation values of RFCs with loading of BaF. The solid line represents the

experimental and the dotted line represents the calculated values. From the figure it is clear that the experimental values and the calculated values using equation.6.2 are in good agreement.

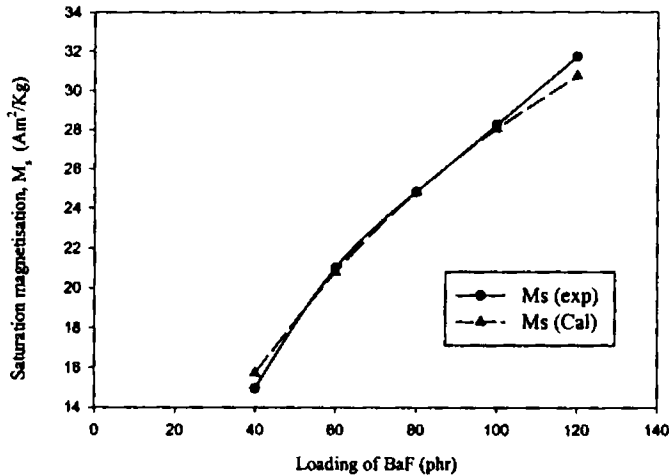


**Fig 6.22 Experimental and calculated values of saturation magnetisation of NR based RFCs containing BaF**

Figure 6.23 depicts the variation in experimental and calculated values of saturation magnetisation with the loading of carbon black in the RFC containing 80 phr barium ferrite.

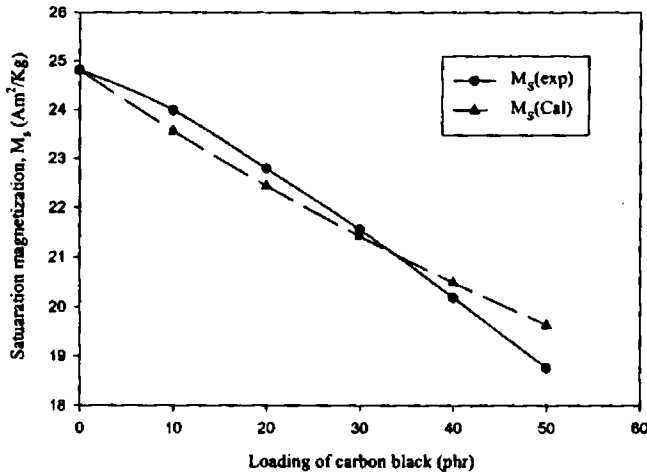


**Fig 6.23 Experimental and calculated values of saturation magnetisation of NR based RFCs containing 80 phr SrF and various loading of carbon black**

As expected the values decreased due to the decrease in the weight fraction of the magnetic component. The saturation magnetisation of RFCs containing different loading of carbon black was calculated by employing equation 6.2 considering carbon black as non magnetic filler. These were then compared with the experimental values. From the figure it was found that that the experimental values agreed well with the calculated values

#### **6.4 CONCLUSION**

Rubber ferrite composites containing barium ferrite and strontium ferrite in natural rubber and nitrile rubber matrix were prepared. Magnetic parameters of the ceramic ferrites as well as that of the RFCs were studied. Study of the magnetic properties indicated the formation of elastomer magnets with suitable saturation magnetisation and magnetic remanence. The saturation magnetisation and the magnetic remanence increased with increase in the loading of barium ferrite and strontium ferrite. The coercivity of the RFCs remained almost same as that of the ceramic component. The effect of carbon black on the magnetic properties of these RFCs was also studied. The magnetic measurements indicated that the saturation magnetisation and the magnetic remanence decreased with the loading of carbon black. However the coercivity was not affected with increasing loading of carbon black. From the magnetic property studies of both natural and nitrile rubber based RFCs containing barium ferrite and strontium ferrite, it can be observed that the matrix material does not have significant effect on saturation magnetisation and magnetic remanence.

By synthesising RFCs, we have the exceptional advantage of modifying saturation magnetisation and magnetic remanence according to the requirement. Hence the desired magnetic property can be imparted by appropriate loading of ferrite fillers. The calculated values tally well with the experimental values of the saturation magnetisation, which indicate that it is possible to modify materials with a definite magnetisation value by appropriate loading of barium ferrite and strontium ferrite filler in both the NR and NBR matrix. Hence the relationship connecting the magnetisation ( $M_s$ ) of RFC with the magnetisation of the respective fillers can be employed to tailor magnetic properties

## REFERENCES

1. Hadfield D, 'Permanent Magnets and Magnetism', John Wiley and sons, Inc. London 1962.
2. Cullity B.D, 'Introduction to Magnetic Materials', 1972, Philippines, Addison-Wesley Publishing Company, Inc.
3. Safari Ardi M, Dick W and McQueen D.H, Plastic Rubber and Composites Processing Applications, **24** (1995) 157-164.
4. Anantharaman M. R, S. Jagatheesan, S. Sindhu, K. A. Malini, C. N. Chinnasamy, A. Narayansamy, P. Kurian and K. Vasudevan, Plastic Rubber and Composites Processing Applications, **27**, 2 (1998) 77-81.
5. Anantharaman M.R, S. Sindhu, S. Jagatheesan, K.A. Malini and Philip Kurian, Journal of Physics D Applied Physics **32** (1999) 1801-1810.
6. Praveen Singh & T.C. Goel: Indian J. Pure and Appl Phys., **38** (2000) 213-219.
7. Anantharaman M. R, P. Kurian, B. Banerjee, E. M. Mohammed, and M. George, Kautschuk Gummi Kunststoffe, (Germany), **49**, 6/96, 424- 426.
8. Jozef Slama, Anna Gruskova, L'udovit Keszegh, Mojmir Kollar: IEEE Trans. Mag., **30**, 2 (1994) 1101-1103.
9. Osawa. Z, K. Kawaguchi, M. Iwata, H.Harada, J.Mater. Sci.**23** (1988) 2637-44.
10. Mitsuo Sugimoto, Journal of American Ceramic Society. **82**, 2 (1999) 269- 279.
11. H. Takei, H. Tokumasu, H. Rikukawa and I. Sasaki, IEEE Trans. Mag. Vol MAJ **23** (1987) 3080-3082.
12. A.M. Sankpal, S.S. Suryavanshi, S.V. Kakatbar, G.G. Tengshe, R.S. Patil, N.D. Chaudhari, S.R. Sawant, J. Mag. Magn. Mater. **186** (1998) 349-356.
13. T. Nakamura, T. Tsutaoka, K. Hatekeyama, J. Mag. Mag. Mater. **138** (1994) 319- 328.
14. K.A. Malini, E.M. Mohammed, S. Sindhu, P.A. Joy, S.K. Date, S.D. Kulkarni, P. Kurian and M.R. Anantharaman, J. Mater. Sci.**36** (2001), 5551-5557.
15. Anantharaman. M.R, K.A. Malini, S.Sindhu, E.M. Mohammed, S.K. Date, P.A. Joy and Philip Kurian, Bull. Mater. Sci., **24**, 6, (2001) 623-631.
16. Smit. J and H.P.J. Wijn, 'Ferrites', 1959, Philips Technical library.

# Chapter 7

---

## SUMMARY AND CONCLUSION

This concluding chapter provides a glimpse of the conclusions drawn from the work carried out on the subject of rubber ferrite composites and the scope for the future work on rubber ferrite composites (RFC).

Composites play a major role in the science and technology of the present day. The magnetic polymer composites especially rubber ferrite composites is one of the many composite materials in which the scientist and engineers are interested and find scope for possible exploitation of commercial applications. Here attempts have been made to prepare magnetic rubber composites. Ferrites are ferrimagnetic materials and come under a group of technologically important magnetic materials, which has received the greatest attention and cannot be easily replaced by any other magnetic materials as they are stable, economical and possess a wide range of applications. Brittleness of the ceramic magnetic materials is one of the difficulties faced in the application point of view. Here the magnetic composites can play a very crucial role. Rubber ferrite composites are magnetic polymer composites made of ferrite fillers and natural or synthetic rubber matrix. This rubber ferrite composite has the advantage of easy fabrication into complex shapes. Flexibility with the required mechanical strength is another hallmark of these composites. These composites can be used as potential microwave absorbers in a wide range of frequencies due to its dielectric properties, low cost, lightweight and

design flexibility. Therefore, preparation and characterisation of RFCs is important and assumes significance

## **7.1 SUMMARY**

The main focus of this study was to synthesise, characterise and investigate the magnetic, dielectric and mechanical properties of rubber ferrite composites based on natural rubber (NR) and nitrile rubber (NBR). Hard ferrites namely barium ferrite (BaF) and strontium ferrite (SrF) in the monophasic form were prepared and characterised. These precharacterised magnetic fillers are then incorporated into two different matrixes, natural and nitrile rubber separately, to produce rubber ferrite composites. The hard ferrites are selected, to produce flexible permanent magnets. The natural rubber is chosen as one of the polymer matrixes because of its easy availability and low cost, whereas the nitrile rubber is selected as the other matrix material considering its superior properties and special purpose application.

The thesis consists of seven chapters, where the **Chapter 1** gives a general introduction to the polymers, rubber ferrite composites, magnetic materials, their classification, applications and the main objectives of the thesis. **Chapter 2** presents a general discussion of the materials used and the experimental techniques employed for the preparation and characterisation of the samples. Chapter 3 to 6 gives the details of the findings of the work carried out on RFCs. The present chapter gives the summary and conclusions of the findings described in each chapter.

**Chapter 3** described the preparation and characterisation of the ferrites and its incorporation into rubber matrixes to produce the rubber ferrite composites. Hexagonal hard ferrites namely barium ferrite and strontium ferrites were prepared by the ceramic techniques. Structural evaluations of the prepared BaF and SrF samples were carried out using X-ray diffraction (XRD) method. These samples were checked for their monophasic characteristics before they were incorporated in to the rubber matrixes. RFCs were prepared by incorporating these precharacterised powder samples into NR and NBR matrixes for various loadings according to a specific recipe. The addition of carbon black is known to reinforce the rubber matrix; moreover studies have indicated that the addition of fillers like

carbon black on rubber ferrite composites enhances the microwave absorbing properties of the composites. Hence the carbon black filled RFCs were prepared by incorporating varying amount of carbon black into RFC containing an optimum quantity of ferrite.

The Cure Characteristics and mechanical properties of the of rubber ferrite composites are discussed in **Chapter 4**. Evaluation of the cure characteristics indicated that RFCs containing barium ferrite and strontium ferrite with and without carbon black reduces both the scorch time and cure time, whereas the minimum and maximum torque values increases with the addition of these materials. The studies also revealed that the processability of the composites is not much affected even up to a loading of 120 phr of ferrite fillers.

Evaluation of the mechanical properties has shown that the addition of magnetic fillers improves the modulus and hardness but slightly reduces the elongation at break. The addition of the ferrites into the natural rubber matrix reduced the tensile strength slightly, because of the inhibition in stress induced crystallization of the NR matrix. But in the case of NBR, the addition of ferrites increases the tensile strength, since it reinforces the NBR matrix. The tensile strength reduced at higher loading of the ferrite filler due to the dilution effect.

The incorporation of carbon black to both natural and nitrile rubber increased the tensile strength significantly, since it is a good reinforcing filler. The studies also indicated that the percolation threshold was not reached for a maximum loading of 120 phr of the filler. Hence after attaining the required magnetic property, if the percolation limit is not reached, the mechanical properties of RFCs can be enhanced by the addition of appropriate amount of carbon black

The dielectric properties of the rubber ferrite composites both with and without carbon black are evaluated and discussed in **Chapter 5**. RFCs intended for microwave applications necessitates an appropriate permeability and permittivity. Hence it is essential to modify the magnetic and dielectric properties. The study of dielectric constant indicated that it decreased with increase of frequency for ceramic samples (BaF and SrF), gum vulcanisates (NR and NBR) and the rubber ferrite composites containing these ferrites both with and without carbon black. The temperature dependence on dielectric constant was also studied and it was



observed that composites were stable up to a maximum temperature of 393K with no visible sign of degradation. The dielectric constant of these materials increased with increasing temperature. But in RFC containing BaF and SrF, the increase in dielectric constant with increase in temperature was not so prominent as in the case of ceramic samples. The carbon black containing RFCs showed a large increase in dielectric constant with temperature.

The dielectric constant of NBR has been found to be greater than that of NR, which indicates that NBR is superior in dielectric properties compared to NR. The addition of the ferrite fillers to both natural and nitrile rubber increased the dielectric constants. The absolute values of the dielectric constant of the composites are found to be greater than that of the gum vulcanisates, but less than that of the ceramic component. It was observed that the dielectric constant increases with increase of volume fraction of the ferrite material. Dielectric constant was found to be maximum for a loading of 120phr. The incorporation of carbon black into these RFCs increased the dielectric constants to a greater extent. In all the cases the dielectric constants increased to a higher value even with the addition of 10 phr of carbon black. Maximum dielectric constant was obtained for a loading of 50phr of carbon black. Moreover the RFCs containing BaF/SrF in nitrile rubber along with carbon black is superior when compared to RFCs based on natural rubber for dielectric applications

The ac conductivity of the ceramic samples, gum vulcanisates and rubber ferrite composites containing SrF with and without carbon black was estimated using the data obtained from the dielectric measurements. The ac conductivity increased with frequency for these materials. NBR gum vulcanisate showed high ac conductivity than that of NR gum vulcanisate. The ac conductivity of the RFCs increased with the increasing loading of SrF. For carbon black containing RFCs the ac conductivity steadily increased with the increasing loading of carbon black.

Magnetic properties of both ceramic fillers and RFCs are evaluated and dealt in **Chapter 6**. The studies of the magnetic properties indicated the formation of elastomer magnets with appropriate value of saturation magnetisation ( $M_s$ ) and magnetic remanence ( $M_r$ ). The saturation magnetisation and the magnetic remanence increase with the increase in the loading of both barium ferrite and strontium ferrite.

The coercivity of these magnetic composites remains almost the same as that of the ceramic ferrite filler. The magnetic properties of the carbon black containing RFCs indicated that the saturation magnetization and the magnetic remanence values decreases with the loading of carbon black. However the coercivity ( $H_c$ ) values remains constant with the increase in loading of carbon black.

The desired saturation magnetisation and magnetic remanence can be imparted by the appropriate loading of ferrite fillers in the rubber matrix. The saturation magnetisation of RFCs can be calculated using the empirical relationship  $M_{rfc} = W_1M_1 + W_2M_2$ , connecting the saturation magnetisation of the RFCs ( $M_{rfc}$ ) with the magnetisation of the respective fillers. The calculated values of the saturation magnetisation agree well with that of the measured values. Hence it is possible to modify these composite materials so as to have a suitable magnetisation value by the appropriate loading of ferrite filler in both the natural and nitrile rubber matrix.

The investigations revealed that the rubber ferrite composites with the required dielectric and magnetic properties can be obtained by the incorporation of ferrite fillers into the rubber matrix, without compromising much on the processability and mechanical properties.

List of abbreviations and symbols are given at the end of the thesis and references at the end of each chapter.

## **7.2 CONCLUSION**

The following conclusions are derived from this work.

- Hard ferrites namely barium ferrite and Strontium ferrite were prepared by the ceramic method.
- These ferrites were characterised using the X-ray powder diffraction technique (XRD).
- Rubber ferrite composites were synthesised by the incorporation of these ferrites into both natural and nitrile rubber.

- The carbon black filled RFCs were prepared by incorporating varying amount of carbon black into the RFC containing an optimum quantity of ferrite.
- The processability of RFCs was not much affected by the filler incorporation.
- The mechanical properties of the RFCs were enhanced by the incorporation of both ferrite filler and carbon black.
- The dielectric constant decreased with frequency for the ceramic ferrites and the composites containing different loadings of BaF and SrF.
- The dielectric constant of RFCs increased with the increasing loading of ferrite fillers
- The dielectric constant of the ceramic samples and RFCs increased with increasing temperature.
- Addition of carbon black into RFCs increased the dielectric constant sharply.
- The dielectric constants were studied up to 393K and it was found that the composites were stable with no visible sign of degradation.
- The ac conductivity of ceramic ferrites and rubber ferrite composites containing SrF with and without carbon black increased with increasing frequency.
- Addition of ferrite fillers imparted magnetic property to the rubber matrixes.
- The saturation magnetisation and the magnetic remanence increased with increase in the loading of barium ferrite and strontium ferrite.
- RFCs can be designed with suitable magnetisation values by the appropriate loading of ferrite filler in both the natural and nitrile rubber matrix.

### **7.3 FUTURE OUTLOOK**

The study of ferrites and rubber ferrite composites is an area, which requires extensive research in the coming years. The techniques like sol-gel, cryochemical, microemulsion, liquid mix and lyophilization can produce ferrites of finer particle size at a lower temperature. Incorporation of these ferrites into different matrixes can lead to the development of magnetic composites with special properties. Some of the areas where more detailed studies required are:

- Embedding of magnetic fillers into Nylon matrix and evaluation of the mechanical, dielectric and magnetic properties is an area having enormous potential.
- Permeability is a determining factor as far as the microwave absorbing properties are concerned. Investigations on the determination of permeability could be undertaken as an extension of the present work.
- Further, scope also exists for incorporating barium and strontium ferrites in matrixes like butyl rubber, polystyrene, polyurethane, polyester etc.
- Morphological studies using optical microscope and scanning electron microscopy can be used to assess the dispersion of the fillers.
- In the present investigation the dielectric studies were limited in the mid-frequency range up to 8MHz. Scope exist to carry out further measurements using network analyser and evaluate the bandwidth of absorption.

## *List Of Abbreviations*

---

A	Area of test sample
AR	Analytical reagent
ASTM	American Society for Testing and Materials
BaF	Barium ferrite
CB	Carbon black
CBS	N-Cyclohexyl benzthiazyl sulphenamide
cps	Centi poise
d	Thickness of the sample
D	Particle size
DOP	Diocetyl phthalate
f	Frequency of the applied field
F	Farad
FOD	Ferrous oxalate dihydrate
h	Hours
HAF	High abrasion furnace black
H <sub>c</sub>	Coercivity
Hz	Hertz
ISNR	Indian Standard Natural Rubber
K	Anisotropy constant
Kg	Kilogram
M	Magnetic moment of the specimen
min	Minutes
ML (1+4) 100°C	Mooney Viscosity determined using large rotor, a preheating time of one minute and rotor run for 4 minutes at 100° C

## ***List of Abbreviations***

---

mm	Millimeter
MPa	Mega Pascal
$M_r$	Magnetic remanence or retentivity
$M_s$	Saturation magnetisation
n	Number of turns per unit length of coil
NBR	Acrylonitrile butadiene rubber
nm	Nano meter
Nm	Newton meter
NR	Natural rubber
Phr	Parts per hundred rubber
RFC	Rubber ferrite composite
rpm	Revolutions per minute
S	Siemens
SrF	Strontium ferrite
$t_{90}$	Optimum cure time
$t_{10}$	Scorch time
$t_5$	Induction time
T	Absolute temperature
UHF	Ultra high frequency
UTM	Universal testing machine
V	Volume loss
VHF	Very high frequency
VSM	Vibrating sample magnetometer
XRD	X-ray powder diffraction
ZnO	Zinc Oxide

## List of Symbols

---

$\mu_r$	Relative permeability
$\chi$	Susceptibility
C and $\theta$	Curie Weiss constants.
$\lambda$	Wavelength of the X-ray radiation
$\beta$	Full width half maximum of the intensity
$\rho$	Density of the sample
$\Delta M$	Mass loss
$\phi$	Magnetic flux
$\mu_0$	Permeability of free space
$\alpha$	Geometric moment decided by position of moment with respect to coil as well as shape of coil.
$\epsilon$	Dielectric constant
$\epsilon_r$	Relative permittivity
$\epsilon_0$	Permittivity of free space
$\epsilon'$	Real part of dielectric permittivity
$\epsilon_r''$	Imaginary part of the dielectric permittivity
$\tan \delta$	Dielectric loss
$\sigma_{ac}$	ac conductivity
$\omega$	Angular frequency

## List of Publications

---

1. **M.A. Soloman**, M.R.Anantharaman and Philip Kurian, Processability and Mechanical Properties of Rubber Ferrite Composites. National Seminar on Current Trends in Macromolecular Chemistry and Technology- MACROSEM 2000, St. Albert's College, Ernakulam, August 23-25 (2000).
2. **M.A.Soloman**, M.R.Anantharaman and Philip Kurian, Dielectric Properties of Rubber Ferrite Composites with and without Carbon Black. Proce.13<sup>th</sup> Kerala State Science Congress, KILA, Thrissur, January 29-31 (2001).
3. **M.A.Soloman**, P.A.Joy, M.R.Anantharaman and Philip Kurian, Processability and Magnetic Properties of Rubber Ferrite Composites containing Barium Ferrite, International Journal of Polymeric Materials. (In press).
4. **M.A.Soloman**, M.R.Anantharaman and Philip Kurian, Dielectric and Mechanical Properties of Rubber Ferrite Composites containing Barium Ferrite, Progress in Rubber and Plastics Technology. (Accepted for publication).
5. **M.A.Soloman**, M.R.Anantharaman and Philip Kurian, Effect of Carbon Black on the Mechanical and Dielectric Properties of Rubber Ferrite Composites containing Barium Ferrite, Plastics Rubber and Composites. (Communicated).
6. **M.A.Soloman**, M.R.Anantharaman and Philip Kurian, Dielectric and Processing Properties of Rubber Ferrite Composites containing Strontium Ferrite, Journal of Elastomers and Plastics. (Communicated).
7. **M.A.Soloman**, P.A.Joy, M.R.Anantharaman and Philip Kurian, Magnetic and Mechanical Properties of Rubber Ferrite Composites containing Strontium Ferrite, European Polymer Journal. (Communicated).

58888'